HEPARAN SULFATE MITIGATES TRANSFORMING GROWTH FACTOR BETA (TGFβ) SIGNALING TO RETAIN PROSTATE STEM CELL STATE

by

SUMIT RAI

(Under the Direction of Lianchun Wang and Houjian Cai)

ABSTRACT

Stem cells are characterized by their ability to self-renew and to give rise to different cell types. In order to exploit their use for regenerative therapies, it is critical to identify molecular mechanisms that regulate the decision between their self-renewal and differentiation under normal physiological conditions and in disease. Heparan sulfate (HS) is a highly sulfated polysaccharide and its synthesis involves various enzymes, among them is the glycosyltransferase *EXT1*, which polymerizes the HS chain. HS is present abundantly on the cell surface and within the basement membrane where it interacts with numerous proteins including growth factors and morphogens thereby regulating important developmental processes in invertebrates and vertebrates. The function of HS in adult stem cell self-renewal and developmental signaling is largely unknown. Prostate stem cell (PrSC) self-renewal and differentiation are controlled by various heparin-binding growth factors and hence HS may be an important component in the modulation of PrSC fate. Ablation of *EXT1*, a HS biosynthetic enzyme leads to HS deficiency in PrSCs. $EXT1^{-/-}$ $p63^{+}$ PrSCs are unable to retain their self-renewal potential, in the *in vitro* sphere assay, and differentiate. The loss of stem cell status is because of enhanced transforming growth factor beta (TGF-β) signaling, promoting differentiation to luminal cell type. Attenuating TGFβ signals partially restores self-renewal property of $EXT1^{-/-}$ PrSCs. Furthermore, HS can maintain PrSC homeostasis by functioning *in cis* or *in trans,* allowing for proper regeneration of the prostate gland. Furthermore, to delineate the epithelial-mesenchymal interactions which ensue during normal development as well as in cancer, we developed a novel *in vitro* co-culture system. Collectively, this study demonstrates that HS is an important modulator of PrSC fate decisions: HS is required for the maintenance of stem cell homeostasis *in cis* or *in trans* fashion.

INDEX WORDS: Heparan Sulfate, Prostate stem cell, Epithelial-Mesenchymal Interactions, Sprouting Angiogenesis, Sphere assay, *In vivo* prostate regeneration, TGFβ signaling

HEPARAN SULFATE MITIGATES TRANSFORMING GROWTH FACTOR BETA (TGFβ) SIGNALING TO RETAIN PROSTATE STEM CELL STATE

by

SUMIT RAI

B.Sc, Bangalore University, India, 2008

M.Sc, School of Regenerative Medicine, Manipal University, India, 2010

A Dissertation Submitted to the Graduate Faculty of The University of Georgia in Partial Fulfillment of the Requirements for the Degree

DOCTOR OF PHILOSOPHY

ATHENS, GEORGIA

2017

HEPARAN SULFATE MITIGATES TRANSFORMING GROWTH FACTOR BETA (TGFβ) SIGNALING TO RETAIN PROSTATE STEM CELL STATE

by

SUMIT RAI

Major Professor: Lianchun Wang
Co-Professor: Houjian Cai

Committee: Lance Wells
Michael Pierce
Michael Tiemeyer
Stephen Dalton

Electronic Version Approved:

Suzanne Barbour
Dean of the Graduate School
The University of Georgia
May 2017

DEDICATION

This dissertation is dedicated to my parents,Vikram and Kavita, who always supported me. Soumya, Aashwin and Vanshree, thanks for always being there for me!

Taronish– Without you, I wouldn't have made it. Thanks for always being there for me

Thanks to my friends here that supported me – especially DJ and Nicky – I am going to miss our scientific and non-scientific discussions that we had.

.

ACKNOWLEDGEMENTS

I want to thank Dr. Lianchun Wang and Dr. Houjian Cai for their mentorship and enthusiasm. I could not have asked for more liberty during my PhD. I also need to mention and thank the people of the Wang and Cai lab, past and present: Wenyuan, Jingwen, Youxi, Cathy, Hong, Sungjin, Qianjin, Meng, Yonjie and Omar. Thanks to my PhD committee members: Dr. Michael Pierce, Dr. Lance Wells, Dr. Michael Pierce, Dr. Stephen Dalton and Dr. Michael Tiemeyer for giving great guidance and advice on my projects and for helping me in my professional endeavors. I would like to thank Julie Nelson for help with the flow cytometry and James barber for help with the confocal microscopy.

TABLE OF CONTENTS

Page

LIST OF TABLES

Page

LIST OF FIGURES

Page

CHAPTER 1

INTRODUCTION AND LITERATURE REVIEW

The prostate, found only in mammals, is a male accessory sex-gland producing the bulk of seminal fluid proteins. In humans, the prostate is a walnut-size structure lacking a lobular structure and is found at the base of the bladder surrounding the urethra. McNeal has defined three morphological areas within the human prostate: the peripheral zone, the transition zone, and the central zone [1, 2] (Fig. 1.1). In contrast, prostate gland in rodents is composed of four distinct lobes: anterior (also known as the coagulating gland), dorsal, lateral and the ventral lobes that produce secretory proteins and exhibit characteristic ductal branching [3]. Although there is no structural analogy between the zones of the human prostate and the lobes of the rodent prostate, several studies argue that the human peripheral zone is similar to rodent dorsolateral lobes. [1]

Mature prostatic ducts consist of three major cell types: luminal epithelial cells which are secretory in nature, basal epithelial cells which line the basement membrane and smooth muscle cells (Fig. 1.2). A subset of rare cells, the neuroendocrine cells, is found interspersed within the basal cell layer. In both species, the luminal cells are columnar, exhibit apicobasal polarity, line the lumen of the prostatic ducts and secrete proteins and fluids from their apical surface. The basal cells, in the human prostate, form a continuous layer between the luminal cells and the basement membrane. However, the mouse prostate has few basal cells that are dispersed forming a discontinuous layer around the

duct. The neuroendocrine cells are found between the epithelial cells of both developing and adult prostate. The basal and luminal cells are derived from the epithelium of the cloaca while the origins of the neuroendocrine cells have been mapped to neural crest cells [4]. The stromal layer of both human and mouse is mostly composed of smooth muscle cells. Other cells include neuronal, lymphoblastic, vascular and fibroblasts. This layer is thicker in the human prostate resulting in higher stromal to epithelial cell population.

Development of the Prostate Gland

The growth and development of the prostate gland, which begins in the fetus, is only accomplished after attaining sexual maturity. During early embryonic development, the cloaca is used for the excretory functions [5]. After about six weeks post-conception in humans and 13.5 days post coitum (dpc) in mice, an urorectal septum develops dividing the cloaca into the digestive tract and the urinary tract [6]. The ventral compartment of the urinary tract thereby formed is called the Urogenital Sinus (UGS). The prostate develops from the UGS whereas other male accessory sex glands develop from the Wolffian duct, a mesodermal structure [7]. The UGS is composed of epithelial cells, derived from the endoderm, surrounded by a mesenchymal layer of mesodermal origin. The UGS is present in both males and female embryo but does not exhibit discernible morphology until 10-12 weeks in humans or 17.5dpc in the mice.

Prostate morphogenesis is initiated by epithelial budding of the UGS wherein urogenital sinus epithelium (UGE) cells proliferate, grow and invade the surrounding urogenital sinus mesenchyme (UGSM). In mice, this happens around 16.5 dpc. These buds grow as solid cords into the UGSM in specific spatial pattern establishing the identity of the

various lobes of the gland [8, 9]. In mice, most of the prostatic ducts remain unbranched until birth. The epithelial cells of the solid prostatic buds co-express cytokeratins 5, 8, 14, and 18, as well as high levels of p63. Postnatally, these solid buds grow into the UGSM and continue branching and canalizing. As canalization commences, the epithelium transforms into two cell types, basal and luminal. In mice, basal epithelial cells are present along the basement membrane forming a discontinuous layer expressing cytokeratins 5 and 14, and p63 [9]. Simultaneously, tall columnar luminal cells, expressing cytokeratins 8 and 18, line the ductal lumen [10]. The prostatic mesenchyme/stroma also can differentiate into a layer of smooth muscle that surrounds the prostatic ducts [11]. In mice, branching morphogenesis is almost entirely complete by postnatal day 15 (P15).

Developmental Cell Signaling

The development of the prostate gland in rodents and humans depends entirely on the androgen secretion by the fetal testes. Also, many signal transduction pathways play an important role in the overall development of the gland. These include fibroblast growth factor (FGF), transforming growth factor β/ bone morphogenetic protein (TGFβ/BMP) and Hedgehog signaling pathways.

Androgen Receptor and Signaling:

Functional androgen receptor (AR) signaling is critical in the formation of the prostate gland [13, 14]. Testes serve as the primary site of testosterone production for the embryo. For prostate development, dihydrotestosterone (DHT) is the required form necessary for prostate development [12]. DHT is the reduced form of testosterone produced intracellularly in the prostate epithelial cells by the enzyme 5α-reductase and has an

increased affinity towards the AR in comparison to testosterone [12]. Any perturbation in AR signaling results in incomplete prostate development, as observed in both humans and mice. In humans, 5α-reductase deficiency results in the absence of the prostate gland even though the development of the seminal vesicles is normal which empties into a vaginal structure not connected to the internal genitalia [13]. Testicular feminization syndrome (Tfm) mice have a frameshift mutation in the AR gene, rendering the male mice androgen insensitive [13]. These mice fail to form the prostate and bear female external genitalia [14].

AR is expressed by the UGSM before and during prostate development, but epithelial AR expression is triggered only after budding and branching morphogenesis [15-17]. Using tissue recombinant experiments, Cunha et al. have demonstrated that mesenchymal AR is responsible for prostate morphogenesis and not the epithelial AR [9, 18]. When wild-type UGSM was recombined with Tfm UGE and implanted under the renal capsule of an adult male mouse, the epithelial cells displayed proliferation and differentiation forming glandular prostate acini in an AR dependent fashion. However, when wild type UGE was recombined with Tfm UGSM prostate morphogenesis was absent with the grafted tissue undergoing vaginal differentiation thus proving that the mesenchymal AR is primarily responsible for the initiation of prostate morphogenesis. Later studies in mice and rat revealed that epithelial AR is necessary for expressing secretory proteins, proliferation of the epithelium and differentiation into the different cells types which is largely dependent on paracrine factors that are under the control of mesenchymal AR [17, 19].

Androgen action is mediated by downstream factors through interaction with nuclear AR, a superfamily of transcription factors [20, 21]. Organ culture studies demonstrated

impairment of prostatic bud formation when male wild-type UGS was removed before fetal testes began producing testosterone. However, this defect can be rescued by supplementing the culture medium with androgen [22]. In contrast, culturing rat male UGS which was removed after the onset of testosterone production, but before the commencement of ductal budding, demonstrated prostate ductal budding in the absence of exogenous androgens [23].

Fibroblast Growth Factor (FGF) Signaling:

Fibroblast growth factors (FGFs) are a family of structurally related polypeptide growth factors and are predominantly expressed during embryogenesis as well as in a restricted fashion in adult tissues [24-26]. FGFs are involved in multiple cellular processes including cell migration, chemotaxis, cell survival, apoptosis, and differentiation. FGFs bind FGF receptors (FGFRs), receptor tyrosine kinases (RTKs) and cause downstream signaling. There are four vertebrate FGF receptors, FGFR1-4. FGFRs consist of an intracellular tyrosine kinase domain, a single transmembrane domain and an extracellular ligand-binding domain containing IgG-like domains. A heparin-binding domain and a cell adhesion homology domain is present between the IgG domains required for interactions with cell surface heparan sulfate proteoglycans and components of the extracellular matrix respectively [27, 28]. FGFs can mediate their effects through various pathways including the Ras/MAPK, PI3K/AKT, STAT and PLC/Ca^{2+}pathways [29]. The MAPK pathway involves binding of docking proteins containing the SH2 domain, such as Grb2, to the phosphotyrosine residues of an activated receptor. Grb2 also binds the guanine nucleotide exchange factor SOS via its SH3domain, which leads to the activation of SOS. Activated SOS, a GTPase, exchanges GDP with GTP in the monomeric G-

protein Ras thereby activating it. Following this, the GTP bound Ras initiates a signaling cascade of various serine/threonine protein kinases including Raf, Mek, and Erk1/2. Phosphorylated Erk1/2 translocates to the nucleus carrying out its functions of transactivating target genes or modulating the activity of other transcriptional regulators [29].

Prostate epithelial expression of FGFR2 plays an essential role in the development of the gland. Conditional loss of FGFR2 in the UGE resulted in the loss of the anterior prostate (AP) and ventral prostate (VP) lobes. The dorsolateral lobes (DLP) in these mice displayed reduced branching and decreased epithelial proliferation. Additionally, the epithelial cells responded poorly to androgen stimulation [30]. Mutant mice harboring UGE specific deletion of *FRS2α,* an adapter protein in the FGF signaling cascade, showed decreased branching of all the prostatic lobes. Interestingly, increase in several pathways regulating branching morphogenesis like BMP4/7, TGFβ, Hoxb13 were differentially modulated in the absence of FGFR22 or FRS2*α.*

Mammals express twenty-two FGF ligands out of which only 18 are able to activate the FGFRs [31]. Currently, only FGF-7 and FGF-10 have been found to be involved in prostate development. They are secreted by the mesenchyme to act on the epithelium which expresses FGFR2iiib, a splice variant of FGFR2 [32]. Organ culture of rat ventral prostate revealed drastically reduced ductal tips when endogenous FGF7 was blocked [33]. On the other hand, FGF7 knockout animals were phenotypically normal suggesting a possibility of functional redundancy of FGF10 [34]. FGF10 alone is not sufficient to induce budding but can promote ductal branching in rats [35]. FGF10 knockout mice

display limited bud formation with significantly reduced prostate development. This phenotype can be rescue by supplementing FGF10 with testosterone [36].

Transforming Growth Factor β (TGFβ) and Bone Morphogenetic Protein (BMP) signaling:

The TGFβ superfamily consists of the TGFβ and BMP proteins sharing a conserved signaling pathway. Both bind to heteromeric receptor complexes consisting of type I and type II serine/threonine receptor subunits. Type II receptors are constitutively active, phosphorylating tyrosines on type I receptors upon ligand binding. Receptors that bind and transduce signals for the TGF-βs are TβR-I and TβR-II. Putative receptors of BMPs are type I receptors: Alk1-3 (type IA or BMPR) and Alk6 (or type IB). Type II receptors that bind BMPs are BMPRII, ActRIIA and ActRIIB. SMAD transduce signals from different members of the TGFβ family. SMAD2/3 are stimulated by TGFβ and activins while SMAD1/5/8 are activated by BMPs [37].

All the three known isoforms of TGFβ ligand (TGFβ1, 2, and 3) are expressed in the prostate [38]. Chang et al have reported localized expression of TGFβ1in the smooth muscle cells surrounding the ducts in rat prostate [39]. Exogenous supplementation of TGFβ1 reduces branching in P0 prostates of rats [38]. Studies on rats and mice, examining the effect of TGFβ1 on epithelial cells showed decreased proliferation in proximal ducts and increased proliferation in distal duct segments [40]. In mouse, this was attributed to increased production of TGFβ1 by the epithelial cells of the proximal tubule [41] demonstrating that TGFβ acts as a negative regulator of prostate epithelial cell growth.

Both BMP4 and BMP7 play a pivotal role in ductal morphogenesis. *In utero* BMP is expressed in the mesenchyme, however, with the onset of ductal morphogenesis, BMP expression is restricted around the epithelia buds [42]. Culturing UGS in the presence of BMP4 suppresses proliferation of epithelial cells and duct formation. BMP4 heterozygous null mouse exhibits substantial increase of ducts in the ventral prostate and anterior prostate thus suggesting an inhibitory role in ductal budding and branching. Exogenous supplementation of BMP7 was found to decrease ductal budding in explant culture while BMP7 null mice show increased ductal budding [43]. The expression of BMP7, before birth, like BMP4 is restricted to the mesenchyme. However, as ductal morphogenesis process, BMP7 expression becomes restricted to the ductal epithelium with highest expression observed in the growing ducts probably acting as a safeguard against the uncontrolled proliferation of cells [35, 43].

Hedgehog signaling pathway:

The Hedgehog (HH) signaling pathway plays a crucial role in the development of the prostate gland. The secreted HH ligand binds to Patched (Ptch), a transmembrane receptor, expressed on the surface of target cells thereby releasing the repression of Smoothened (Smo) leading to transcriptional regulation of various genes by three transcription factors, Gli1, Gli2, and Gli3. Mammals express three HH ligands: Sonic Hedgehog (SHH), Indian Hedgehog (IHH) and Desert hedgehog (DHH) [44]. The developing prostate expresses high levels of SHH [45]. The expression of SHH in the UGE increases as ductal budding increases. This expression is maintained until ductal branching commences when SHH levels decrease steadily and tapers off to a measurable but low level in the adult [46, 47]. In rats, SHH is localized to the distal tip epithelium as

the ducts grow and branch [48] with the mesenchyme expressing Ptc1 and Gli1, the SHH target genes [47].

Podlasek et al. reported inhibition of prostate morphogenesis when SHH signaling was blocked using a neutralizing antibody in grafted UGS [46]. However, a number of following studies, both in rat and mouse, found normal prostate morphogenesis independent of SHH signaling with UGS from a SHH null mouse exhibiting normal prostate morphogenesis when grafted [49-51]. Interestingly, the levels of IHH were found to be upregulated in these null embryos providing functional redundancy in rescuing HH signaling [45]. The effect of HH on prostate morphogenesis was found to be stage specific with HH promoting epithelial proliferation and budding before birth while inhibiting epithelial proliferation and ductal branching postnatally [52].

Epithelial-Mesenchymal Interactions in Prostate Development:

The growth factors and androgen secreted by the stromal compartment serve an essential role in the development of the prostate gland. Prostate morphogenesis is a highly complex process involving paracrine and juxtacrine interactions between the stroma and the epithelium [53-59], maintaining a balance between survival, proliferation, differentiation and apoptosis. These cellular processes vary between the basal and luminal compartment resulting in cell turnover differences [60, 61]. The stromal cells secretes many growth factors out of which TGF, FGF, EGF, HGF and IGF are involved in cell proliferation and differentiation.

IGF family of proteins are homologs of insulin and promote proliferation of prostate epithelial cells [62]. Basal cells express type I IGF receptors which bind to both IGF-I and IGF-II, with IGF-1 being a more potent mitogen [63, 64]. Presence of IGF-1 in

primary cultures of prostate epithelial cells is necessary for their survival and growth [65].

Multiple members of FGF family are expressed in the prostate (FGF-1, 2, 3, 5, 7, 8 and 10). FGFRs have been identified both in the stroma and the epithelium where they are involved in stimulating proliferation of the stromal cells except FGF10 and FGF7 which act on epithelial cells [66, 67].

EGF promotes growth of the epithelium. TGF-α, a member of the EGF family, binds to the same receptor as EGF and is involved in the differentiation of the prostate epithelium [68, 69].

HGF/scatter factor receptor, c-MET, is located on the basal cells of the prostatic epithelium and is involved in inhibiting proliferation and promoting differentiation in normal prostate epithelial cells [70, 71].

Prostate Stem Cells:

Early studies have revealed that the adult mouse prostate undergoes involution in response to androgen depletion or castration. This was found largely due to apoptosis of the androgen dependent luminal cells while the basal cells were not affected. Supplementation with androgen resulted in rapid regeneration of a fully functional tissue. The cycle of androgen ablation and replacement could be repeated multiple times suggesting the existence of stem cells possessing the property of self-renewal and multi-lineage differentiation. It has been found that prostate stem cells are harbored within the basal cells layer and are characterized by their androgen independence as well as expression of many stem cell genes like telomerase, p63 and Bcl-2.

Functional Assays Characterizing Prostate Stem/Progenitor Cells:

Two dimensional (2D) and three-dimensional (3D) culture systems have been employed to identify progenitor cells in mouse and human tissues. However, very few studies have been able to support prolonged *in-vitro* culturing and quantification of self-renewal capacity of prostate stem cells. In an effort to define these properties of murine stem/progenitor cells, a regeneration assay was devised using the classical tissue fragment recombination assay [72]. In this assay, single cells from adult mouse prostate are combined with UGSM cells and implanted under the kidney capsule of an immuno-deficient male mouse. UGSM is known to play a supportive as well as an instructive role in prostate morphogenesis during development through induction of proliferation and differentiation of the stem cells by secreting andromedins. The regenerated glandular structures resembles the mouse prostate tissue. The glands are lined by a single layer of epithelial cells, with all the three major cell types present, surrounding a fluid filled epithelium [73, 74]. In addition, when prostatic epithelial cells expressing different fluorescent proteins were used in this regeneration assay, the resulting glands were composed of cells expressing only a single color, advocating for the presence of cells in the prostate capable of undergoing multilineage differentiation [73]. This assay therefore makes it possible to quantify the functions of these stem cells by genetically manipulating them since these glands are formed by single cells. Also, fractionation of the epithelial population based on their surface antigen profile allows for the comparison of the regenerative potential of various subpopulations. The regenerated tissue also exhibits several cycles of involution and regeneration in response to androgen deprivation and

replacement [75]. The primary regenerated prostate tissue can be serially passaged 2-3 times supporting the self-renewal property of the cells [75].

Although the regeneration assay is robust, it is time consuming and technically challenging. To bypass these inherent difficulties, a surrogate *in vitro* sphere assay was developed. In this assay, a small fraction of prostate epithelial cells clonally form spheroids when cultured in a 3D matrix of Matrigel [74]. These spheroids can be serially passaged for several generations confirming self-renewal capacity of sphere forming cells. These sphere forming cells are not functionally equivalent to stem cells as they are unable to regenerate glandular structure when used in the *in vivo* regeneration assay. This also raises the possibility that sphere-forming cells *in vitro* and the prostate-regenerating cells *in vivo* are probably two different subpopulations of prostate epithelial cells. Other groups have also reported different sphere assays for the study of prostate stem cells wherein these sphere forming cells retain the capability of regenerating prostate glandular structure when combined with UGSM [76, 77].

Using these assays, a number of groups have identified human and murine stem/progenitor cells. Regeneration as well as the sphere assay has helped several groups identify Stem cell antigen-1 (Sca1) expressing cells to have regenerative capacity [73, 78]. Studies subsequently have shown that markers such as CD49f, Trop2 and CD166 further enrich for stem cell activity within the Sca1+ population [79-81]. Single murine prostate cells displaying the antigenic profile Lin-Sca-1^{+}CD44^{+}CD133^{+}CD117^{+} can regenerate the prostate tissue [82]. All these cells display a basal cell phenotype in accordance with the hypothesis that basal cells possess the stem cell activity.

Using the prostate regeneration assay, Goldstein et al. showed that the prostate stem cell activity is enriched in the $CD49f^{+}Trop2^{+}$ human prostate basal cells [83, 84]. Interestingly, Garraway et al. showed that the basal prostate cells that form prostate spheres may not be equivalent to the cells that regenerate tubular structures in the prostate regeneration assay demonstrating that $Epcam^{+}CD44^{-}CD49f^{Hi}$ cells are the tubule regenerating prostate stem cell population while $Epcam^{+}CD44^{+}CD49f^{Hi}$ cells are the sphere-forming cells [85]. CD133 is another marker that has been reported to enrich prostate stem cell activity. Richardson et al showed that integrin $\alpha2\beta1^{Hi}CD133^{+}$ cells from human prostate tissues can reconstitute prostatic-like acini [86].

In vivo Characterization of Prostate Stem/Progenitor Cells:

The development of the *in vivo* regeneration assay has provided a platform to study the behavior of prostate stem cells under varied settings, developmental or pathophysiological. However, a major drawback of this assay is that the prostate cells are in direct contact with the UGSM cells known to apply strong reprogramming pressure. Several groups have investigated if the regenerative capacity of basal cells in this assay is required for the maintenance of prostate epithelium *in vivo* by tracking fates of labeled luminal and basal cells *in vivo*. The two labeling techniques have led to similar conclusions that independent sustenance of luminal and basal cells *in vivo*. Lineage tracing has also provided information regarding epithelial hierarchy during development of the gland. Using labeled luminal and basal cells to study postnatal development of the prostate, Ousset et al. found that only a fraction of basal cells possessed stem cell capacity and were able to differentiate to both basal and luminal cells [87]. Therefore, the basal cells could give rise to luminal cells by generating unipotent luminal cells or a

transit amplifying cell. In contrast, luminal cells at this state displayed lineage restriction and only possess unipotent differentiation potential.

Glycosaminoglycans:

Glycosaminoglycans (GAGs) are linear polysaccharides that are ubiquitously present and involved in mediating developmental, physiological and patho-physiological processes. They are composed of repeating disaccharide units of N-acetyl-hexosamine and a hexuronic acid (Glucuronic or Iduronic acid). Differenet types of GAGs vary in their composition of the disaccharide units. Heparan Sulfate (HS), Keratan Sulfate (KS) and Hyaluronic Acid (HA) contain N-acetyl-glucosamine (GlcNAc) while Chondroitin Sulfate (CS) and Dermatan Sulfate (DS) consist of N-Acetyl-galactosamine (GalNAc) (Table 1.1). The backbone of GAGs are derived from five precursor molecules: UDP-GlcNAc, UDP-GalNAc, UDP-GlcA, UDP-Xyl and UDP-Gal. The backbone of GAGs is further sulfated wherein 3′-phosphoadenosine 5′-phosphosulfate (PAPS) provides sulfate moieties for the process [88-90]. Except for HA, all the other GAGs are highly sulfated. GAGs are abundantly present on the cell surface as well as in the basement membrane attached covalently to a core protein. The types of GAG chains, their number, amount of sulfation, and variation in their length as well as their arrangement on the core protein confer diversity to the core proteoglycans. This is reflected by multiple functions of proteoglycans, most of which are highly dependent on the GAG chains.

Heparan Sulfate Proteoglycans:

Heparan sufate proteoglycans (HSPGs) are glycoconjugates composed of a core protein covalently linked to one or more HS GAG chains [91-93]. These HSPGs are abundantly present on the cell surface (including Syndecans and Glypicans) and in the ECM

(including perlecan and agrin) where they are well documented to interact with multitude of proteins including growth factors, morphogens, extra cellular matrix proteins, adhesion molecules and proteases.

There are three major classes of HSPGs: transmembrane syndecans, glycosylphosphatidylinositol (GPI) anchored glypicans and extracellular HSPGs like agrin and perlecan (Fig. 1.3). Syndecans contain a transmembrane region, a short but conserved C-terminal cytoplasmic tail and an extracellular domain containing GAG attachment sites [94]. There are four vertebrate syndecans designated as syndecan 1-4. Syndecans primarily carry HS chains but syndecan 1 and 4 may also bear CS chains [95]. Syndecans are capable of forming dimers and higher order oligomers. While multiple syndecan members are expressed by most cells, their expression is cell, tissue and development specific [96]. Glypicans comprise a family of GPI-anchored proteoglycans bearing a globular domain which contains a characteristic pattern of 14 cysteine residues and an extended domain with attachment sites exclusively for HS. Like syndecans, glypican (glypican 1-6) expression is tissue- and developmental stage- regulated. It has been suggested that attachment of glypicans *via* the GPI anchor may target them to lipid rafts which are believed to serve as signaling centers on the plasma membrane. Thus this interaction could be important to facilitate their interaction with specific signaling molecules [97]. The HSPGs perlecan and agrin are mainly present in the ECM where they are involved in maintaining basement membrane structure as well as in modulating various signaling transduction events. Perlecan is a large multidomain proteoglycan that is expressed in basement membranes, mesenchymal and connective tissues. Perlecan contains attachment sites for both HS and CS at its N-terminal domain. HS of perlecan

has been implicated in sequestering and storing of growth factors as well as acting as a low-affinity co-receptor [98].

Biosynthesis of Heparan Sulfate:

Biosynthesis of HS chains begins in the Golgi. The first step involves the formation of a tetrasaccharide linker composed of GlcAβ(1→3)Galβ(1→3)Galβ(1→4)Xylβ1 at specific serine residue/s of the core protein [99-101] (Fig. 1.4). The assembly of this linker initiates with the addition of a xylose residue to a serine by Xylosyltransferase (XylT) I or II, depending on the organism and cell type. This follows attachment of a galactose residue by galactosyltransferase-I (GalT-I). Once this disaccharide linker is formed an atypical secretory pathway kinase, family with sequence similarity 20 member B (FAM20B), phosphorylates xylose at the 2-O position [102, 103]. FAM20B dependent xylose phosphorylation potentiates the activity of galactosyltransferase-II (GalT-II) in adding the second galactose residue. The absence GalT-II activity results in incomplete linkages capped with sialic acid. Before the addition of glucuronic acid, the phosphate on the xylose is removed by 2-Phosphoxylose Phosphatase (XYLP) [104]. Glucuronyltransferase-I (GlcAT-I) then proceeds to add a glucuronic acid residue completing the formation of the tetrasaccharide linker. It has been shown that GlcAT-I interacts and regulates the localization of XYLP. The addition of GlcA by GlcAT-I is concurrent with rapid XYLP-dependent dephosphorylation. Inability to remove the phosphate from xylose prevents formation of the tetrasaccharide linkage [104]. Exostosin like 2 (EXTL2) encodes the α1,4-N-acetylhexosaminyltransferase that transfers GlcNAc/GalNAc to the tetrasaccharide linker initiating heparin/heparan sulfate polymerization, differentiating it from the chondroitin sulfate/dermatan sulfate synthesis

[105, 106]. After the addition of the GlcNAc residue, polymerization of the HS backbone is initiated by alternate addition of β1,4-linked GlcA and α1,4-linked GlcNAc units to the non-reducing end of the growing polymer by co-polymerases Exostosin 1 (Ext1) and Exostosin 2 (Ext2) which are bifunctional glycosyltransferases harboring both GlcA- and GlcNAc-transferase (GlcA-TII and GlcA-TII) activity [107-110]. Although Ext1 is capable of polymerizing HS chain *in vitro* there seems to be an absolute requirement for the two enzymes to work in sync *in vivo* since absence of one leads to disruption in HS biosynthesis [111, 112]. As heparan sulfate chain is being elongated, the N-deacetylase N-sulfotransferases (NDST) substitute the N-acetyl groups with N-sulfate groups of some GlcNAc residues. There are four isoforms of NDST (NDST1-4) each exhibiting striking differences in the proportion of N-deacetylation and N-sulfation activities [113]. These regions undergo further modifications by a number of enzymes including epimerization of GlcA to Iduronic acid (IdoA) by C5-epimerase, advancing towards O-sulfation at various positions by iduronosyl 2-O-sulfotransferase (HS2st), glucosaminyl 6-O-sulfotransferases (HS6sts) and 3-O-sulfotransferases (HS3sts). Three isoforms of HS6st and seven isoforms of HS3st have been described, whereas only one isoform of C5-epimerase and HS2st has been found. These modification steps are found to be highly regulated with enzymes using products of preceding enzymatic reaction as substrates. However, certain *in vitro* and cell based studies have revealed otherwise. Modifications of the HS structure, though mostly occurring in the Golgi, are not restricted within the cell. The HS chains are post-synthetically remodeled at the cell surface by extracellular endosulfatases (Sulf) removing 6-O sulfates from GlcNAc residues. These HS chains can also by degraded by an endoglycosidase, heparanase. There are two isoforms of sulfatase

and heparanases. The sulfation and epimerization modifications, both intra- and extracellularly, are not evenly spread across the HS chains giving rise to variable HS sequences. For example NDSTs give rise to segments with unmodified *N*-acetylated disaccharide units (NA domains), sequences of *N*-sulfated disaccharide units (NS domains) and regions composed of alternating *N*-sulfated and *N*-acetylated disaccharides (NA/NS domains). Interestingly, these modification are not random and have been shown to be under tight regulation. As the sequence and sulfation pattern of HS chains dictates interaction with a plethora of binding partners, these modifications fine-tune spatiotemporal regulatory functions of HS during development and in disease progression.

Interaction of heparan sulfate with proteins:

HSPGs hold several important roles during development, in tissue homeostasis and injury repair. The structural diversity of HS chains impart HSPGs with the capacity to perform diverse physiological functions which can be cell specific, tissue specific or ubiquitous [92] (Fig. 1.5). Syndecans are primarily associated with anchoring the cells to heparin-binding domain of extra cellular matrix proteins thus relaying extracellular signal to the cytoskeleton and intracellular machinery. By providing this physical link between ECM, cytoskeletal proteins and intracellular signaling components, HSPGS are able to modulate basic cellular functions including cell adhesion, migration, etc. [114, 115]. A more tissue and organ-restricted role of HSPGs is found in hepatic cells for lipid metabolism where they mediate clearance of lipoproteins independent of LDL receptors, the primary lipoprotein uptake receptor [116].

HS/Heparin Binding Determinants on Proteins:

The heterogeneous and highly complex structure of HS chains, even within the same cell, allows for interaction with numerous proteins. Cardin and Weintraub compared the amino acid sequence of heparin binding domains of multiple proteins and identified two motifs: XBBXBX and XBBBXXBX (where B is a basic and X a hydrophobic and or a neutral amino acid residue) [117]. Utilizing molecular modeling methods, it was found that the secondary structure these motifs was displayed in a fashion that facilitates interaction with the negatively charged sulfate groups of heparin. GAG binding sites are often exposed along one end of helical conformations or are wrapped around β-pleated sheets. Twelve heparin-binding proteins containing the Cardin-Weintraub sequence are known [118]. However, the motif hypothesis does not hold true as these motifs are not ubiquitously present in other heparin-binding proteins. A turn-rich TXXBXXTBXXXTBB binding motif (T, turn; B, basic arginine/lysine; X, hydropathic residue) was discovered by comparing heparin binding sites of FGF1, FGF2 and TGFβ. This topology was found to be important as affinity studies revealed stronger interaction between cyclic peptides and heparin than acyclic peptides [119]. This strongly suggests that protein conformation plays an essential role in mediating HS/heparin interaction. For example protein conformation is believed to play an essential role in mediating interaction between Antithrombin III and heparin as the protein does not contain contiguous binding sites thus requiring proper positioning of the basic amino acids [120]. Van der Waals forces, hydrogen bonds and hydrophobic interactions with the carbohydrate backbone are well known to participate in interactions between proteins and GAGs [118]. Several known heparin-binding domains contain amino acids like arginine

and lysine that can form hydrogen bonds. Using peptide libraries, it was observed that hydrogen bonding significantly increases heparin binding affinity [121].

Protein binding determinants on Heparan Sulfate/Heparin chains:

Due to the presence of multiple sulfate groups, HS chains inherently carry high negative charges. Therefore, many of the proteins thus bind to HS due to electrostatic interactions. The structure of HS required to interact with a plethora of binding partners has been extensively studied in context of the FGF family of proteins, specifically FGF1 and FGF2. Structural and biochemical studies have shown that chain length, sulfation pattern and conformation of HS is crucial in FGF binding and activity. FGF2 binds to heparin/HS pentasaccharide containing an IdoA2S-GlcNS disaccharide while FGF1 recognizes octasaccharide bearing an IdoA2S-GlcNS6S-IdoA2S trisaccharide motif [122, 123]. Crystal structures of heparin–FGF complexes have illustrated that the heparin interacts with both FGF as well as the FGFR forming a ternary complex [124, 125]. A minimum of 8-mer heparin oligosaccharides are needed for complex formation with increased stability observed with decasaccharides. Furthermore, FGF-FGFR complexes are stabilized by increasing the amount of 2-O and 6-O sulfation though there does not seem to be a preference between the two sulfations indicating a lack of selectivity with regards to carbohydrate structure [126]. Conclusions about structural requirements of HS for interaction with FGF can also been made from mouse models deficient in HS biosynthetic enzymes. Mice deficient in GlcA C5-epimerase and 2-O-sulfotransferase appear normal [127, 128]. 2OST mice exhibits increased 6-O- and N-sulfation such that overall sulfation remains the same. Hence the stability of FGF-oligosaccharide-FGFR complexes may depend on the overall level of O-sulfation rather than their specific

positions on the glycan. Conversely, recent studies have demonstrated specificity of FGF-FGFR complexes in their binding to HS of specific disaccharide compositions indicating that positions of sulfate groups may be important [129].

Heparan Sulfate and Prostate Stem Cells:

HS has been implicated in regulating various developmental processes through their ability to interact with numerous proteins that include growth factors and morphogens. HS modifying enzyme, Hs6st1, which adds 6-O sulfate groups to the HS backbone is expressed abundantly at the tips of growing epithelial buds, the site of prostate development, within the embryo [130]. These buds are well documented to be enriched in stem cell population. Interestingly, the mesenchyme surrounding the bud expresses high levels of Sulf1, an enzyme that removes 6-O sulfates from the HS chain, probably functioning to spatially limit the activity of various HS-dependent signaling events. Immunohistochemical studies have revealed the presence of highly sulfated HS structure within these buds. As self-renewal and differentiation are controlled by various heparin-binding growth factors, HS may play an important role in the modulation of prostate stem cell fate decisions. To date, the functional roles of HS in prostate stem cell biology are not well defined. My study addresses the role of HS in prostate stem cell self-renewal, differentiation and developmental cell signaling.

References

1. McNeal, J.E., *[Origin and development of carcinoma of the prostate]*. Aktuelle Urol, 2003. **34**(2): p. 81-2.
2. Hayashi, N., et al., *Morphological and functional heterogeneity in the rat prostatic gland.* Biol Reprod, 1991. **45**(2): p. 308-21.
3. Sugimura, Y., G.R. Cunha, and A.A. Donjacour, *Morphogenesis of ductal networks in the mouse prostate.* Biol Reprod, 1986. **34**(5): p. 961-71.
4. Szczyrba, J., et al., *Neuroendocrine Cells of the Prostate Derive from the Neural Crest.* J Biol Chem, 2017. **292**(5): p. 2021-2031.
5. Seifert, A.W., B.D. Harfe, and M.J. Cohn, *Cell lineage analysis demonstrates an endodermal origin of the distal urethra and perineum.* Dev Biol, 2008. **318**(1): p. 143-52.
6. Hynes, P.J. and J.P. Fraher, *The development of the male genitourinary system. I. The origin of the urorectal septum and the formation of the perineum.* Br J Plast Surg, 2004. **57**(1): p. 27-36.
7. Prins, G.S. and O. Putz, *Molecular signaling pathways that regulate prostate gland development.* Differentiation, 2008. **76**(6): p. 641-59.
8. Timms, B.G., T.J. Mohs, and L.J. Didio, *Ductal budding and branching patterns in the developing prostate.* J Urol, 1994. **151**(5): p. 1427-32.
9. Cunha, G.R., et al., *The endocrinology and developmental biology of the prostate.* Endocr Rev, 1987. **8**(3): p. 338-62.
10. Hayward, S.W., et al., *Epithelial development in the rat ventral prostate, anterior prostate and seminal vesicle.* Acta Anat (Basel), 1996. **155**(2): p. 81-93.

11. Hayward, S.W., et al., *Stromal development in the ventral prostate, anterior prostate and seminal vesicle of the rat.* Acta Anat (Basel), 1996. **155**(2): p. 94-103.

12. Wilson, J.D. and R.E. Gloyna, *The intranuclear metabolism of testosterone in the accessory organs of reproduction.* Recent Prog Horm Res, 1970. **26**: p. 309-36.

13. Siiteri, P.K. and J.D. Wilson, *Testosterone formation and metabolism during male sexual differentiation in the human embryo.* J Clin Endocrinol Metab, 1974. **38**(1): p. 113-25.

14. Lyon, M.F. and S.G. Hawkes, *X-linked gene for testicular feminization in the mouse.* Nature, 1970. **227**(5264): p. 1217-9.

15. Shannon, J.M. and G.R. Cunha, *Autoradiographic localization of androgen binding in the developing mouse prostate.* Prostate, 1983. **4**(4): p. 367-73.

16. Takeda, H., T. Mizuno, and I. Lasnitzki, *Autoradiographic studies of androgen-binding sites in the rat urogenital sinus and postnatal prostate.* J Endocrinol, 1985. **104**(1): p. 87-92.

17. Prins, G.S. and L. Birch, *The developmental pattern of androgen receptor expression in rat prostate lobes is altered after neonatal exposure to estrogen.* Endocrinology, 1995. **136**(3): p. 1303-14.

18. Cunha, G.R. and L.W. Chung, *Stromal-epithelial interactions--I. Induction of prostatic phenotype in urothelium of testicular feminized (Tfm/y) mice.* J Steroid Biochem, 1981. **14**(12): p. 1317-24.

19. Donjacour, A.A. and G.R. Cunha, *Assessment of prostatic protein secretion in tissue recombinants made of urogenital sinus mesenchyme and urothelium from normal or androgen-insensitive mice.* Endocrinology, 1993. **132**(6): p. 2342-50.

20. Liao, S. and S. Fang, *Receptor-proteims for androgens and the mode of action of androgens on gene transcription in ventral prostate.* Vitam Horm, 1969. **27**: p. 17-90.

21. Nuclear Receptors Nomenclature, C., *A unified nomenclature system for the nuclear receptor superfamily.* Cell, 1999. **97**(2): p. 161-3.

22. Cunha, G.R., *The role of androgens in the epithelio-mesenchymal interactions involved in prostatic morphogenesis in embryonic mice.* Anat Rec, 1973. **175**(1): p. 87-96.

23. Lasnitzki, I. and T. Mizuno, *Induction of the rat prostate gland by androgens in organ culture.* J Endocrinol, 1977. **74**(1): p. 47-55.

24. Haub, O. and M. Goldfarb, *Expression of the fibroblast growth factor-5 gene in the mouse embryo.* Development, 1991. **112**(2): p. 397-406.

25. Feldman, B., et al., *Requirement of FGF-4 for postimplantation mouse development.* Science, 1995. **267**(5195): p. 246-9.

26. Hartung, H., et al., *Murine FGF-12 and FGF-13: expression in embryonic nervous system, connective tissue and heart.* Mech Dev, 1997. **64**(1-2): p. 31-9.

27. Ornitz, D.M., *FGFs, heparan sulfate and FGFRs: complex interactions essential for development.* Bioessays, 2000. **22**(2): p. 108-12.

28. Pellegrini, L., *Role of heparan sulfate in fibroblast growth factor signalling: a structural view.* Curr Opin Struct Biol, 2001. **11**(5): p. 629-34.

29. Bottcher, R.T. and C. Niehrs, *Fibroblast growth factor signaling during early vertebrate development.* Endocr Rev, 2005. **26**(1): p. 63-77.

30. Lin, Y., et al., *Fibroblast growth factor receptor 2 tyrosine kinase is required for prostatic morphogenesis and the acquisition of strict androgen dependency for adult tissue homeostasis.* Development, 2007. **134**(4): p. 723-34.

31. Beenken, A. and M. Mohammadi, *The FGF family: biology, pathophysiology and therapy.* Nat Rev Drug Discov, 2009. **8**(3): p. 235-53.

32. Thomson, A.A. and G.R. Cunha, *Prostatic growth and development are regulated by FGF10.* Development, 1999. **126**(16): p. 3693-701.

33. Sugimura, Y., et al., *Keratinocyte growth factor (KGF) can replace testosterone in the ductal branching morphogenesis of the rat ventral prostate.* Int J Dev Biol, 1996. **40**(5): p. 941-51.

34. Guo, L., L. Degenstein, and E. Fuchs, *Keratinocyte growth factor is required for hair development but not for wound healing.* Genes Dev, 1996. **10**(2): p. 165-75.

35. Huang, L., et al., *The role of Fgf10 signaling in branching morphogenesis and gene expression of the rat prostate gland: lobe-specific suppression by neonatal estrogens.* Dev Biol, 2005. **278**(2): p. 396-414.

36. Donjacour, A.A., A.A. Thomson, and G.R. Cunha, *FGF-10 plays an essential role in the growth of the fetal prostate.* Dev Biol, 2003. **261**(1): p. 39-54.

37. Hinck, A.P., *Structural studies of the TGF-betas and their receptors - insights into evolution of the TGF-beta superfamily.* FEBS Lett, 2012. **586**(14): p. 1860-70.

38. Itoh, N., et al., *Developmental and hormonal regulation of transforming growth factor-beta1 (TGFbeta1), -2, and -3 gene expression in isolated prostatic epithelial and stromal cells: epidermal growth factor and TGFbeta interactions.* Endocrinology, 1998. **139**(3): p. 1378-88.

39. Chang, W.Y., et al., *Neonatal estrogen exposure alters the transforming growth factor-beta signaling system in the developing rat prostate and blocks the transient p21(cip1/waf1) expression associated with epithelial differentiation.* Endocrinology, 1999. **140**(6): p. 2801-13.

40. Tomlinson, D.C., et al., *Differential effects of transforming growth factor-beta1 on cellular proliferation in the developing prostate.* Endocrinology, 2004. **145**(9): p. 4292-300.

41. Salm, S.N., et al., *TGF-{beta} maintains dormancy of prostatic stem cells in the proximal region of ducts.* J Cell Biol, 2005. **170**(1): p. 81-90.

42. Lamm, M.L., et al., *Mesenchymal factor bone morphogenetic protein 4 restricts ductal budding and branching morphogenesis in the developing prostate.* Dev Biol, 2001. **232**(2): p. 301-14.

43. Grishina, I.B., et al., *BMP7 inhibits branching morphogenesis in the prostate gland and interferes with Notch signaling.* Dev Biol, 2005. **288**(2): p. 334-47.

44. Shaw, A. and W. Bushman, *Hedgehog signaling in the prostate.* J Urol, 2007. **177**(3): p. 832-8.

45. Doles, J., et al., *Functional compensation in Hedgehog signaling during mouse prostate development.* Dev Biol, 2006. **295**(1): p. 13-25.

46. Podlasek, C.A., et al., *Prostate development requires Sonic hedgehog expressed by the urogenital sinus epithelium.* Dev Biol, 1999. **209**(1): p. 28-39.

47. Lamm, M.L., et al., *Sonic hedgehog activates mesenchymal Gli1 expression during prostate ductal bud formation.* Dev Biol, 2002. **249**(2): p. 349-66.

48. Pu, Y., L. Huang, and G.S. Prins, *Sonic hedgehog-patched Gli signaling in the developing rat prostate gland: lobe-specific suppression by neonatal estrogens reduces ductal growth and branching.* Dev Biol, 2004. **273**(2): p. 257-75.

49. Freestone, S.H., et al., *Sonic hedgehog regulates prostatic growth and epithelial differentiation.* Dev Biol, 2003. **264**(2): p. 352-62.

50. Wang, B.E., et al., *Inhibition of epithelial ductal branching in the prostate by sonic hedgehog is indirectly mediated by stromal cells.* J Biol Chem, 2003. **278**(20): p. 18506-13.

51. Berman, D.M., et al., *Roles for Hedgehog signaling in androgen production and prostate ductal morphogenesis.* Dev Biol, 2004. **267**(2): p. 387-98.

52. Yu, M. and W. Bushman, *Differential stage-dependent regulation of prostatic epithelial morphogenesis by Hedgehog signaling.* Dev Biol, 2013. **380**(1): p. 87-98.

53. Liu, A.Y., et al., *Cell-cell interaction in prostate gene regulation and cytodifferentiation.* Proc Natl Acad Sci U S A, 1997. **94**(20): p. 10705-10.

54. Hayward, S.W., et al., *A functional model of adult human prostate epithelium. The role of androgens and stroma in architectural organisation and the maintenance of differentiated secretory function.* J Cell Sci, 1992. **102 (Pt 2)**: p. 361-72.

55. Grant, E.S., K.W. Batchelor, and F.K. Habib, *Androgen independence of primary epithelial cultures of the prostate is associated with a down-regulation of androgen receptor gene expression.* Prostate, 1996. **29**(6): p. 339-49.

56. Timms, B.G., et al., *Instructive induction of prostate growth and differentiation by a defined urogenital sinus mesenchyme.* Microsc Res Tech, 1995. **30**(4): p. 319-32.

57. Kinbara, H., et al., *Evidence of stem cells in the adult prostatic epithelium based upon responsiveness to mesenchymal inductors.* Prostate, 1996. **29**(2): p. 107-16.

58. Bayne, C.W., et al., *A novel coculture model for benign prostatic hyperplasia expressing both isoforms of 5 alpha-reductase.* J Clin Endocrinol Metab, 1998. **83**(1): p. 206-13.

59. Lang, S.H., et al., *Prostate epithelial cell lines form spheroids with evidence of glandular differentiation in three-dimensional Matrigel cultures.* Br J Cancer, 2001. **85**(4): p. 590-9.

60. Sugimura, Y., et al., *Whole-mount autoradiography study of DNA synthetic activity during postnatal development and androgen-induced regeneration in the mouse prostate.* Biol Reprod, 1986. **34**(5): p. 985-95.

61. Lee, C., *Role of androgen in prostate growth and regression: stromal-epithelial interaction.* Prostate Suppl, 1996. **6**: p. 52-6.

62. Cohen, P., et al., *Insulin-like growth factors (IGFs), IGF receptors, and IGF-binding proteins in primary cultures of prostate epithelial cells.* J Clin Endocrinol Metab, 1991. **73**(2): p. 401-7.

63. Fiorelli, G., et al., *Insulin-like growth factor-I receptors in human hyperplastic prostate tissue: characterization, tissue localization, and their modulation by chronic treatment with a gonadotropin-releasing hormone analog.* J Clin Endocrinol Metab, 1991. **72**(4): p. 740-6.

64. Cohen, P., et al., *Elevated levels of insulin-like growth factor-binding protein-2 in the serum of prostate cancer patients.* J Clin Endocrinol Metab, 1993. **76**(4): p. 1031-5.

65. McKeehan, W.L., P.S. Adams, and D. Fast, *Different hormonal requirements for androgen-independent growth of normal and tumor epithelial cells from rat prostate.* In Vitro Cell Dev Biol, 1987. **23**(2): p. 147-52.

66. Yan, G., et al., *Exon switching and activation of stromal and embryonic fibroblast growth factor (FGF)-FGF receptor genes in prostate epithelial cells accompany stromal independence and malignancy.* Mol Cell Biol, 1993. **13**(8): p. 4513-22.

67. Lu, W., et al., *Fibroblast growth factor-10. A second candidate stromal to epithelial cell andromedin in prostate.* J Biol Chem, 1999. **274**(18): p. 12827-34.

68. Sherwood, E.R. and C. Lee, *Epidermal growth factor-related peptides and the epidermal growth factor receptor in normal and malignant prostate.* World J Urol, 1995. **13**(5): p. 290-6.

69. Derynck, R., *The physiology of transforming growth factor-alpha.* Adv Cancer Res, 1992. **58**: p. 27-52.

70. Gmyrek, G.A., et al., *Normal and malignant prostate epithelial cells differ in their response to hepatocyte growth factor/scatter factor.* Am J Pathol, 2001. **159**(2): p. 579-90.

71. van Leenders, G., et al., *Intermediate cells in normal and malignant prostate epithelium express c-MET: implications for prostate cancer invasion.* Prostate, 2002. **51**(2): p. 98-107.

72. Cunha, G.R. and B. Lung, *The possible influence of temporal factors in androgenic responsiveness of urogenital tissue recombinants from wild-type and androgen-insensitive (Tfm) mice.* J Exp Zool, 1978. **205**(2): p. 181-93.

73. Xin, L., D.A. Lawson, and O.N. Witte, *The Sca-1 cell surface marker enriches for a prostate-regenerating cell subpopulation that can initiate prostate tumorigenesis.* Proc Natl Acad Sci U S A, 2005. **102**(19): p. 6942-7.

74. Xin, L., et al., *Self-renewal and multilineage differentiation in vitro from murine prostate stem cells.* Stem Cells, 2007. **25**(11): p. 2760-9.

75. Lawson, D.A., et al., *Prostate stem cells and prostate cancer.* Cold Spring Harb Symp Quant Biol, 2005. **70**: p. 187-96.

76. Barclay, W.W., et al., *Characterization of adult prostatic progenitor/stem cells exhibiting self-renewal and multilineage differentiation.* Stem Cells, 2008. **26**(3): p. 600-10.

77. Shi, X., J. Gipp, and W. Bushman, *Anchorage-independent culture maintains prostate stem cells.* Dev Biol, 2007. **312**(1): p. 396-406.

78. Burger, P.E., et al., *Sca-1 expression identifies stem cells in the proximal region of prostatic ducts with high capacity to reconstitute prostatic tissue.* Proc Natl Acad Sci U S A, 2005. **102**(20): p. 7180-5.

79. Goldstein, A.S., et al., *Trop2 identifies a subpopulation of murine and human prostate basal cells with stem cell characteristics.* Proc Natl Acad Sci U S A, 2008. **105**(52): p. 20882-7.

80. Lawson, D.A., et al., *Isolation and functional characterization of murine prostate stem cells.* Proc Natl Acad Sci U S A, 2007. **104**(1): p. 181-6.

81. Jiao, J., et al., *Identification of CD166 as a surface marker for enriching prostate stem/progenitor and cancer initiating cells.* PLoS One, 2012. **7**(8): p. e42564.

82. Leong, K.G., et al., *Generation of a prostate from a single adult stem cell.* Nature, 2008. **456**(7223): p. 804-8.

83. Goldstein, A.S., et al., *Purification and direct transformation of epithelial progenitor cells from primary human prostate.* Nat Protoc, 2011. **6**(5): p. 656-67.

84. Goldstein, A.S., et al., *Identification of a cell of origin for human prostate cancer.* Science, 2010. **329**(5991): p. 568-71.

85. Guo, C., et al., *Epcam, CD44, and CD49f distinguish sphere-forming human prostate basal cells from a subpopulation with predominant tubule initiation capability.* PLoS One, 2012. **7**(4): p. e34219.

86. Richardson, G.D., et al., *CD133, a novel marker for human prostatic epithelial stem cells.* J Cell Sci, 2004. **117**(Pt 16): p. 3539-45.

87. Ousset, M., et al., *Multipotent and unipotent progenitors contribute to prostate postnatal development.* Nat Cell Biol, 2012. **14**(11): p. 1131-8.

88. Sugahara, K. and H. Kitagawa, *Heparin and heparan sulfate biosynthesis.* IUBMB Life, 2002. **54**(4): p. 163-75.

89. Silbert, J.E. and G. Sugumaran, *Biosynthesis of chondroitin/dermatan sulfate.* IUBMB Life, 2002. **54**(4): p. 177-86.

90. Itano, N. and K. Kimata, *Mammalian hyaluronan synthases.* IUBMB Life, 2002. **54**(4): p. 195-9.

91. Esko, J.D. and S.B. Selleck, *Order out of chaos: assembly of ligand binding sites in heparan sulfate.* Annu Rev Biochem, 2002. **71**: p. 435-71.

92. Bishop, J.R., M. Schuksz, and J.D. Esko, *Heparan sulphate proteoglycans fine-tune mammalian physiology.* Nature, 2007. **446**(7139): p. 1030-7.

93. Bernfield, M., et al., *Functions of cell surface heparan sulfate proteoglycans.* Annu Rev Biochem, 1999. **68**: p. 729-77.

94. Yoneda, A. and J.R. Couchman, *Regulation of cytoskeletal organization by syndecan transmembrane proteoglycans.* Matrix Biol, 2003. **22**(1): p. 25-33.

95. Carey, D.J., *Syndecans: multifunctional cell-surface co-receptors.* Biochem J, 1997. **327 (Pt 1)**: p. 1-16.

96. Kim, C.W., et al., *Members of the syndecan family of heparan sulfate proteoglycans are expressed in distinct cell-, tissue-, and development-specific patterns.* Mol Biol Cell, 1994. **5**(7): p. 797-805.

97. Song, H.H. and J. Filmus, *The role of glypicans in mammalian development.* Biochim Biophys Acta, 2002. **1573**(3): p. 241-6.

98. Knox, S.M. and J.M. Whitelock, *Perlecan: how does one molecule do so many things?* Cell Mol Life Sci, 2006. **63**(21): p. 2435-45.

99. Zhang, L., G. David, and J.D. Esko, *Repetitive Ser-Gly sequences enhance heparan sulfate assembly in proteoglycans.* J Biol Chem, 1995. **270**(45): p. 27127-35.

100. Zhang, L. and J.D. Esko, *Amino acid determinants that drive heparan sulfate assembly in a proteoglycan.* J Biol Chem, 1994. **269**(30): p. 19295-9.

101. Lindahl, U., et al., *The Role of Serine in the Linkage of Heparin to Protein.* J Biol Chem, 1965. **240**: p. 2817-20.

102. Koike, T., et al., *FAM20B is a kinase that phosphorylates xylose in the glycosaminoglycan-protein linkage region.* Biochem J, 2009. **421**(2): p. 157-62.

103. Wen, J., et al., *Xylose phosphorylation functions as a molecular switch to regulate proteoglycan biosynthesis.* Proc Natl Acad Sci U S A, 2014. **111**(44): p. 15723-8.

104. Koike, T., et al., *Identification of phosphatase that dephosphorylates xylose in the glycosaminoglycan-protein linkage region of proteoglycans.* J Biol Chem, 2014. **289**(10): p. 6695-708.

105. Kitagawa, H., H. Shimakawa, and K. Sugahara, *The tumor suppressor EXT-like gene EXTL2 encodes an alpha1, 4-N-acetylhexosaminyltransferase that transfers N-acetylgalactosamine and N-acetylglucosamine to the common glycosaminoglycan-protein linkage region. The key enzyme for the chain initiation of heparan sulfate.* J Biol Chem, 1999. **274**(20): p. 13933-7.

106. Wuyts, W., et al., *Identification and characterization of a novel member of the EXT gene family, EXTL2.* Eur J Hum Genet, 1997. **5**(6): p. 382-9.

107. Lind, T., et al., *The putative tumor suppressors EXT1 and EXT2 are glycosyltransferases required for the biosynthesis of heparan sulfate.* J Biol Chem, 1998. **273**(41): p. 26265-8.

108. McCormick, C., et al., *The putative tumor suppressors EXT1 and EXT2 form a stable complex that accumulates in the Golgi apparatus and catalyzes the synthesis of heparan sulfate.* Proc Natl Acad Sci U S A, 2000. **97**(2): p. 668-73.

109. McCormick, C., et al., *The putative tumour suppressor EXT1 alters the expression of cell-surface heparan sulfate.* Nat Genet, 1998. **19**(2): p. 158-61.

110. Senay, C., et al., *The EXT1/EXT2 tumor suppressors: catalytic activities and role in heparan sulfate biosynthesis.* EMBO Rep, 2000. **1**(3): p. 282-6.

111. Busse, M. and M. Kusche-Gullberg, *In vitro polymerization of heparan sulfate backbone by the EXT proteins.* J Biol Chem, 2003. **278**(42): p. 41333-7.

112. Kim, B.T., et al., *In vitro heparan sulfate polymerization: crucial roles of core protein moieties of primer substrates in addition to the EXT1-EXT2 interaction.* J Biol Chem, 2003. **278**(43): p. 41618-23.

113. Aikawa, J., et al., *Multiple isozymes of heparan sulfate/heparin GlcNAc N-deacetylase/GlcN N-sulfotransferase. Structure and activity of the fourth member, NDST4.* J Biol Chem, 2001. **276**(8): p. 5876-82.

114. LeBaron, R.G., et al., *Adhesion of glycosaminoglycan-deficient chinese hamster ovary cell mutants to fibronectin substrata.* J Cell Biol, 1988. **106**(3): p. 945-52.

115. McQuade, K.J. and A.C. Rapraeger, *Syndecan-1 transmembrane and extracellular domains have unique and distinct roles in cell spreading.* J Biol Chem, 2003. **278**(47): p. 46607-15.

116. MacArthur, J.M., et al., *Liver heparan sulfate proteoglycans mediate clearance of triglyceride-rich lipoproteins independently of LDL receptor family members.* J Clin Invest, 2007. **117**(1): p. 153-64.

117. Cardin, A.D. and H.J. Weintraub, *Molecular modeling of protein-glycosaminoglycan interactions.* Arteriosclerosis, 1989. **9**(1): p. 21-32.

118. Gandhi, N.S. and R.L. Mancera, *The structure of glycosaminoglycans and their interactions with proteins.* Chem Biol Drug Des, 2008. **72**(6): p. 455-82.

119. Fromm, J.R., et al., *Interaction of fibroblast growth factor-1 and related peptides with heparan sulfate and its oligosaccharides.* Arch Biochem Biophys, 1997. **346**(2): p. 252-62.

120. Capila, I. and R.J. Linhardt, *Heparin-protein interactions.* Angew Chem Int Ed Engl, 2002. **41**(3): p. 391-412.

121. Caldwell, E.E., et al., *Importance of specific amino acids in protein binding sites for heparin and heparan sulfate.* Int J Biochem Cell Biol, 1996. **28**(2): p. 203-16.

122. Faham, S., et al., *Heparin structure and interactions with basic fibroblast growth factor.* Science, 1996. **271**(5252): p. 1116-20.

123. Kreuger, J., et al., *Sequence analysis of heparan sulfate epitopes with graded affinities for fibroblast growth factors 1 and 2.* J Biol Chem, 2001. **276**(33): p. 30744-52.

124. Pellegrini, L., et al., *Crystal structure of fibroblast growth factor receptor ectodomain bound to ligand and heparin.* Nature, 2000. **407**(6807): p. 1029-34.

125. Schlessinger, J., et al., *Crystal structure of a ternary FGF-FGFR-heparin complex reveals a dual role for heparin in FGFR binding and dimerization.* Mol Cell, 2000. **6**(3): p. 743-50.

126. Jastrebova, N., et al., *Heparan sulfate-related oligosaccharides in ternary complex formation with fibroblast growth factors 1 and 2 and their receptors.* J Biol Chem, 2006. **281**(37): p. 26884-92.

127. Bullock, S.L., et al., *Renal agenesis in mice homozygous for a gene trap mutation in the gene encoding heparan sulfate 2-sulfotransferase.* Genes Dev, 1998. **12**(12): p. 1894-906.

128. Li, J.P., et al., *Targeted disruption of a murine glucuronyl C5-epimerase gene results in heparan sulfate lacking L-iduronic acid and in neonatal lethality.* J Biol Chem, 2003. **278**(31): p. 28363-6.

129. Zhang, F., et al., *Compositional analysis of heparin/heparan sulfate interacting with fibroblast growth factor.fibroblast growth factor receptor complexes.* Biochemistry, 2009. **48**(35): p. 8379-86.

130. Buresh-Stiemke, R.A., et al., *Distinct expression patterns of Sulf1 and Hs6st1 spatially regulate heparan sulfate sulfation during prostate development.* Dev Dyn, 2012. **241**(12): p. 2005-13.

131. Abate-Shen, C. and M.M. Shen, *Mouse models of prostate carcinogenesis.* Trends Genet, 2002. **18**(5): p. S1-5.

132. Marker, P.C., et al., *Hormonal, cellular, and molecular control of prostatic development.* Dev Biol, 2003. **253**(2): p. 165-74.

133. Kraushaar, D.C., S. Dalton, and L. Wang, *Heparan sulfate: a key regulator of embryonic stem cell fate.* Biol Chem, 2013. **394**(6): p. 741-51.

134. Kreuger, J., et al., *Interactions between heparan sulfate and proteins: the concept of specificity.* J Cell Biol, 2006. **174**(3): p. 323-7.

Figures:

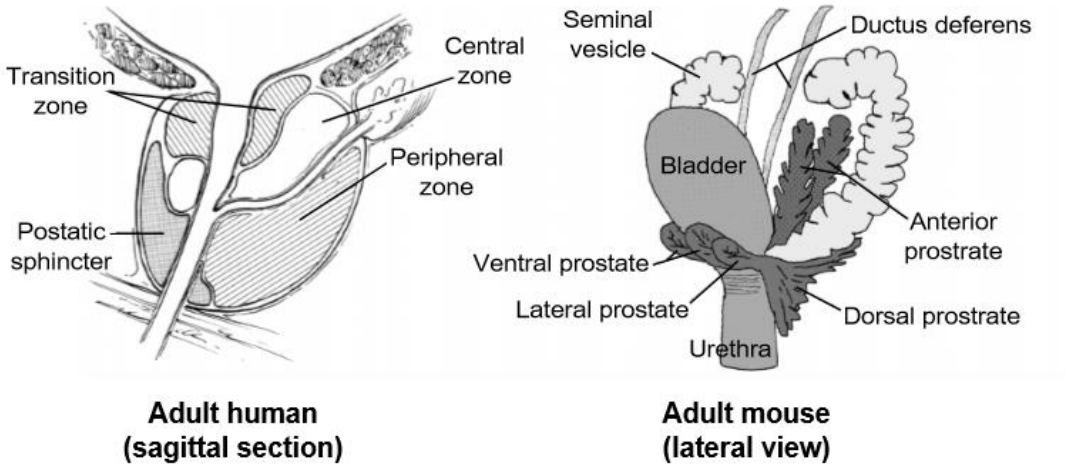

Figure 1.1 Schematic illustration of the anatomy of the human (A) and mouse (B) prostate. Human prostate is located under the bladder, connected to seminal vesicle and urethra. The mouse prostate location is similar to human with some morphology differences. It has several lobes; include coagulating gland (CG) or arterial prostate, ampullary glands, dorsal-lateral prostate and ventral prostate. Adapted from [131].

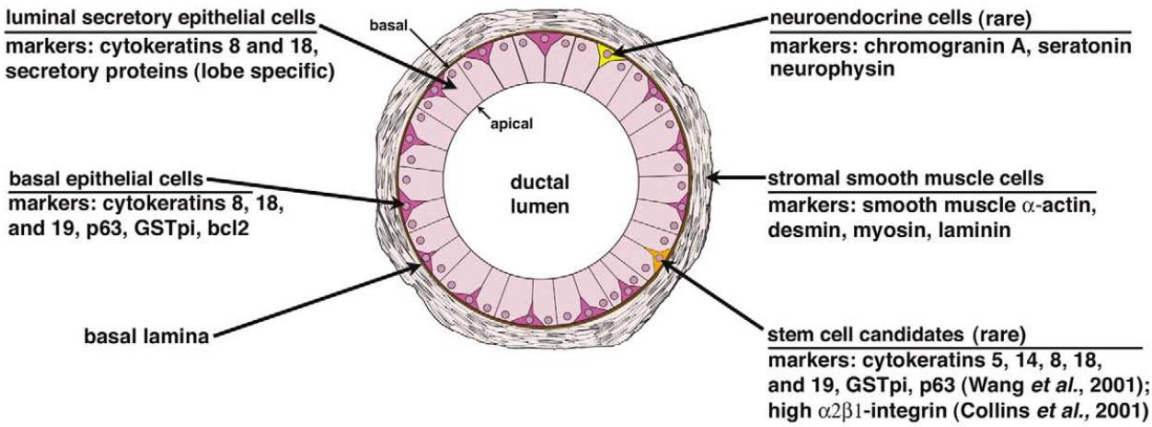

Figure 1.2 Schematic depiction of the prostatic epithelial cell types. Prostatic epithelium is mainly composed of basal and luminal cells along with a minor population of neuroendocrine cells. In normal prostate epithelium, a single layer of luminal cell and basal cells along with the basement membrane forms the wall of the prostate duct. Adapted from [132].

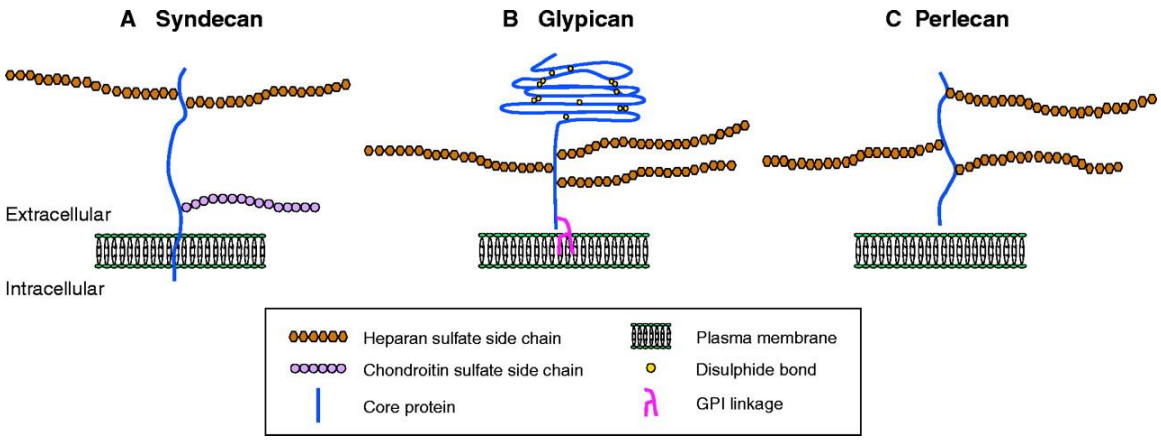

Figure 1.3. Types of heparan sulfate proteoglycans. Syndecans are transmembrane proteins. Glypicans are GPI-anchored proteins and perlecan is secreted into the extracellular space. Adapted from [102].

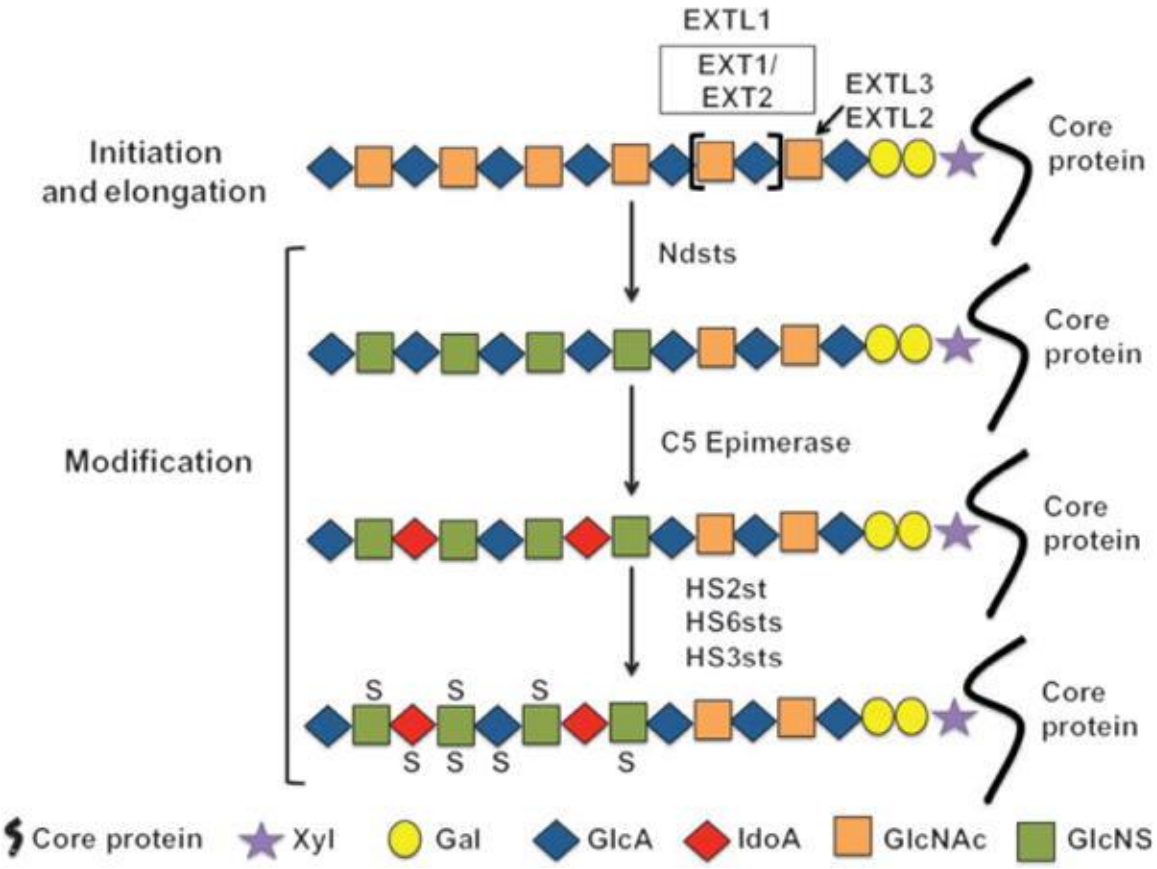

Figure 1.4. Heparan sulfate (HS) biosynthesis. In mammals, as many as 26 enzymes participate in the formation of HS chains. Important for HS backbone formation is the co-polymerase complex composed of EXT1 and EXT2 that have both GlcA-transferase and GlcNAc-transferase activity. Adapted from [133]

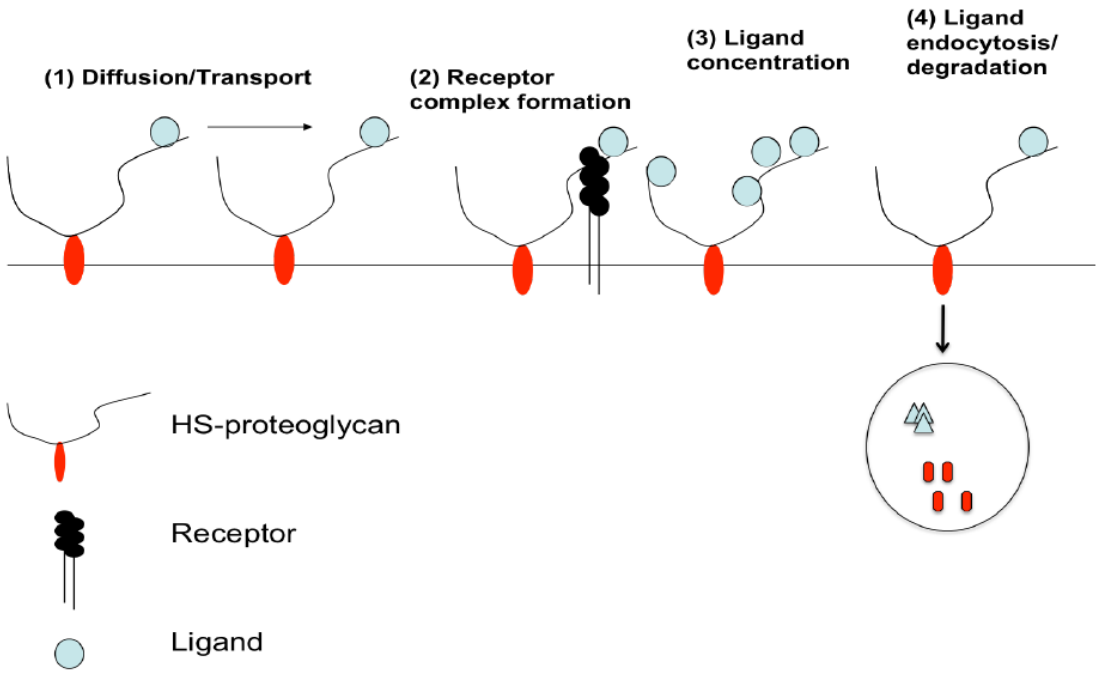

Figure 1.5. Proposed models for modulation of cell signaling by heparan sulfate. Morphogen gradient formed requires HS for cell-to-cell movement (1). HSPGs function as co-receptors for efficient signal transduction events (2). Ligand binding to HS chains enhances local ligand concentrations (3) or may facilitate ligand internalization (4). Modified from [134].

Tables:

Table 1.1. Glycosaminoglycans. Glycosaminoglycans are composed repeating disaccharide units of an uronic acid and hexosamine sugar. The backbone is sulfated except in the case of Hyaluronan.

Name	Uronic acid/ Hexose	Hexosamine	Linkage geometry
Heparan Sulfate	GlcA/ IdoA	GlcNAc	**-4**GlcUAβ**1-4**GlcNAcα**1-**
Chondroitin Sulfate	GalA	GalNAc	**-4**GlcUAβ**1-3**GalNAcβ**1-**
Dermatan Sulfate	GlcA/IdoA	GalNAc	**-4**IdoUAβ**1-3**GalNAcβ**1-**
Keratan Sulfate	Gal	GlcNAc	**-3**Galβ**1-4**GlcNAcβ**1-**
Hyaluronic Acid	GlcA	GlcNAc	**-4**GlcUAβ**1-3**GlcNAcβ**1-**

Table 1.2 Heparin/heparan sulfate-binding proteins (incomplete list)

Ligands	Heparan sulfate binding proteins
Growth factors	HB-EGFs (Heparin Binding Epidermal Growth Factors), FGFs (Fibroblast Growth Factors), VEGF (Vascular Endothelial Growth Factor), PDGF (Platelet-Derived Growth Factor), TGF-β (Transforming Growth Factor-β), HGF (Hepatocyte Growth Factor)
Extracellular matrix	Collagens, Fibronectin, Laminin, Tenascin, Thrombospondin I and II, Vitronectin
Morphogens	BMP 2, 4 and 7 (bone morphogenetic protein), Hh (Hedgehog) , Wnt (Wingless wg), Sprouty
Tissue remodeling factors	Tissue plasminogen activator; Plasminogen activator inhibitor; Protease nexin 1
Adhesion molecules and chemokines	L-selectin and P-selectin, N-CAM(Neural Cell Adhesion Molecule), PECAM-1(Platelet Endothelial Cell Adhesion Molecule) , MAC-1(Monocyte Adhesion Molecule) and chemokines, such as SDF-1
Anti-angiogenic factors	Angiostatin, Endostatin
Coagulation	Antithrombin III, Factor Xa, Thrombin
Lipid Metabolism	Lipoprotein lipase, Hepatic lipase, Phospholipase, ApoB, ApoE

Adapted from [93]

CHAPTER 2

HEPARAN SULFATE MITIGATES TRANSFORMING GROWTH FACTOR BETA (TGFβ) SIGNALING TO RETAIN PROSTATE STEM CELL STATE

Sumit Rai, Houjian Cai and Lianchun Wang. To be submitted to The Journal of Biological Chemistry.

Abstract

The prostate stem cells are responsible for prostate regeneration in adult, but the molecular mechanisms that control the cell status, including self-renewal and differentiation, are incompletely understood. In this study, we examined the functional role of heparan sulfate (HS) in regulating prostate stem cell maintenance and tissue regeneration. We show that ablation of prostate stem cell HS expression by inactivating *Ext1*, the gene essential for HS biosynthesis, diminished prostate sphere formation *in vitro*. Loss of HS expression reduced $p63^+$ stem cells and $CK5^+$ progenitor cells with an increase in differentiated $CK8^+$ cells and perturbed cell cycle. We further demonstrate that HS deficiency up-regulated TGFβ signaling. Treatment with TGFβ inhibitor or overexpression of dominant negative TGFβ receptor partially reversed the disrupted sphere formation activity in HS-deficient prostate stem cells. In the *in vivo* tissue recombination assay, while loss of HS in both urogenital sinus mesenchyme and epithelial cell compartments disrupted prostate tissue regeneration, which correlates with reduced p63+ stem cells, the retention of HS expression in either one of the compartments sustained normal prostate tissue regeneration. We conclude that HS mitigates TGFβ signaling to essentially sustain self-renewal of stem cells in adult prostate and functions both *in-cis* and *in-trans* to facilitate prostate regeneration.

Introduction:

The Prostate is a male accessory gland that contains two major epithelial cell types: secretory luminal cells which contribute to the bulk of seminal fluid and basal cells lining the basement membrane [1]. There also exists a small population of neuroendocrine cells within the basal cell layer regulating the activity of the two other epithelial lineages [2].

The adult prostate is capable of undergoing multiple cycles of atrophy following castration while re-administration of androgen results in regeneration of the gland. The prostate atrophy results from apoptosis of mostly luminal cells attesting to the presence of stem cells in the androgen-independent basal cell layer [3, 4]. Dye efflux studies [5, 6], as well as the presence of replication quiescent BrdU-label retaining cells [7], have further supported this claim. Recently, several studies have successfully isolated functional prostate stem cells (PrSCs) identified by their cell surface marker expression [8-12]. The molecular mechanisms and the regulatory networks required for the maintenance of their stem cell state, as well as external cues driving their differentiation, have been under intense investigation [13]. For example, transforming growth factor β (TGFβ) signaling induces rat prostate basal cells to differentiate into luminal cells [14] while TGFβ also maintains dormancy of PrSCs in the proximal region of prostate ducts [15], highlighting the spatiotemporal regulation of TGFβ signaling on PrSC functional status.

Heparan sulfate (HS) is a linear anionic polysaccharide expressed ubiquitously on the cell surface and in the extracellular matrix where it is covalently linked to core proteins to form heparan sulfate proteoglycans (HSPGs). The biosynthesis of HS chains begins in the Golgi through the sequential activity of various glycosyltransferases [16, 17]. A heterodimer of two glycosyltransferases, composed of Exostosin 1 (*Ext1*) and Exostosin 2 (*Ext2*), initiates HS biosynthesis by polymerizing the chain backbone by the alternate addition of N-acetyl glucosamine (GlcNAc) and D-glucuronic (GlcA) residues. As the chain is being elongated, a number of glycosyltransferases sequentially modify the chain resulting in N-deacetylation, N-sulfation of GlcNAc and epimerization of GlcA to iduronic acid followed by addition of 2-O, 6-O and 3-O sulfation modifications.

However, the modification reactions are incomplete, resulting in a highly heterogeneous structure. The synthesized HS chains can be further amenable to post-synthetic modification by 6-O-sulfatases (Sulf) at the cell surface by removing the 6-O sulfates of GlcNAc residues. The biosynthetic modifications and the post-synthetic remodeling work together to generate unique ligand-binding sites for various protein ligands including growth factors and morphogens, such as fibroblast growth factor (FGF), Wnt, Hedgehog (Hh), TGF and bone morphogenetic protein (BMP) which are known to critically modulate organ development [18-22]. Intriguingly, HS structure has been shown to be tissue, cell-type and developmental stage-specific, highlighting that HS may play cell-specific and a spatiotemporal regulatory functions [23].

In previous studies we and others discovered that HS regulates self-renewal and differentiation of mouse embryonic stem cells via facilitation of FGF and/or BMP signaling [24-32]. HS has also been found to modulate adult stem cells function in different tissues [31-36]. Interestingly, a recent study characterized the expression patterns of HS biosynthetic enzymes in the developing mouse prostate by *in situ* hybridization and observed the *heparan sulfate 6-O-sulfotransferase-1* (*HS6st1*), the enzyme that adds 6-O-sulfation modification during HS biosynthesis, is uniquely expressed at the tip of elongating epithelial buds where PrSCs are enriched [37]. This led us to hypothesize that HS critically modulates PrSC functions. To test this idea, we inactivated HS biosynthetic gene *Ext1* expression in mouse PrSCs and examined its consequence on PrSC functions. We observed that the *Ext1* inactivation inhibits self-renewal, differentiation and proliferation of PrSCs in the *in vitro* sphere formation. These defects correlate with enhanced TGFβ signaling and the self-renewal defect was rescued

by TGFβ signaling inhibition, including both through specific TGFβ signaling inhibitor treatment and overexpression of dominant negative TGFβRII. These observations suggest that HS attenuates TGFβ signaling to maintain PrSC self-renewal. In the *in vivo* prostate regeneration assay, while loss of HS in both urogenital sinus mesenchyme and epithelial cell compartment inhibited prostate tissue regeneration, the retention of HS in either compartment sustained prostate tissue regeneration potential. We conclude that HS mitigates TGFβ signaling to essentially sustain self-renewal of stem cells in adult prostate and functions to facilitate prostate regeneration.

Results

Loss of HS expression diminishes self-renewal activity in adult PrSCs - Stem cells from adult prostate, like mammary gland and brain, can be propagated as spheres [38, 39]. These prostate spheres clonally arise from the PrSCs located in the epithelial compartment when cultured within Matrigel [12]. As this assay allows for long-term serial passaging of spheres, it presents a reliable tool to assess self-renewal potential of PrSCs. To determine the role of HS in PrSC self-renewal, single prostate epithelial cell (PrEC) suspension from *Ext1*$^{f/f}$ mice was infected with lentivirus encoding Cre-recombinase or lentivector backbone (mock-) and grown in matrigel to form spheres (Fig. 2.1A). As expected, *Ext1* expression was lost from spheres formed by cells which had undergone Cre-mediated recombination as manifested by the appearance of the mutant *Ext1* allele (*Ext1*$^{-/-}$) in genomic DNA PCR analysis (Fig. 2.1B) and by loss of HS expression indicated by diminished cell surface anti-HS antibody 10E4 staining (Fig. 2.1C). Interestingly, after 8-10 days in culture, cells which were mock infected or infected with Cre expressing lentvirus, formed spheres with comparable efficiency, and

the size of the *Ext1*-deficient (*Ext1*$^{-/-}$) spheres appeared to be smaller, but the difference did not reach a statistical significance (Fig. 2.1D). However, when single cells dissociated from primary spheres (1° spheres) were assessed for their secondary sphere (2° sphere) forming capacity, the *Ext1*$^{-/-}$ cells were unable to form spheres. The PrECs from the primary *Ext1*$^{-/-}$ spheres formed dramatically reduced number of 2° spheres and most remained as single cells, compared to mock-infected primary spheres which retained a high sphere formation activity (Fig. 2.1E). This observation illustrate that HS is essentially required for PrSCs to maintain their self-renewal activity.

HS functions in trans to sustain HS-deficient PrSCs to from primary spheres – HS can function both *in cis* and *in trans* to modulate cell functions [40, 41]. In our sphere assay, the primary spheres, mock- or Cre infected, did not display a significant difference in number or size, raising a possibility that the Cre-infected sphere may represent a chimera composed of both HS-deficient and HS-expressing cells, the latter may function to sustain HS-deficient PrSCs to form sphere in the primary sphere assay. To vigorously assess this possibility, we employed a *Rosa26*$^{mt/mG}$ reporter strain that exhibits a switch from membrane-bound tdTomato to membrane-bound EGFP in the presence of Cre-recombinase [42] (Fig. 2.2A). PrECs isolated from *Rosa26*$^{mT/mG}$*Ext1*$^{f/f}$ mice were infected with Cre expressing lentivirus and cultured in Matrigel to form primary spheres. Interestingly, Cre-mediated loss of tdTomato with the consequent expression of EGFP was non-uniform and the majority of Cre expressing prostate spheres retained tdTomato expression, indicating that majority of the primary spheres formed are HS-deficient and HS-expressing cell chimeras (Fig. 2.2B, 2.2C). Interestingly, a decrease in sphere size was observed in the few spheres exhibiting complete loss of Tdtomato fluorescence (Fig.

2.2D). Furthermore, infected PrECs were sorted at the onset of fluorescence expression, around day 4, of primary sphere formation and used for 2° sphere formation. The mock-infected PrECs formed abundant spheres, whereas no sphere was formed from the Cre-infected PrECs (data not shown). Taken together, these observations strongly suggest that loss of the obvious phenotype in HS-deficient primary spheres is due to the absence of global Cre expression within the sphere and support that HS expressed by the non-Cre-infected neighbor cells functions *in trans* to sustain *Ext1*$^{-/-}$ primary sphere formation of *Ext1*$^{-/-}$ PrSCs.

Loss of HS expression diminishes p63^{+} *stem cells and disturbs PrSC differentiation* - Prostate spheres are primarily formed from p63^{+} stem cells of the basal cell compartment [43]. To determine if the diminished sphere formation capacity of the HS depleted PrSCs was due to loss of p63^{+} cell population, qPCR analysis was performed on cells 16-18 h after initiation of the 2° sphere formation (Fig. 2.3A). A reduction in *p63* levels was observed, indicating that HS deficiency indeed reduces p63^{+} stem cells leading to diminished self-renewal activity in the *Ext1*$^{-/-}$ PrSCs (Fig. 2.3A). The qPCR analysis also detected a reduction in the basal/progenitor marker CK5 expression along with increased expression of luminal cell specific marker CK8 in the *Ext1*$^{-/-}$ PrECs (Fig. 2.3B). These observations indicate that loss of HS expression also promotes the CK5^{+} basal/progenitor cells to differentiate into mature CK8^{+} luminal cells and reveal that loss of HS expression also disturbs PrSC differentiation during sphere formation.

The above transcript analysis examined infected PrECs only 16-18 h after the initiation of 2° sphere assay, suggesting that the altered expressions of p63, CK5 and CK8 might already exist at the end stage of primary sphere assay. Meanwhile, we also noticed that

the size of the Cre-infected primary spheres were slightly smaller, suggesting that effects of HS deficiency on PrSC functions might be just emerging towards the later stages of primary formation assay and could be detected microscopically (Fig. 2.1D). To test this idea, we stained the sphere sections for $p63^+$, $CK5^+$ or $CK8^+$ cells. In the mock-infected primary spheres, the $p63^+$ cells were abundant and presented only in the outer layers, whereas the other cells showed a uniform expression of CK5 with minimal CK8 staining (Fig. 2.3C). In contrast, in the Cre-infected primary spheres, the $p63^+$ cells remained to present in the outer layers, but the numbers were dramatically reduced, accompanied with reduced $CK5^+$ cells and increased $CK8^+$ cells (Fig. 2.3C). The reduction of $p63^+$ cells was further confirmed in Western blot analysis (Fig. 2.3C). These marker gene transcript and protein expression analyses indicate that loss of HS reduces $p63^+$ expression and promotes CK5 progenitor cells differentiation into mature $CK8^+$ cells, leading to $p63^+$ stem cell exhaustion and the subsequent loss of self-renewal activity.

Loss of HS impairs cell cycle progression - HS is known to interact with many growth factors and cytokines mediating cell growth and proliferation [44]. To assess if the loss of secondary sphere formation is also attributed to impaired cell cycle progression, we performed cell cycle analysis on HS-deficient PrECs sorted from primary spheres and were cultured for 12-16hrs in the second sphere assay. Cell cycle analysis revealed significantly lower number of HS-deficient cells were in proliferating G2-M phases (Fig. 2.4A, 9% in HS-deficient cells vs 30% in wildtype control). We further determined the expression profile of cell cycle regulators including cyclins, cyclin-dependent kinase (CDKs) and cyclin-dependent kinase inhibitors (CKIs) in the cells. HS-deficient cells showed significantly decreased expressions of CDK4 and of Cyclins A2, B1, and D1

accompanied with upregulated expression of p21, a cyclin-dependent kinase inhibitor, known to potently inhibit cell cycle progression (Fig. 2.4B-D), all supporting a cell proliferation arrest in the HS-deficient cells. This data strongly suggest that loss of HS attenuates signals mediating proliferation of PrECs. We also assessed if loss of HS induces apoptosis attributing to the diminished sphere formation of the HS-deficient PrECs by measuring the expressions of Bcl2, Bax and Caspase 3. These surveyed genes did not show altered expression (Fig. 2.4E), excluding the possibility of increased apoptosis during sphere formation.

Attenuating TGFβ signaling in HS-deficient PrSCs rescues sphere formation – The homeostasis of PrSCs in adult prostate is the net outcome of a variety of signaling networks including growth factors, morghogens and adhesion molecules [45, 46]. Among these signaling networks, TGFβ signaling is the crucial overall regulator and functions to maintain dormancy of PrSCs in adult prostate [14, 15]. HS is known to regulate TGFβ signaling in various cell types including epithelial cells [47, 48]. We therefore asked if HS regulates TGFβ signaling to sustain self-renewal activity of PrSCs. We profiled the expression of TGFβ receptors and ligands, and found that TGFβR2 and TGFβ2 expression were significantly increased in the HS-deficient cells (Fig. 2.5A-C). In contrast, the HS-deficient PrECs showed reduced expression of TGFβRIII (betaglycan) that is known to be transcriptionally repressed by TGFβ signals [49]. The expression of a number of TGFβ responsive genes involved in inhibiting epithelial cell growth was also observed including increased expressions of the transcription factors 4E-BP1 and ZFP36L1 and down-regulated expression of E2F1. Similarly, the expressions of TGFβ target genes were altered too. We observed that the expressions of the inhibitor of

differentiation (Id) family of proteins (Id1 and Id3) were reduced in the HS-deficient PrECs. The altered expressions of aforementioned transcription factors and the target genes suggest that loss of HS expression up-regulates TGFβ signal in the mutant PrECs. To determine if the up-regulated TGFβ signals results in diminished self-renewal activity of the HS-deficient PrSCs, TGFβ signaling was blocked in the second sphere formation assay by adding SB-431542, a specific TGFβRI inhibitor, in the culture medium. SB-431542 treatment increased sphere formation of HS-deficient PrSCs both in number and size, showing a significant rescuing effect (Fig. 2.5D). To alternatively confirm this finding, dominant negative TGFBR2 (TGFBR2-DN) was lentivirally introduced to overexpress in the *Ext1*$^{-/-}$ PrECs. Genetic inhibition of the TGFβ signals by TGFBR2-DN overexpression similarly increase sphere formation of the *Ext1*$^{-/-}$ PrECs (Fig. 2.5E, F). In together, our observations from different aspects support that loss of HS enhances TGFβ signals to diminish sphere formation, and we conclude that HS mitigates TGFβ signals to essentially sustain self-renewal activity of PrSCs.

HS functions in both in cis and in trans to retain PrSC homeostasis and to sustain efficient prostate regeneration in vivo - The development of prostate gland is a highly orchestrated process requiring intimate regulatory crosstalk between the epithelial and the stromal compartment. The urogenital sinus mesenchyme (UGSM) is well documented to exert supportive as well as inductive signals in the formation of the prostate gland [50]. In the *in vivo* regeneration assay, UGSM cells instruct PrSCs present in the adult prostate to form regenerated prostate tissue [51]. We asked if HS expressed in UGSM or PrSC compartment is required for PrSC-driving prostate regeneration. To address this question, tissue recombination experiments were carried out wherein HS was depleted from either

PrEC or UGSM compartment or both. At the end of the eight-week period, regenerated prostate grafts were harvested, weighed and histologically analyzed (Fig. 2.6A-C). In the wild type experimental setting the regeneration, as expected, was efficient, whereas in the setting where HS is deficient in both PrEC and UGSM compartments, the formed grafts were smaller in size and showed very a few prostate tubular structure, correlating to lower p63+ stem cell activity, demonstrating that the loss of HS expression dramatically disrupted prostate regeneration and PrSC homeostasis (Fig. 2.8). In the experimental settings where deficiency of HS is only in one compartment, either in PrSCs or UGSM, the formed grafts showed size and tubular structure comparable to the wildtype grafts, revealing that HS expressed by PrECs and UGSMs functions *in cis* and or *in trans,* respectively, to sustain prostate regeneration and PrSC homeostasis *in vivo*.

Discussion

The role of HS in regulation of embryonic stem cell fate has been extensively investigated [24-27, 29, 52]. Recent studies, however, have expanded to examine the roles of HS in adult stem cell status. Convincing evidence demonstrate that HS is essential for self-renewal or homeostasis of stem cells in skeletal muscle, epidermis, neural tissue, bone marrow, salivary gland, testis and intestine [53] [54], [31, 32, 34, 55-57]. In our current study, we provide *in vitro* and *in vivo* evidence demonstrating that HS is a crucial regulator of self-renewal of stem cells in prostate gland and is required to fulfill PrSCs capacity to regenerate prostate tissue.

The prostate develops from the urogenital sinus during later embryonic development. Paracrine interactions between UGSM and the urogenital sinus epithelium are required for proper prostate development. Strikingly, several paracrine growth factors that

essentially regulate prostate development bind HS including FGF10, BMP4 and BMP7. FGF10 is expressed in UGSM and located adjacent to the epithelial bud-forming region. FGF10 promotes epithelial cell proliferation and bud outgrowth by binding to FGF receptor (FGFR)-2-IIIb expressed in urogenital sinus epithelium [58]. FGF10-null urogenital sinus fails to develop into prostates [59] and conditional loss of FGFR and the FGFR2 substrate-2α in the developing prostates impairs branching morphogenesis [60, 61] . These observations illustrate that the paracrine FGF10 signaling promotes growth and /or branching morphogenesis. BMP4 and BMP7 are expressed at the peri-epithelial mesenchyme and adjacent to the most proximal portion of the prostatic buds of developing prostate [62-64]. Exogenous BMP4 and BMP7 both impaired urogenital sinus bud development in culture and the knockout mice containing null alleles for either *BMP4* or *BMP7* each show increased prostatic branching [64, 65]. These observations show that the paracrine BMP4 and BMP7 signaling inhibits epithelial cell growth and branching during prostate development. Interestingly, a recent study reported the exogenous BMP4 and BMP7 induces *Sulf1* expression in the UGMS in *in vitro* organ culture, decreases epithelial HS 6-O-sulfaiton, and reduces intracellular signaling of urogenital sinus epithelium in response to FGF10 stimulation, revealing a pivotal role of HS in regulating cross-talk of BMP and FGF10 signaling in the developing prostate [66]. Our current study uncovered that HS mitigates TGFβ signaling to essentially sustain self-renewal activity of PrSCs. Paracrine TGFβ signaling has been shown to be required for UGSM to induce endoderm-derived epithelia and stem cells to from prostate [67], therefore our results reveal that HS regulates TGFβ signaling to facilitate prostate development too. However, in our study, inhibition of TGFβ signaling by SB-431542 or

overexpression of TGFBR2-DN both only partially rescue the self-renewal activity of the HS-deficient PrSCs, suggesting that other HS-dependent pathway signaling are required to acquire full self-renewal activity. Recent study showed that FGFR2 signaling preserves stemness and prevents differentiation of PrSCs from the basal compartment [68], raising a high possibility the loss of HS also impairs the FGFR2 signaling leading to loss of stemness and differentiation of the PrSCs attributing to our observed self-renewal defect phenotype of the HS-deficint PrSCs. This interesting aspect will be explored in our further studies.

An early study examined androgen dependence of HS biosynthesis in the prostate following castration and subsequent androgen-treatment-induced regeneration [69]. HS content was significantly decreased following castration and increased after androgen replacement treatment, highlighting that HS may be critically required for androgen-primed prostate regeneration. In our tissue recombination experiment, we provide the first evidence demonstrating that HS indeed is essential for proper prostate regeneration. We investigated further and delineated that HS mitigates TGFβ signaling to sustain self-renewal activity. It would be very interesting to ablate HS expression in prostate epithelium in adult mice and test if epithelial HS is required in prostate regeneration and if this regulation depends on HS-TGFβ signaling axis. In addition, reported studies highlighted the critical importance 6-O-sulfation of HS in prostate development [66, 70] and in modulation of TGFβ signaling to main glomerular integrity [71, 72]. Therefore, it would be interesting to determine if the HS-dependent PrSC self-renewal and androgen-induced prostate regeneration also require specific HS structure, such as highly 6-O-sulfated HS motifs, *in vivo*.

HS has been known to positively or negatively modulate TGFβ signaling in various cellular or tissue contexts via different modes of action. For example, in mouse periocular mesenchyme HS deficiency specifically inhibits TGFβ2 signaling manifested by diminished phosphorylation of Smad2 [73]. While examination of CHO cells, TGFβ1 induces transcriptional activation of plasminogen activator inhibitor-1 and growth inhibition more potently in CHO cell mutants deficient in HS (CHO-677 cells) than in wildtype CHO-K1 cells, showing that HS inhibits TGFβ1 signaling [74]. Currently, three modes of action for HS to modulate TGFβ signaling have been proposed. In the first mode of action, HS modulates the diffusion and the gradient of TGFβ within the local environment. As a good example, the *Drosophila* TGFβ homolog, Dpp, moves along the cell surface via HS to restrict extracellular diffusion to maintain proper TGFβ signaling [75]. In the second mode of action, HS functions as a co-receptor to facilitate the interaction between TGFβ and the receptors on cell surface. The prototype of this co-receptor mode was established from studies of the function of HS in FGF signaling. HS has been shown to interact simultaneously with FGF2 and FGFR to form a 2:2:1 functional complex to be essential for FGFR signaling activation [76]. In the third mode of action, cell surface HS decreases the ratio of TGFβ binding to TGFβR-II and TGFβR-I, facilitating caveolae/lipid-raft-mediated endocytosis and rapid degradation of TGFβ1 to attenuated TGFβ1 signaling [74]. Among these three modes of action, the first two modes act to enhance, but the third mode to inhibit TGFβ signaling. In current study, we observed that PrECs express both TGFβR-II and TGFβR-I, and HS mitigates TGFβ signaling to sustain self-renewal activity of PrSCs, indicating HS acts in the third mode to regulate PrSC function status. It would be very interesting to determine if HS deficiency

alters the binding ratio of TGFβ1/2 to TGFβR-II and TGFβR-I to confirm this proposition.

We also observed loss of HS reduces $CK5^+$ progenitor cells accompanied with increase in terminally differentiated $CK8^+$ luminal cells, revealing that HS regulates prostate progenitor cell differentiation too. Our current study has not investigated further to delineate the underlying molecular mechanism. TGFβ is known to promote differentiation of PrSCs towards luminal cell fate [14, 15]. Danielpour showed that in the absence of growth factors rat prostate epithelial cell line, NRP-152, undergoes luminal differentiation [14]. This differentiation involves an increase in the levels of TGFβ2, TGFβ3, and TGFβR2, which mirrors the altered expression of TGFβs and TGFβRs in our HS-deficient PrECs, suggesting that HS may regulate TGFβ signaling to modulate differentiation of $CK5^+$ cells to $CK8^+$ cells too.

Recent studies have revealed that, except for *in cis* function, HS expressed in adjacent cells may function *in trans* to sustain HS-dependent signaling in HS-deficient cells [40, 41]. In our *in vitro* sphere formation and the *in vivo* tissue recombinant prostate regeneration experiments, we provide clear evidence showing that HS functions both *in cis* and *in trans* to sustain self-renewal activity of PrSCs and prostate regeneration. The *in trans* function of HS-expressing cells has helped to interpret the relative normal primary sphere formation efficiency of Cre-infected PrECs. It is possible that the loss of HS biosynthesis as well as degradation of secreted HSPGs exhibit a time lag from the time Cre is expressed, about 3-4 days after lentiviral infection, and thus can support the growth of these “HS-deficient” spheres. This may represent another major reason to explain why the HS deficient PrSCs completely lost self-renewal activity in the secondary, but not

during the primary sphere formation. This potential explanation has also been strongly supported by our additional finding that the Cre-expressing PrECs from day 4 primary spheres could not form any secondary sphere.

In conclusion, our current studies reveal that HS is a crucial regulator of self-renewal and homeostasis of PrSCs. Our molecular dissection studies determine that the regulatory function of HS on PrSCs is partially mediated by mitigation of TGFβ signaling pathway activity. We also showed that HS is essential for prostate regeneration. These findings lay a solid foundation for further studies to understand any other HS-dependent signaling that critically regulates PrSC functions as well as any specific HS functional motifs are needed.

Materials and Methods

Mice - All animals received humane care in compliance with the protocol approved by the Institutional Animal Care and Use Committee (IACUC) of the University of Georgia. The conditional *Ext1* mice (*Ext1*$^{f/f}$) were kindly provided by Dr. Yu Yamaguchi (Sanford Burnham Prebys Medical Discovery Institute, La Jolla, CA, USA) [77]. *PB-Cre4* mice [78] (official strain nomenclature: *Tg(Pbsn-cre)4Prb*) were obtained from the NCI-Frederick mouse repository while the Rosa26$^{mT/mG}$ double fluorescence reporter mice[42] (official strain nomenclature: *Gt(ROSA)26Sor*$^{tm4(ACTB-tdTomato,-EGFP)Luo}$/J) were obtained from the Jackson Laboratory (Bar Harbor, ME). *Ext1*$^{f/f}$ female mice were crossed with *Pb-Cre4* and *Rosa26*$^{mT/mG}$ male mice to generate *Pb-Cre4 Ext1*$^{f/f}$ and *Rosa26*$^{mT/mG}$ *Ext1*$^{f/f}$ mice. Mice were genotyped by PCR using mouse genomic DNA from tail biopsy specimens. The sequences of genotyping primers and the expected PCR product sizes are listed in Supplementary Table 1. PCR products were separated on 2% agarose gels and

visualized via ethidium bromide under UV light. The C57BL/6 and CB.17SCID/SCID (SCID) mice were obtained from Charles River (Wilmington, MA).

Lentivirus generation and infection - Codon-optimized Cre recombinase (iCre) was cloned using the *XbaI* site of an FU-CRW vector or FU-CGW [79], generating the FU-Cre-CRW and FU-Cre-CGW vector. In this vector, iCre is driven by a human *Ubiquitin* promoter and is followed by a CMV promoter driving the expression of a monomeric red fluorescent protein (RFP) or enhanced green fluorescent protein (EGFP), respectively. pCMV5 HA-TBRII (delta Cyt) was a gift from Dr. Joan Massague (Memorial Sloan Kettering Cancer Center, Addgene plasmid # 14051) [80]. The encoded gene was PCR amplified (primers listed in Supplementary Table 2), verified by sequencing and cloned into the FU-CRW lentiviral vector using the EcoRI and XbaI sites. Lentivirus production and titration were performed as described previously [81]. Dissociated prostate cells were infected with the lentivirus using the spinoculation method at 750g for 120 min at 25 °C [51]. All procedures followed the safety guidelines and regulations of The University of Georgia.

Prostate sphere and regeneration assay - 4- to 8-week old male mice were killed by carbon dioxide inhalation. Prostates were dissected, minced into small pieces with a steel blade, and digested with collagenase I (GIBCO, 190 units/ml) in 10 ml of DMEM 10% FBS (GIBCO) at 37°C for 90 min. PrECs were pelleted, washed once with Ca^{2+} and Mg^{2+} PBS and trypsinized with 0.05% Trypsin/EDTA for 5 min at 37°C. Trypsin is inactivated by addition of equal volume of media containing 10% FBS. The cells were then passed 4-5 times through 21G needle followed by $25^{1/2}$ G needle and 40 μm nylon mesh (BD Biosciences, San Jose, CA) to obtain a single cell suspension. Cells were

washed twice with DMEM 10% FBS, resuspended in 1 ml of DMEM 10% FBS, and counted. Cells are infected with required lentiviruses at a multiplicity of infection of 10-20. The infected cells were collected, washed and finally resuspended in 50 µL prostate epithelial growth medium (PrEGM) (#CC-3166, Lonza, Walkersville, MD). 50 µl of cell suspension were mixed with 50 µL of Matrigel (#356234, Corning) and plated around the rims of the wells in a 12-well cell culture plate. After the cell-Matrigel mixture solidified at 37 °C for 45 min, 1 mL of PrEGM was added. Cells were cultured for 8-10 days to allow viral integration and Cre-RFP/EGFP expression. Prostate spheres were defined as spheroids with a diameter ≥ 40 µm after eight days of culture. After the RFP/EGFP expression was confirmed, dispase, to a final conc. of 1mg/ml, was added to digest the matrigel matrix and harvest the spheres. Spheres were collected by passing through a 40 µm nylon mesh to remove single cells while the spheres were retained. Spheres were trypsinized for 10 min at RT with 0.05% Trypsin-EDTA. Digested cells were passed through a $27^{1/2}$ G needle thrice and filtered by a 40 µm cell strainer. Cells were then resuspended in an appropriate volume of PrEGM medium, counted, mixed with Matrigel and cultured for 8-10 days as mentioned above to form secondary spheres. In some cases, dissociated primary sphere cells were sorted based on fluorescence before seeding them in culture for secondary sphere formation.

In the prostate regeneration assay, mock- or iCre infected PrECs ($1x10^5$ cells/graft) were combined with mock- or iCre-infected UGSM ($1x10^5$ cells/graft) together with 20 µL of collagen type I (neutral pH, #354236, Corning). After overnight incubation, grafts were implanted under the kidney capsule in SCID mice by survival surgery with a subcutaneous testosterone pellet (12.5 mg of androgen per pellet, 90-day release;

Innovative Research of America). All animals were maintained and used according to the surgical and experimental procedures approved by the IACUC of the University of Georgia.

Manipulation of signaling pathways - SB431542 was purchased from LC Laboratories (Woburn, MA), dissolved in DMSO and added at concentrations reported in literature in our second sphere formation assay [45]. The cell culture media was replaced every 48 hrs.

RNA isolation and qRT–PCR analysis - Total RNA was isolated from cells using the RNeasy Plus Mini kit (Qiagen, Valencia, CA). Reverse transcription was performed using the high capacity cDNA reverse transcription kit (Thermo –Fischer Scientific). qRT–PCR was performed using the PerfeCTa SYBR Green FastMix (Quanta Bio, Beverly, MA) on an ABI Step one plus real-time PCR system (Applied Biosystems, Foster City, CA). Primer sequences for qPCR are listed in Supplementary Table 3.

Western Blotting - Prostate spheres were passed through a 40 µm nylon mesh and spheres lysed in RIPA buffer (20 mM Tris-HCl, pH 7.5, 150 mM NaCl, 1 mM Na_2EDTA, 1 mM EGTA, 1% NP-40, 1% sodium deoxycholate, 2.5 mM sodium pyrophosphate, 1 mM β-glycerophosphate and 1 mM Na_3VO_4) with protease inhibitors (Roche Applied Science) and phosphatase inhibitors 2 and 3 (Sigma). Protein concentrations were determined using a Bradford Assay kit (Bio-Rad). Protein was separated in 10% SDS/PAGE and transferred onto a 0.2 µm Nitrocellulose membrane (Amersham Biosciences, Arlington Heights, IL). The membrane was blocked with 5% skim milk, and subsequently incubated with primary antibodies listed in Supplementary Table 4 at 4 °C O/N followed by incubation with peroxidase-conjugated goat anti-mouse IgG or goat anti-rabbit IgG

(CST, Danvers, MA), and developed with Amersham ECL reagent (GE Healthcare Ltd., Buckinghamshire, UK).

FACS - FACS analyses and sorting of RFP/EGFPexpressing cells were performed by using the Bio-Rad S3 cell sorter (Bio-rad, Hercules, CA) (Fig. 2.7). For cell cycle analysis, dissociated primary sphere cells were seeded in matrigel for 16-20hrs. They were harvested, dissociated to single cells and stained with Hoechst 33342 ready flow reagent (Thermo Fischer Scientific) for 1hr at 37°C and analyzed on HyperCyAn analyzer (Beckman Coulter, Indianapolis, IN). The cell cycle data was analyzed using the ModFit software (Verity software house)

Histology and immunostaining - H&E staining and immunofluorescence staining were performed using standard protocols on 5-μm paraffin sections. Primary antibodies and dilutions used are listed in the Supplementary Table 4. Slides were blocked with 3% BSA (Gold Bio, St. Louis, MO) and incubated with primary antibodies diluted in 3% BSA overnight at 4 °C. Slides were washed with and incubated with secondary antibodies (diluted 1:500 in 0.05% Tween 20 in phosphate-buffered saline (PBST)) labeled with Alexa Fluor 488 or 594 (Invitrogen/Molecular Probes). Sections were counterstained with 4',6-diamidino-2-phenylindole (DAPI) (Sigma-Aldrich). Immunofluorescence staining was imaged using a Carl Zeiss Axio Observer A1 fluorescence microscope or a Nikon A1 confocal microscope (10X, 20X and 40X objectives).

References

1. Wang, Y., et al., *Cell differentiation lineage in the prostate.* Differentiation, 2001. **68**(4-5): p. 270-9.
2. Aumuller, G., et al., *Semiquantitative morphology of human prostatic development and regional distribution of prostatic neuroendocrine cells.* Prostate, 2001. **46**(2): p. 108-15.
3. Kyprianou, N. and J.T. Isaacs, *Activation of programmed cell death in the rat ventral prostate after castration.* Endocrinology, 1988. **122**(2): p. 552-62.
4. English, H.F., R.J. Santen, and J.T. Isaacs, *Response of glandular versus basal rat ventral prostatic epithelial cells to androgen withdrawal and replacement.* Prostate, 1987. **11**(3): p. 229-42.
5. Bhatt, R.I., et al., *Novel method for the isolation and characterisation of the putative prostatic stem cell.* Cytometry A, 2003. **54**(2): p. 89-99.
6. Sabnis, N.G., et al., *The Efflux Transporter ABCG2 Maintains Prostate Stem Cells.* Mol Cancer Res, 2017. **15**(2): p. 128-140.
7. Tsujimura, A., et al., *Proximal location of mouse prostate epithelial stem cells: a model of prostatic homeostasis.* J Cell Biol, 2002. **157**(7): p. 1257-65.
8. Goldstein, A.S., et al., *Trop2 identifies a subpopulation of murine and human prostate basal cells with stem cell characteristics.* Proc Natl Acad Sci U S A, 2008. **105**(52): p. 20882-7.
9. Jiao, J., et al., *Identification of CD166 as a surface marker for enriching prostate stem/progenitor and cancer initiating cells.* PLoS One, 2012. **7**(8): p. e42564.

10. Xin, L., D.A. Lawson, and O.N. Witte, *The Sca-1 cell surface marker enriches for a prostate-regenerating cell subpopulation that can initiate prostate tumorigenesis.* Proc Natl Acad Sci U S A, 2005. **102**(19): p. 6942-7.

11. Lawson, D.A., et al., *Isolation and functional characterization of murine prostate stem cells.* Proc Natl Acad Sci U S A, 2007. **104**(1): p. 181-6.

12. Xin, L., et al., *Self-renewal and multilineage differentiation in vitro from murine prostate stem cells.* Stem Cells, 2007. **25**(11): p. 2760-9.

13. Strand, D.W. and A.S. Goldstein, *The many ways to make a luminal cell and a prostate cancer cell.* Endocr Relat Cancer, 2015. **22**(6): p. T187-97.

14. Danielpour, D., *Transdifferentiation of NRP-152 rat prostatic basal epithelial cells toward a luminal phenotype: regulation by glucocorticoid, insulin-like growth factor-I and transforming growth factor-beta.* J Cell Sci, 1999. **112 (Pt 2)**: p. 169-79.

15. Salm, S.N., et al., *TGF-{beta} maintains dormancy of prostatic stem cells in the proximal region of ducts.* J Cell Biol, 2005. **170**(1): p. 81-90.

16. Bernfield, M., et al., *Functions of cell surface heparan sulfate proteoglycans.* Annu Rev Biochem, 1999. **68**: p. 729-77.

17. Esko, J.D. and S.B. Selleck, *Order out of chaos: assembly of ligand binding sites in heparan sulfate.* Annu Rev Biochem, 2002. **71**: p. 435-71.

18. Ornitz, D.M., *FGFs, heparan sulfate and FGFRs: complex interactions essential for development.* Bioessays, 2000. **22**(2): p. 108-12.

19. Baeg, G.H., et al., *Heparan sulfate proteoglycans are critical for the organization of the extracellular distribution of Wingless.* Development, 2001. **128**(1): p. 87-94.

20. Ortmann, C., et al., *Sonic hedgehog processing and release are regulated by glypican heparan sulfate proteoglycans.* J Cell Sci, 2015. **128**(12): p. 2374-85.

21. Lyon, M., G. Rushton, and J.T. Gallagher, *The interaction of the transforming growth factor-betas with heparin/heparan sulfate is isoform-specific.* J Biol Chem, 1997. **272**(29): p. 18000-6.

22. Kuo, W.J., M.A. Digman, and A.D. Lander, *Heparan sulfate acts as a bone morphogenetic protein coreceptor by facilitating ligand-induced receptor hetero-oligomerization.* Mol Biol Cell, 2010. **21**(22): p. 4028-41.

23. Sarrazin, S., W.C. Lamanna, and J.D. Esko, *Heparan sulfate proteoglycans.* Cold Spring Harb Perspect Biol, 2011. **3**(7).

24. Kraushaar, D.C., S. Dalton, and L. Wang, *Heparan sulfate: a key regulator of embryonic stem cell fate.* Biol Chem, 2013. **394**(6): p. 741-51.

25. Kraushaar, D.C., et al., *Heparan sulfate facilitates FGF and BMP signaling to drive mesoderm differentiation of mouse embryonic stem cells.* J Biol Chem, 2012. **287**(27): p. 22691-700.

26. Kraushaar, D.C., Y. Yamaguchi, and L. Wang, *Heparan sulfate is required for embryonic stem cells to exit from self-renewal.* J Biol Chem, 2010. **285**(8): p. 5907-16.

27. Johnson, C.E., et al., *Essential Alterations of Heparan Sulfate During the Differentiation of Embryonic Stem Cells to Sox1-Enhanced Green Fluorescent*

Protein-Expressing Neural Progenitor Cells. STEM CELLS, 2007. **25**(8): p. 1913-1923.

28. Baldwin, R.J., et al., *A Developmentally Regulated Heparan Sulfate Epitope Defines a Subpopulation with Increased Blood Potential During Mesodermal Differentiation.* STEM CELLS, 2008. **26**(12): p. 3108-3118.
29. Sasaki, N., et al., *Heparan sulfate regulates self-renewal and pluripotency of embryonic stem cells.* J Biol Chem, 2008. **283**(6): p. 3594-606.
30. Dejima, K., et al., *Novel contact-dependent bone morphogenetic protein (BMP) signaling mediated by heparan sulfate proteoglycans.* J Biol Chem, 2011. **286**(19): p. 17103-11.
31. Levings, D.C., T. Arashiro, and H. Nakato, *Heparan sulfate regulates the number and centrosome positioning of Drosophila male germline stem cells.* Mol Biol Cell, 2016. **27**(6): p. 888-96.
32. Saez, B., et al., *Inhibiting stromal cell heparan sulfate synthesis improves stem cell mobilization and enables engraftment without cytotoxic conditioning.* Blood, 2014.
33. Nurcombe, V. and S.M. Cool, *Heparan sulfate control of proliferation and differentiation in the stem cell niche.* Critical reviews in eukaryotic gene expression, 2007. **17**(2): p. 159-171.
34. Helledie, T., et al., *Heparan sulfate enhances the self-renewal and therapeutic potential of mesenchymal stem cells from human adult bone marrow.* Stem Cells Dev, 2012. **21**(11): p. 1897-910.

35. Watson, H.A., et al., *Heparan sulfate inhibits hematopoietic stem and progenitor cell migration and engraftment in mucopolysaccharidosis I.* J Biol Chem, 2014. **289**(52): p. 36194-203.

36. Hayashi, Y., S. Kobayashi, and H. Nakato, *Drosophila glypicans regulate the germline stem cell niche.* J Cell Biol, 2009. **187**(4): p. 473-80.

37. Buresh-Stiemke, R.A., et al., *Distinct expression patterns of Sulf1 and Hs6st1 spatially regulate heparan sulfate sulfation during prostate development.* Dev Dyn, 2012. **241**(12): p. 2005-13.

38. Dontu, G., et al., *In vitro propagation and transcriptional profiling of human mammary stem/progenitor cells.* Genes Dev, 2003. **17**(10): p. 1253-70.

39. Reynolds, B.A. and S. Weiss, *Clonal and population analyses demonstrate that an EGF-responsive mammalian embryonic CNS precursor is a stem cell.* Dev Biol, 1996. **175**(1): p. 1-13.

40. Jakobsson, L., et al., *Heparan Sulfate in trans Potentiates VEGFR-Mediated Angiogenesis.* Developmental Cell, 2006. **10**(5): p. 625-634.

41. Nakato, H. and J.P. Li, *Functions of Heparan Sulfate Proteoglycans in Development: Insights From Drosophila Models.* Int Rev Cell Mol Biol, 2016. **325**: p. 275-93.

42. Muzumdar, M.D., et al., *A global double-fluorescent Cre reporter mouse.* Genesis, 2007. **45**(9): p. 593-605.

43. Huang, Y., et al., *Prostate Sphere-forming Stem Cells Are Derived from the P63-expressing Basal Compartment.* J Biol Chem, 2015. **290**(29): p. 17745-52.

44. Bishop, J.R., M. Schuksz, and J.D. Esko, *Heparan sulphate proteoglycans fine-tune mammalian physiology.* Nature, 2007. **446**(7139): p. 1030-7.

45. Valdez, J.M., et al., *Notch and TGFbeta form a reciprocal positive regulatory loop that suppresses murine prostate basal stem/progenitor cell activity.* Cell Stem Cell, 2012. **11**(5): p. 676-88.

46. Witte, J.S., *Prostate cancer genomics: towards a new understanding.* Nat Rev Genet, 2009. **10**(2): p. 77-82.

47. Eickelberg, O., et al., *Betaglycan inhibits TGF-beta signaling by preventing type I-type II receptor complex formation. Glycosaminoglycan modifications alter betaglycan function.* J Biol Chem, 2002. **277**(1): p. 823-9.

48. Qiu, H., et al., *Quantitative phosphoproteomics analysis reveals broad regulatory role of heparan sulfate on endothelial signaling.* Mol Cell Proteomics, 2013. **12**(8): p. 2160-73.

49. Hempel, N., et al., *Expression of the type III TGF-beta receptor is negatively regulated by TGF-beta.* Carcinogenesis, 2008. **29**(5): p. 905-12.

50. Cunha, G.R. and B. Lung, *The importance of stroma in morphogenesis and functional activity of urogenital epithelium.* In Vitro, 1979. **15**(1): p. 50-71.

51. Xin, L., et al., *In vivo regeneration of murine prostate from dissociated cell populations of postnatal epithelia and urogenital sinus mesenchyme.* Proc Natl Acad Sci U S A, 2003. **100 Suppl 1**: p. 11896-903.

52. Lanner, F., et al., *Heparan sulfation-dependent fibroblast growth factor signaling maintains embryonic stem cells primed for differentiation in a heterogeneous state.* Stem Cells, 2010. **28**(2): p. 191-200.

53. Dos Santos, M., et al., *Perlecan expression influences the keratin 15-positive cell population fate in the epidermis of aging skin.* Aging (Albany NY), 2016. **8**(4): p. 751-68.

54. Pawlikowski, B., et al., *Regulation of skeletal muscle stem cells by fibroblast growth factors.* Dev Dyn, 2017. **246**(5): p. 359-367.

55. Buono, M., et al., *Sulfatase modifying factor 1-mediated fibroblast growth factor signaling primes hematopoietic multilineage development.* J Exp Med, 2010. **207**(8): p. 1647-60.

56. Takemura, M. and H. Nakato, *Drosophila Sulf1 is required for the termination of intestinal stem cell division during regeneration.* J Cell Sci, 2017. **130**(2): p. 332-343.

57. Patel, V.N., et al., *Hs3st3-modified heparan sulfate controls KIT+ progenitor expansion by regulating 3-O-sulfotransferases.* Dev Cell, 2014. **29**(6): p. 662-73.

58. Huang, L., et al., *The role of Fgf10 signaling in branching morphogenesis and gene expression of the rat prostate gland: lobe-specific suppression by neonatal estrogens.* Dev Biol, 2005. **278**(2): p. 396-414.

59. Donjacour, A.A., A.A. Thomson, and G.R. Cunha, *FGF-10 plays an essential role in the growth of the fetal prostate.* Dev Biol, 2003. **261**(1): p. 39-54.

60. Lin, Y., et al., *Fibroblast growth factor receptor 2 tyrosine kinase is required for prostatic morphogenesis and the acquisition of strict androgen dependency for adult tissue homeostasis.* Development, 2007. **134**(4): p. 723-34.

61. Zhang, Y., et al., *Role of epithelial cell fibroblast growth factor receptor substrate 2alpha in prostate development, regeneration and tumorigenesis.* Development, 2008. **135**(4): p. 775-84.

62. Abler, L.L., et al., *A high-resolution molecular atlas of the fetal mouse lower urogenital tract.* Dev Dyn, 2011. **240**(10): p. 2364-77.

63. Prins, G.S., et al., *The role of estrogens in normal and abnormal development of the prostate gland.* Ann N Y Acad Sci, 2006. **1089**: p. 1-13.

64. Lamm, M.L., et al., *Mesenchymal factor bone morphogenetic protein 4 restricts ductal budding and branching morphogenesis in the developing prostate.* Dev Biol, 2001. **232**(2): p. 301-14.

65. Grishina, I.B., et al., *BMP7 inhibits branching morphogenesis in the prostate gland and interferes with Notch signaling.* Dev Biol, 2005. **288**(2): p. 334-47.

66. Buresh-Stiemke, R.A., et al., *Distinct expression patterns of Sulf1 and Hs6st1 spatially regulate heparan sulfate sulfation during prostate development.* Developmental Dynamics, 2012. **241**(12): p. 2005-2013.

67. Li, X., et al., *Urothelial transdifferentiation to prostate epithelia is mediated by paracrine TGF-beta signaling.* Differentiation, 2009. **77**(1): p. 95-102.

68. Huang, Y., et al., *Type 2 Fibroblast Growth Factor Receptor Signaling Preserves Stemness and Prevents Differentiation of Prostate Stem Cells from the Basal Compartment.* J Biol Chem, 2015. **290**(29): p. 17753-61.

69. Terry, D.E. and A.F. Clark, *Glycosaminoglycans in the three lobes of the rat prostate following castration and testosterone treatment.* Biochem Cell Biol, 1996. **74**(5): p. 653-8.

70. Buresh, R.A., et al., *Sulfatase 1 is an inhibitor of ductal morphogenesis with sexually dimorphic expression in the urogenital sinus.* Endocrinology, 2010. **151**(7): p. 3420-31.

71. Takashima, Y., et al., *Heparan sulfate 6-O-endosulfatases, Sulf1 and Sulf2, regulate glomerular integrity by modulating growth factor signaling.* Am J Physiol Renal Physiol, 2016. **310**(5): p. F395-408.

72. Lee, J., et al., *Structural determinants of heparin-transforming growth factor-beta1 interactions and their effects on signaling.* Glycobiology, 2015. **25**(12): p. 1491-504.

73. Iwao, K., et al., *Heparan sulfate deficiency leads to Peters anomaly in mice by disturbing neural crest TGF-beta2 signaling.* J Clin Invest, 2009. **119**(7): p. 1997-2008.

74. Chen, C.L., S.S. Huang, and J.S. Huang, *Cellular heparan sulfate negatively modulates transforming growth factor-beta1 (TGF-beta1) responsiveness in epithelial cells.* J Biol Chem, 2006. **281**(17): p. 11506-14.

75. Belenkaya, T.Y., et al., *Drosophila Dpp morphogen movement is independent of dynamin-mediated endocytosis but regulated by the glypican members of heparan sulfate proteoglycans.* Cell, 2004. **119**(2): p. 231-44.

76. Pellegrini, L., et al., *Crystal structure of fibroblast growth factor receptor ectodomain bound to ligand and heparin.* Nature, 2000. **407**(6807): p. 1029-34.

77. Inatani, M., et al., *Mammalian brain morphogenesis and midline axon guidance require heparan sulfate.* Science, 2003. **302**(5647): p. 1044-6.

78. Wu, X., et al., *Generation of a prostate epithelial cell-specific Cre transgenic mouse model for tissue-specific gene ablation.* Mech Dev, 2001. **101**(1-2): p. 61-9.

79. Xin, L., et al., *Progression of prostate cancer by synergy of AKT with genotropic and nongenotropic actions of the androgen receptor.* Proc Natl Acad Sci U S A, 2006. **103**(20): p. 7789-94.

80. Siegel, P.M., et al., *Transforming growth factor beta signaling impairs Neu-induced mammary tumorigenesis while promoting pulmonary metastasis.* Proc Natl Acad Sci U S A, 2003. **100**(14): p. 8430-5.

81. Cai, H., et al., *Collaboration of Kras and androgen receptor signaling stimulates EZH2 expression and tumor-propagating cells in prostate cancer.* Cancer Res, 2012. **72**(18): p. 4672-81.

Figures:

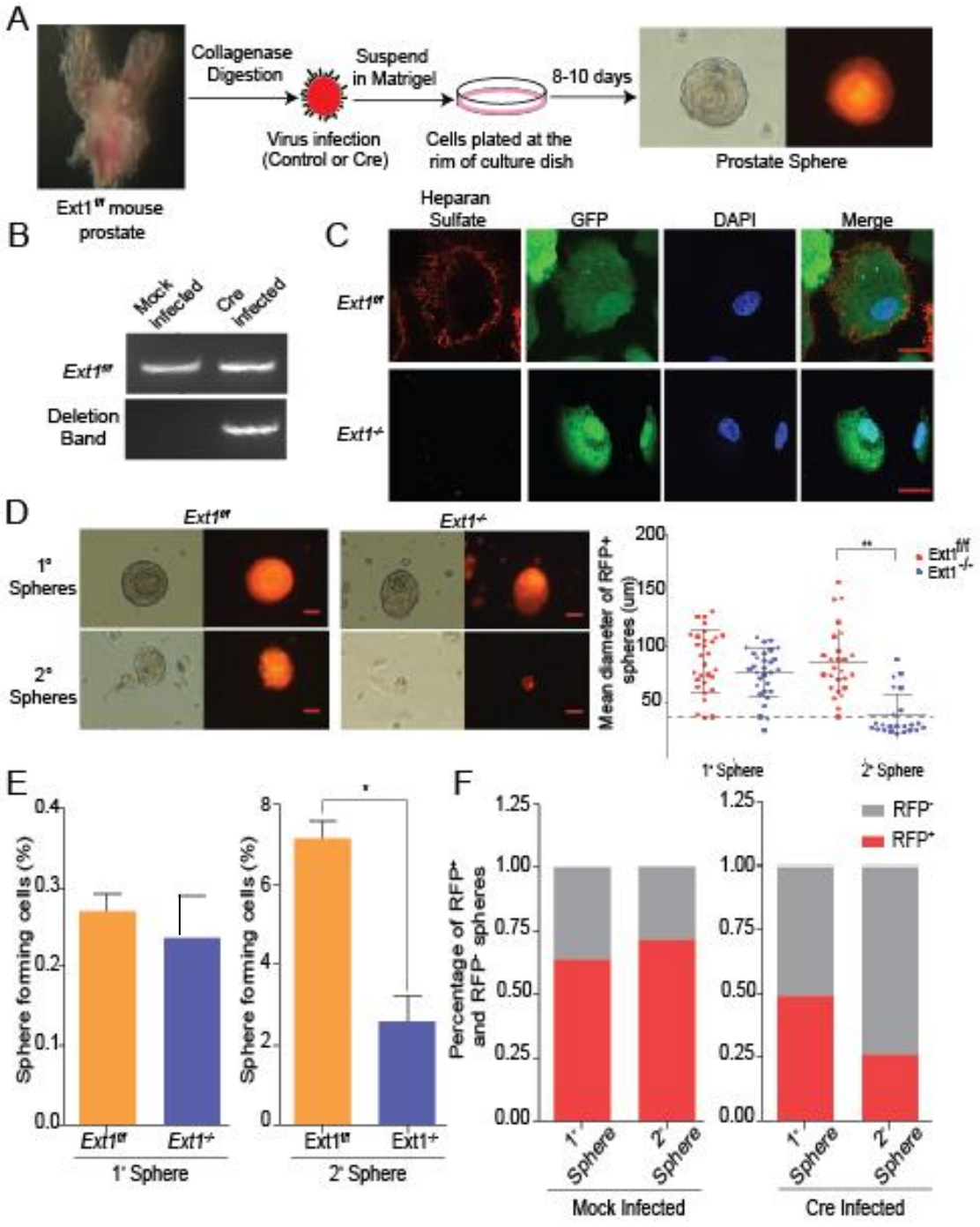

Figure 2.1 Loss of HS expression diminishes self-renewal activity in adult PrSCs (A) Schematic representation of sphere forming assay. The Ext1$^{f/f}$ cells were transduced with control or Cre by lentiviral infection (with the RFP marker). The transduced cells were

mixed with matrigel and plated at the rim of petri dish. After 8-10 days incubation, prostate spheroids were formed. The RFP expression indicated that the sphere was transduced with Cre or control gene. (B) PCR analysis of genomic DNA isolated from mock and Cre transduced prostate spheres. Loss of Ext1 due to Cre transduction led to the detection of a PCR product, which did not occur in the wild type sphere. (C) Anti-HS antibody staining (10E4) of mock or Cre transduced PrECs (Scale = 25 μm) (D) Phase and fluorescence images and the size distribution (diameter) of spheres derived from control ($Ext1^{f/f}$) or Cre ($Ext1^{-/-}$) transduced groups in primary sphere (1°) and secondary (2°) spheres (Scale = 25μm) were recorded. Only spheres with the diameter ≥ 40 μm were counted. (E) The percentage of sphere formation from the control (*Ext1*$^{f/f}$ cells) or Cre ($Ext1^{-/-}$) transduced prostate epithelial cells were calculated in the primary and second generations. Error bars represent means and SD from triplicate experiments. *p < .05. (F) Bar graph comparing the percentage of red (RFP^{+}) spheres in the primary and second of prostate sphere culture.

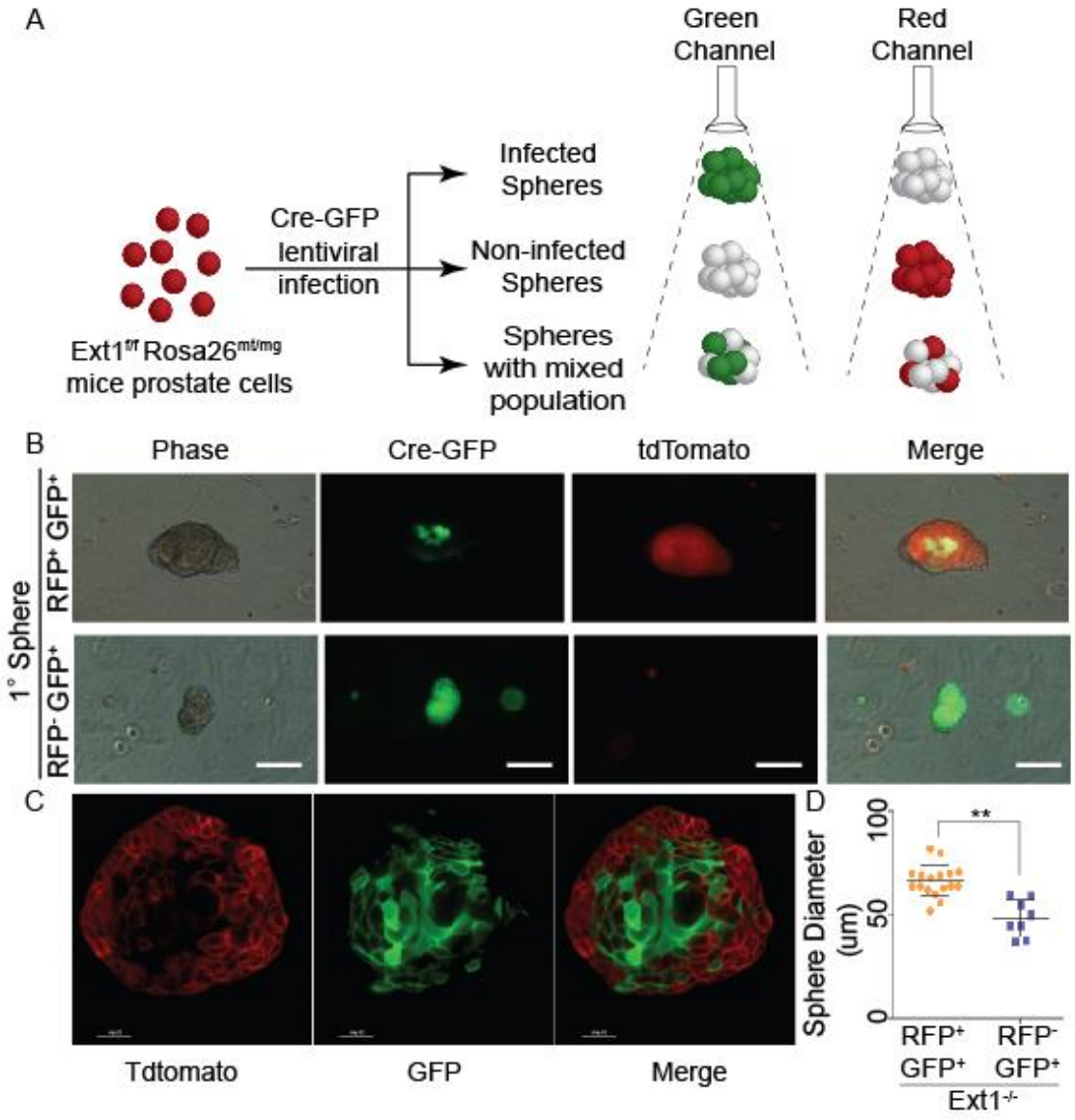

Figure 2.2 HS functions *in trans* to sustain HS-deficient PrSCs to from primary spheres. (A) Schematic representation of the strategy employed in determining Cre expression in prostate spheres formed by Ext1$^{f/f}$ Rosa26$^{mt/mg}$ prostate cells. (B) Fluorescence image of Cre infected primary (1°) prostate spheres from *Ext1$^{f/f}$ Rosa26$^{mt/mg}$* prostate cells (Scale = 50µm). (C) Confocal image of Cre infected primary (1°) prostate sphere from *Ext1$^{f/f}$ Rosa26$^{mt/mg}$* prostate cells (Scale = 25µm). (D) Bar graphs comparing the sphere size *Ext1$^{-/-}$* primary (1°) spheres. Results show means ± SD from three

independent experiments. Statistical significance was assessed by Student's t-test (**$p < .01$).

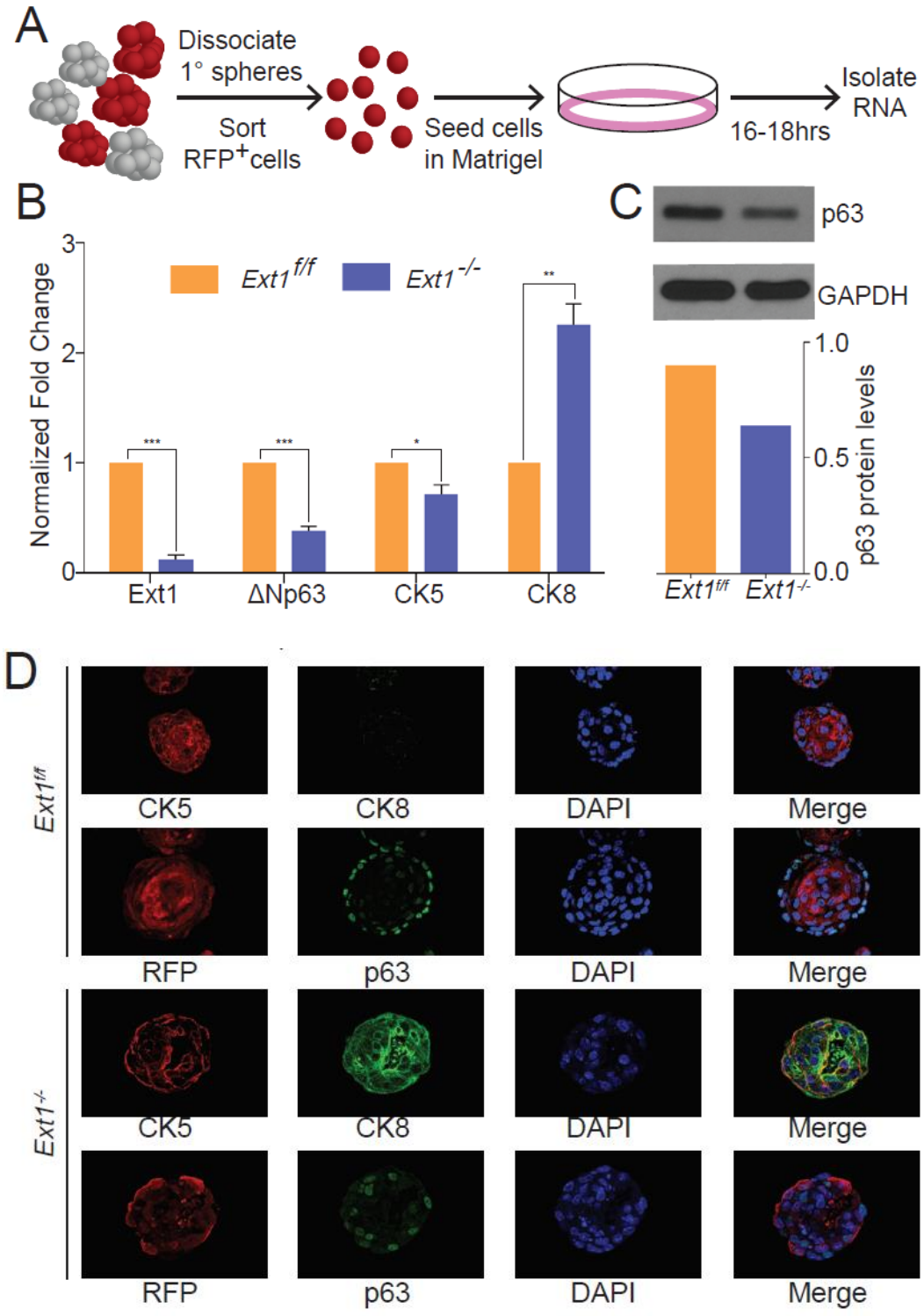

Figure 2.3 Loss of HS expression diminishes p63^{+} stem cells and disturbs PrSC differentiation. (A) Schematic representation of mRNA isolation from secondary spheres. Dissociated primary prostate cells were transduced with Cre (with RFP marker)

by lentiviral infection. After 8-10 days, the primary spheres were dissociated into single cells. The RFP^+ cells were enriched by Flow Cytometry, and reseeded in matrigel for recovery after cell sorting. Total RNA was isolated after 16-18 h incubation. (B) qRT-PCR analysis for expression levels of Ext1 and lineage markers [p63, cytokeratin (CK) 5, and CK 8) of the above short-cultured RFP^+ cells. Fold Change normalized to Gapdh. Results represent the $\text{mean} \pm \text{SD}$ of three independent experiments. Statistical significance was assessed by Student's t-test ($^*p < .05$, $^{**}p < .01$, $^{***}p < .001$). (C) Western blot analysis and quantification of p63 protein levels in mock or Cre transduced primary spheres. (D) Immuno-histochemical staining for CK5, CK8, RFP, and p63 in primary spheres of $Ext1^{f/f}$ or $Ext1^{-/-}$.

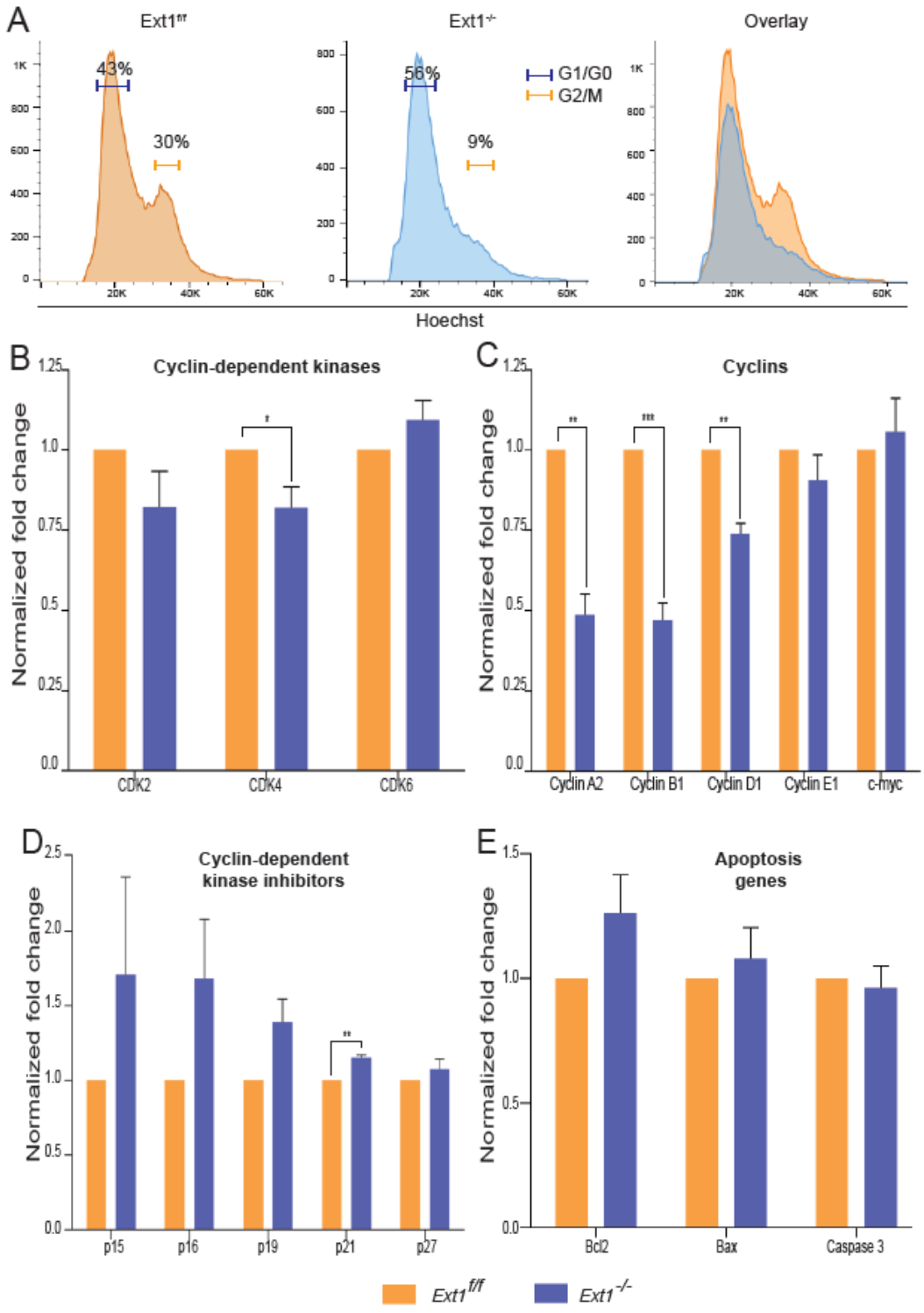

Figure 2.4 Loss of HS impairs cell cycle progression. (A) The primary prostate spheres derived from *Ext1*$^{f/f}$ or *Ext1*$^{-/-}$ was dissociated, seeded in Matrigel for 16-20hrs and subjected to cell cycle analysis by using Hoechst 33342. (B-E) qRT-PCR analysis of cell

cycle regulators including (B) cyclin dependent kinases (CDKs), (C) cyclins, (D) CDK inhibitors (CKIs), and (E) apoptotic genes of the above cells. Fold Change normalized to Gapdh. Results represent the mean ± SD of three independent experiments. Statistical significance was assessed by Student's t-test (*$p < .05$, **$p < .01$, ***$p < .001$).

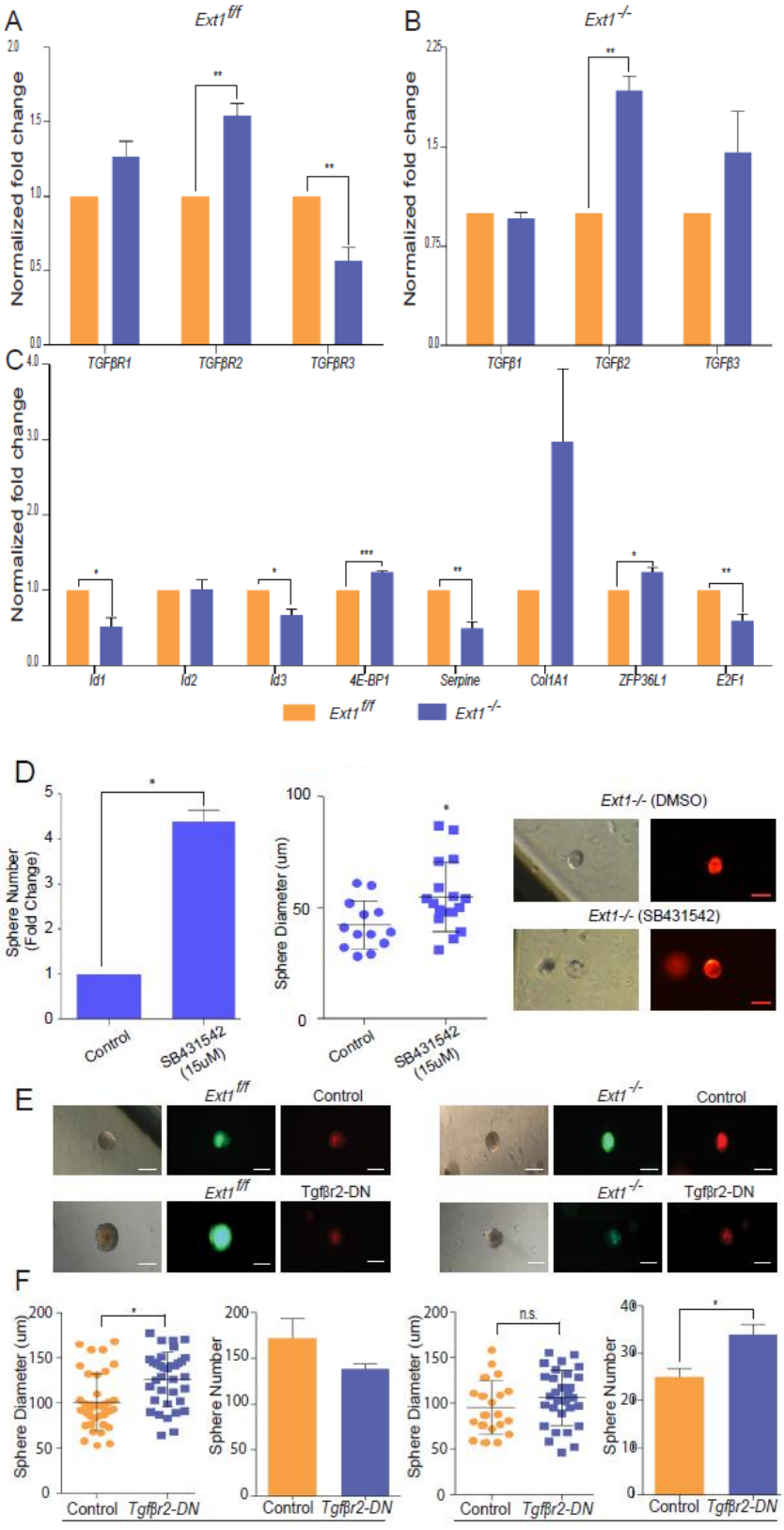
A
Ext1 f/f
Normalized fold change
TGFβR1
TGFβR2
TGFβR3
B
Ext1 -/-
Normalized fold change
TGFβ1
TGFβ2
TGFβ3
C
Normalized fold change
Id1
Id2
Id3
4E-BP1
Serpine
Col1A1
ZFP36L1
E2F1
Ext1 f/f
Ext1 -/-
D
Sphere Number (Fold Change)
Control
SB431542 (15uM)
Sphere Diameter (um)
Control
SB431542 (15uM)
Ext1-/- (DMSO)
Ext1-/- (SB431542)
E
Ext1 f/f
Control
Ext1 -/-
Control
Ext1 f/f
Tgfβr2-DN
Ext1 -/-
Tgfβr2-DN
F
Sphere Diameter (um)
Control
Tgfβr2-DN
Sphere Number
Control
Tgfβr2-DN
Sphere Diameter (um)
n.s.
Control
Tgfβr2-DN
Sphere Number
Control
Tgfβr2-DN

Figure 2.5 Attenuating TGFβ signaling in HS-deficient PrSCs rescues sphere formation. (A-C) qRT-PCR analysis to assess expression levels of TGFbetaR1/2/3 (A), TGFβ ligands (TGFbeta1/2/3) (B), and the signaling pathway downstream target genes including ld1/2/3, 4E-BP1, Serpine, Col1A1, ZFP36L1, and E2F1 (C) in prostate spheroid cells derived from *Ext1*$^{f/f}$ or *Ext1*$^{-/-}$. Results show means ± SD from three independent experiments. Statistical significance was assessed by Student's t-test (*p < .05, **p < .01, ***p < .001). (D-F) The number and size of the second generation of *Ext1*$^{-/-}$ spheres were enhanced in either SB43154 treatment (D) or overexpression of TGFβR2-DN (E-F). Scale = 100 μm.

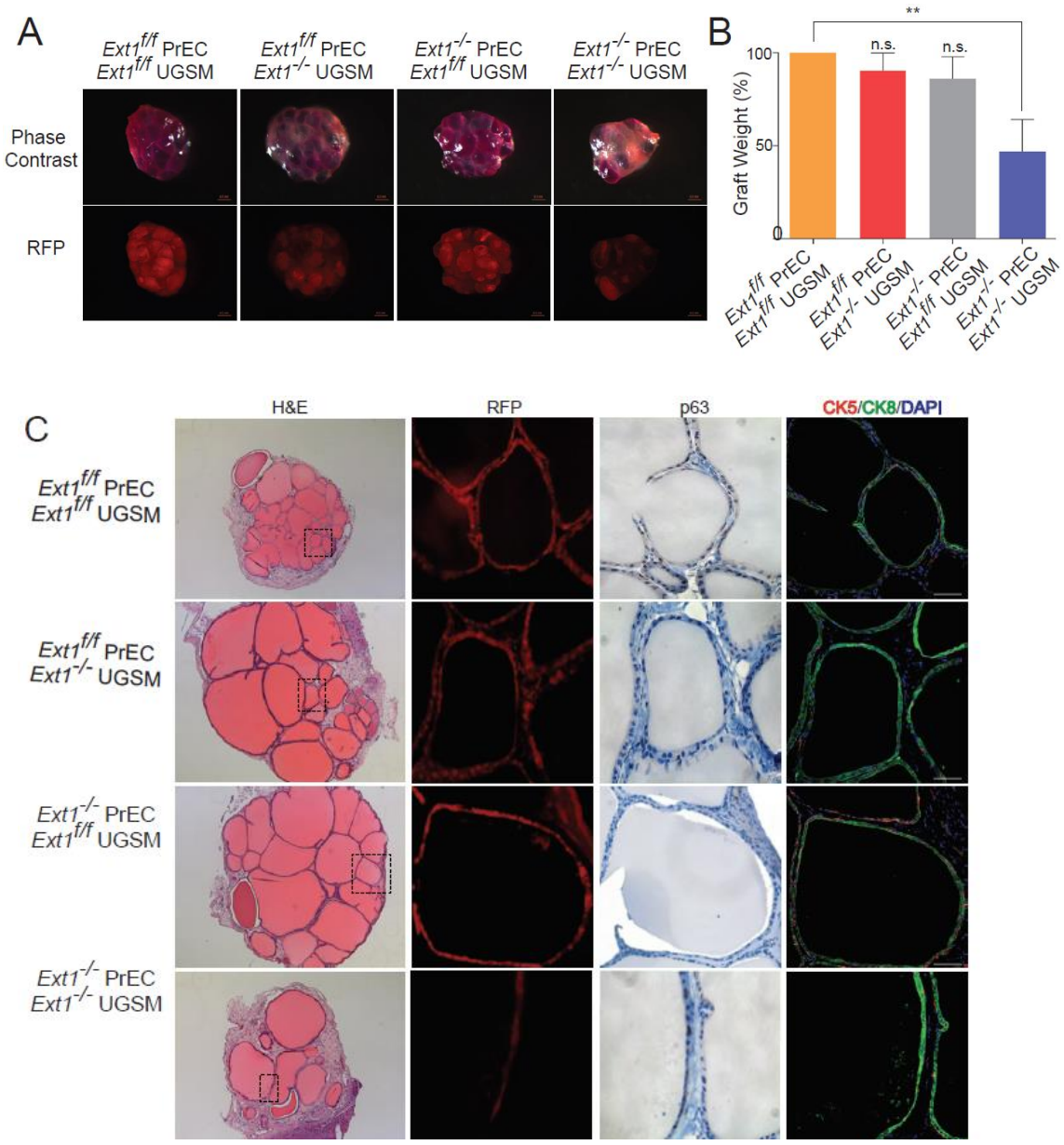

Figure 2.6 HS functions in both *in cis* and *in trans* to retain PrSC homeostasis and to sustain efficient prostate regeneration *in vivo*. (A-B) The global view (A) and weight (B) of regenerated prostate tissue. Scale bar: 0.5mm. Results show percentage mean ± SD from three independent experiments. Statistical significance was assessed by Student's t-test (**$p < 0.01$). (C) H&E (scale bar: 200μm), RFP, and

immunohistochemistry analysis on the expression of p63, CK5, and CK8 (Scale bar: 50μm).

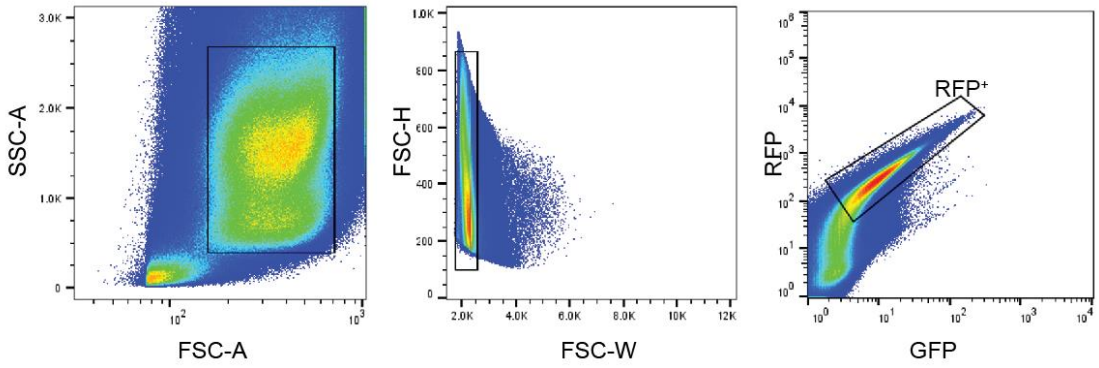

Supplementary Figure 2.7 Flow cytometry gating to sort RFP$^+$ cells. Gating strategy to sort RFP expressing PrECs from dissociated primary spheres.

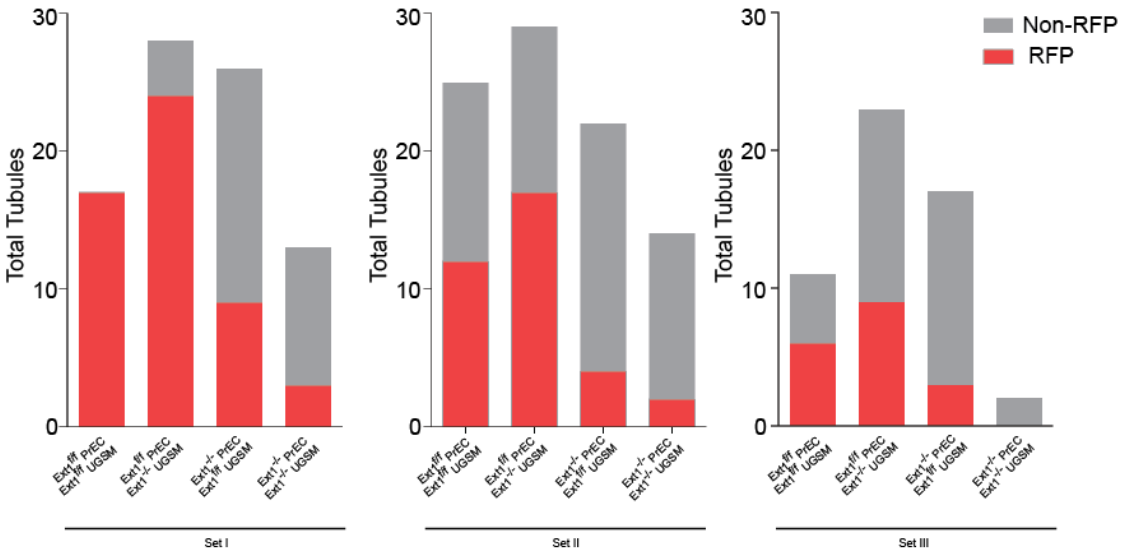

Total Tubules							
		Set I		Set II		Set III	
		Total Tubules	RFP+	Total Tubules	RFP+	Total Tubules	RFP+
PrEC	UGSM						
Ext1f/f	Ext1f/f	17	17	25	12	11	6
Ext1f/f	Ext1-/-	28	24	29	17	23	9
Ext1-/-	Ext1f/f	26	9	22	4	17	3
Ext1-/-	Ext1-/-	13	3	14	2	2	0

Supplementary Figure 2.8 Quantification of tubules in regenerated prostate grafts.

Quantification of mock or Cre transduced tubules (RFP^{+}) and in the regenerated prostate grafts.

Supplementary Table 2.1

Primers for mouse genotyping

Primer	Sequence (5'-3')	Amplicon Size	Comments
Burn 51	GGAGTGTGGATGAGTTGAAG	460bp : floxed allele 389bp : WT allele	Distinguishes between WT and floxed *Ext1* allele
Burn 52	CAACACTTTCAGCTCCAGTC		
Burn 51	GGAGTGTGGATGAGTTGAAG	500bp	Detects *Ext1* deletion band
Burn 29	GAGAACAGGTACCCATGTTC		
P021	CTGAAGAATGGGACAGGCATTG	393bp	Detects the presence of Pb-Cre
C031	CATCACTCGTTGCATCGACC		
oIMR7318	CTC TGC TGC CTC CTG GCT TCT	250bp	Detects Rosa26 WT allele
oIMR7319	CGA GGC GGA TCA CAA GCA ATA		
oIMR7318	CTC TGC TGC CTC CTG GCT TCT	330bp	Detects Rosa26$^{mt/mg}$ allele
oIMR7320	TCA ATG GGC GGG GGT CGT T		

Supplementary Table 2.2

Primers for amplification of truncated TGFβR2 from pCMV5 HA-TBRII (delta Cyt) plasmid

Primer	Sequence (5'-3')	Comments
Forward Primer	AAATCTAGAGCCACCATGGGTCGGGGGCTGCTC	TCTAGA - XbaI restriction site GCCACC - Kozak Sequence
Reverse Primer	AAAAAGAATTCTCATGAACTCAGCTTCTGCTGCCG	GAATTC – EcoRI restriction site

Supplementary Table 2.3

Primers for mouse qRT-PCR:

Primer	Sequence (5'-3')	Amplicon Size
Ext1 Forward	TGGAGTCCTGCTTCGATTTC	72bp
Ext1 Reverse	CTTTCTGCTGCGGGTACAC	
ΔNp63 Forward	ACAATGCCCAGACTCAATTT	88bp
ΔNp63 Reverse	GAGGAGCCGTTCTGAATCTG	
CK5 Forward	GAGATCGCCACCTACAGGAA	117bp
CK5 Reverse	TCCTCCGTAGCCAGAAGAGA	
CK8 Forward	GACATCGAGATCACCACCTA	125bp
CK8 Reverse	GATGAACTCAGTCCTCCTGA	
CDK2 Forward	CTCATCAAGAGCTATCTGTTCC	105bp
CDK2 Reverse	TGCATTGATAAGCAGGTTCT	
CDK4 Forward	GCAGTCTACATACGCAACA	139bp
CDK4 Reverse	AGGCAATCCAATGAGATCAA	
CDK6 Forward	GACTTGACCACTTACTTGGATA	118bp
CDK6 Reverse	GCACTACTCTGTGAGAATGAA	
CyclinA2 Forward	GTCCTTGCTTTTGACTTGGC	139bp
CyclinA2 Reverse	ACGGGTCAGCATCTATCAAAC	
CyclinB1 Forward	AGCGAAGAGCTACAGGCAAG	113bp
CyclinB1 Reverse	TCACACACAGGCACCTTCTC	
CyclinD1 Forward	GCCCTCCGTATCTTACTTCAAG	145bp

CyclinD1 Reverse	GCGGTCCAGGTAGTTCATG	
p15 Forward	CTTTGTGTACCGCTGGGAAC	104bp
p15 Reverse	TTAGCTCTGCTCTTGGGATTG	
p16 Forward	GTGTGCATGACGTGCGGG	146bp
p16 Reverse	GCAGTTCGAATCTGCACCGTAG	
p19 Forward	GCTCTGGCTTTCGTGAACATG	137bp
p19 Reverse	TCGAATCTGCACCGTAGTTGAG	
p21 Forward	TTGCACTCTGGTGTCTGAGC	112bp
p21 Reverse	TCTGCGCTTGGAGTGATAGA	
p27 Forward	GTGGACCAAATGCCTGACTC	122bp
p27 Reverse	TCTGTTCTGTTGGCCCTTTT	
TGFβR1 Forward	TAGCAGCAGACAACAAAGAC	115bp
TGFβR1 Reverse	CCTTCCACAGTAACAGTGTATC	
TGFβR2 Forward	CCAAGTCGGATGTGGAAATGG	103bp
TGFβR2 Reverse	GCCATGACATCACTGTTAAA	
TGFβR3 Forward	GGGAGGTTCACATCCTAAAC	81bp
TGFβR3 Reverse	GGTTCAGATGCAGGGTAAC	
TGFβ1 Forward	GAAGCGGACTACTATGCTAAA	94bp
TGFβ1 Reverse	TACTGTGTGAGATGTCTTTGG	
TGFβ2 Forward	GAGGGATCTTGGATGGAAATG	112bp
TGFβ2 Reverse	GAGGACTTTGGTGTGTTGAG	
TGFβ3 forward	GCATCCACTGTCCATGTCAC	109bp
TGFβ3 Reverse	CCATGGTCATCTTCATTGTCC	

Id1 Forward	AGAACCGCAAAGTGAGCAAG	66bp
Id1 Reverse	GCTGCAGGTCCCTGATGTAG	
Id2 Forward	GCAAAGTACTCTGTGGCTAAA	131bp
Id2 Reverse	CCTGGTGAAATGGCTGATAA	
Id3 Forward	CTGCTACGAGGCGGTGTG	175bp
Id3 Reverse	CACCTGGCTAAGCTGAGTGC	
Col1a1 Forward	GCCAAGAAGACATCCCTGAAG	104bp
Col1a1 Reverse	ATTGTGGCAGATACAGATCAA	
ZFP36L1 Forward	GGGTAACAAGATGCTCAACTA	140bp
ZFP36L1 Reverse	GGTTCTGATGGAACTTGGAGC	
4E-BP1 Forward	GGTCACTAGCCCTACCAG	112bp
4E-BP1 Reverse	GTCCATCTCAAATTGTGACTCT	
E2F1 Forward	CAACTGCTTTCGGAGGACT	149bp
E2F1 Reverse	GTCTCTGAAGAATCCACAGCTT	

Supplementary Table 2.4

Antibodies for Immunohistochemistry and Western Blot

Antibody	Company, Catalog Number	Usage, Dilution
CK5	Covance #PRB-160P	IHC: 1:1000
CK8	Covance #MMS-162P	IHC: 1:2000, WB: 1:1000
p63	Santa Cruz, 4A4	IHC: 1:100, WB: 1:1000
RFP	Rockland, #600-401-379	IHC: 1:1000
Ki67	Novus, #NB500-170	IHC: 1:100
Cleaved Caspase 3	Cell Signaling, #9661	IHC: 1:500
Smad3	Cell Signaling, #9513	WB: 1:1000
pSmad3	NBP1-77836SS	WB: 1:1000
Akt	Cell Signaling, #46917	WB: 1:1000
pAkt	Cell Signaling, #4060	WB: 1:1000
GAPDH	Cell Signaling, #2118	WB: 1:5000

CHAPTER 3

NOVEL CO-CULTURE SYTEM TO INVESTIGATE EPITHELIAL-STROMAL INTERACTION DURING PROSTATE ORGANOGENESIS AND CARCINOGENESIS

Sumit Rai, Lianchun Wang and Houjian Cai. To be submitted to The Journal of Biological Methods.

Abstract

Prostaspheres formation is an experimental approach to study self-renewal and differentiation potential of prostate stem/progenitor cells *in vitro*. The formation of spheroid is clonal in origin, and solely relies on the intrinsic potential of progenitor cells. However, epithelial-stromal interaction is essential in organogenesis, spheroid formation does not impart information regarding to the contribution of stromal compartment. To assess and quantify the contribution of stromal microenvironment to the spheroid formation, we have developed an *in vitro* 3D co-culture assay wherein prostate epithelial stem/progenitor cells form spheres in the presence of stromal cells isolated from the urogenital sinus mesenchymal cells. The number of sphere increases 2-fold in the co-culture assay in comparison to using epithelium alone. The assay allows evaluating the reciprocal epithelium-stromal interaction and provides reliable quantification about the effect of the stromal cells on the epithelial progenitor cells. The 3D co-culture *in vitro* system possesses the advantage of being amenable to altering gene expression in either epithelial or stromal cells, and will be suitable to quantify the potential of the stem/progenitor cells under various combinations of gene expression.

Introduction

Prostate is a male accessory gland comprising of stromal and epithelial compartment [1]. The prostate epithelium is composed of three major cell types: luminal cells which are secretory in nature, basal cells that line the basement membrane and neuroendocrine cells regulating epithelial cell growth [2]. The adult prostate is capable of undergoing multiple cycles of atrophy and regeneration following androgen depletion and supplementation,

respectively [3]. This shrinkage was found largely due to apoptosis of luminal cells attesting the presence of progenitor cells in the androgen independent condition [4].

Recent efforts have been directed towards evaluating the stem/progenitor cell characteristics of isolated prostate epithelial cells in culture. One of the experimental approaches is by growing the isolated cells as prostaspheres in a matrix of matrigel [5]. The PrSCs have been shown to be capable of undergoing self-renewal as well differentiation in this culture system. The spheroids are clonal in origin, and express cell cytokeratin 5 (CK5) and/or p63 along the outer rim of the sphere. This model system also serves as an excellent experimental approach to study molecular mechanisms and regulatory networks required for the maintenance of stem cell characteristics as well as external cues to facilitate the differentiation.

Stem cell localizes at a particle niche in numerous stem cell models [6], suggesting the essential role in the maintenance of stem/progenitor activity. Numerous studies have demonstrated that reciprocal interactions between the epithelial and stromal compartment are essential for stem cell function [7, 8]. The stromal cells have also been shown to promote tumor progression [9]. However, the measurement of the stromal contribution is limited through utilization of transgenic animal model or *in vivo* regeneration assays which are time intensive in studying normal prostate development or carcinogenesis.

Here we present an experimental approach to study the stromal-epithelial interaction in an *in vitro* co-culture system. This approach involves growing PrSCs as spheres in the presence of stromal cells. This assay allows for easy manipulation of gene expression in both epithelial and stromal cells, one at a time or together thus providing a platform to

screen a combination of diverse conditions. This assay will provide an addition to the *in vivo* models for understanding the regulatory circuits that exists between the epithelial-stromal compartments during development as well as the extent of their participation during carcinogenesis.

Materials:

REAGENTS

- Male C57/BL6 mice (6-12 weeks old) (Housed and bred in accordance with Division of Laboratory Animal Medicine regulations.)

Caution: All experiments involving live rodents must abide by institutional regulations.

- Dulbecco's modified Eagle medium (DMEM) (Thermo Fischer Scientific, Cat. No. 12100-061)
- RPMI (Roswell Park Memorial Institute) 1640 medium (Thermo Fischer Scientific, Cat. No. 11875119)
- 1x PBS (Thermo Fischer Scientific, Cat. No. 10010049)
- Fetal bovine serum (Omega Scientific, Cat. No. FB-01)
- NuSerum (BD Biosciences, Cat. No. 355504)

Critical: Nu-serum has been found to support optimal growth of UGSM cells.

- Dihydrotestosterone (DHT) (Sigma Aldrich)(see REAGENT SETUP)

Caution: FDA clearance required to procure DHT.

- Insulin (Thermo Fischer Sceintific, Cat No. 12585014)
- Glutamax (Thermo Fisher Scientific, Cat. No. 35050061)
- Penicillin/Streptomycin (Thermo Fischer Scientific, Cat. No. 15140-122)
- Collagenase I (Thermo Fischer Scientific, Cat. No. 17018029)
- Dispase (Thermo Fischer Scientific, Cat. No. 17105041)
- DNase I (Sigma, Cat. No. 10104159001)
- 0.05%Trypsin-EDTA (Thermo Fischer Scientific, Cat. No. 25300054)
- 2.5% Trypsin (Thermo Fischer Scientific, Cat. No. 15090046)
- PrEGM (Clonetics/LonzaCat. No. CC-3165)
- Matrigel (Corning, Cat. No. 354234)

EQUIPMENT

- Cell culture disposables: Petri dishes (BD Biosciences), Centrifuge tubes (Eppendorf), pipettes, pipette tips, filter units(Millipore)
- 12-well tissue culture plates (Corning, Cat. No. 3513)
- 21-gauge, 25-gauge, and 28-gauge needles (BD Biosciences)
- 10ml syringes (BD Biosciences, Cat. No. 309604)
- 0.2μm syringe filters (Pall Corporation, Cat. No. 4187)
- Single edge blades (Polysciences, Cat. No. 08410-1)
- Dissecting scissors, dissecting forceps (Roboz)
- Dissecting microscope (Olympus)
- Nylon mesh 40um pore size (BD Biosciences)

- Cell culture centrifuge (Beckman Coulter)
- Tissue culture hood
- CO_2 incubator set to 8% CO_2 and 37°C
- Inverted microscope with fluorescence, phase contrast objectives (phase x4, x10, x20) from Zeiss
- Rotator at 37° incubator
- Cavity slide (Ted Pella, Cat. No. 260241)

REAGENT SETUP

- **Harvest medium:** DMEM containing 10% FBS, 1X Glutamax and 1X penicillin/streptomycin solution. Store at 4°C for a month.
- **Collagenase solution:** Weigh appropriate amount and dissolve collagenase type I in RPMI medium such that 1ml has 1900 units. Filter through a 0.22µm filter unit. Prepare 500ul aliquots and store at −20°C. Thaw and use at a final concentration of 190 units/ml
- **Dispase solution:** Weigh appropriate amount of Dispase and dissolve in PrEGM medium to a concentration of 20 mg/ml (20X). Filter through 0.22µm filter unit and store as 500ul aliquots at −20°C. Thaw immediately before use and add to Matrigel to a final concentration of 1mg/ml (1X) i.e. 50ul for a well containing 1ml medium.

- **PrEGM medium:** Add the thawed supplements to the basal medium. Aliquot into 40 ml aliquots. Store an aliquot at 4°C for a month and freeze the remaining aliquots for long term storage at −20°C.
- **Dihydrotestosterone (DHT) stock:** Dissolve in ethanol to a final concentration of 10^{-3} M. Store at −20°Cfor up to a year.
- **1% Trypsin:** Dilute the 2.5% Trypsin to 1% in sterile 1x PBS and make 500ul one time use aliquots. Store at -20°C.
- **Medium for growing UGSM cells:** DMEM-High Glucose is supplemented with 5% FBS, 5% NuSerum, 1X Glutamax, 1X penicillin/streptomycin solution, 0.01μM DHT, 25ug/ml insulin. Store at 4°C for a month.

PROCEDURE

a) Isolation of Prostate Epithelial Cells:

1. Harvest the prostate from a 4-8 week old mouse and place it in a petri dish containing cold harvest media
2. Clean the prostate of seminal vesicles, urinary bladder, ureter, etc. Refer to Fig. 3.1 for visual aid.

Tip: Do not discard the urethra as recent reports have demonstrated the presence of stem/progenitor cells at the proximal end of the urethra. Remove the muscle tissue around the urethra by gently pulling with fine tweezers.

3. Transfer the prostate tissue and the urethra to a new petri-dish and mince it with a razor blade.

4. Transfer the minced tissue to a 15ml falcon tube containing 5ml pre-warmed digestion media per prostate tissue.
5. Incubate the tube at 37°C on a rotator for 90 min.
6. After incubation, gently pass the cells through 22 ½ G needle 4-5 times

Caution: Be gentle and do not put excessive pressure as it will result in rupturing and consequent loss of cells.

7. Spin the cells down at 1800rpm for 5 min
8. Discard the supernatant and wash the cell pellet in 5ml of pre-warmed PBS
9. Spin the cells down at 1800rpm for 5 min
10. Discard the supernatant and add 2ml of 0.05% trypsin/EDTA per prostate. Incubate the tube in a 37°C water bath for 5 min
11. Add equal volume of FBS containing media and pipette the cell suspension with a 1ml pipette 5-6 times
12. Pass the cell suspension gently through 22 ½ G syringe 4-5 times
13. Pass the cells 5-6 times through 25 ½ G needle
14. Strain the cells through a 40um cell strainer to remove any cell clumps
15. Spin down the cells at 1800rpm for 5 minutes
16. Resuspend the cells in harvest media.
17. Count the cells using hemocytometer

Note: The number of cells obtained per prostate varies from $5x10^5$ to $1x10^6$ cells

b) Culturing prostaspheres:

1. Dilute the cells in PrEGM media to a final cell density of 10,000 cells per 50ul media

Tip: One can also infect the cells to over-express or downregulate gene expression in PrSCs using lentivirus at this step. The cells are infected at an MOI of 20-50 using the spinoculation method. The cell suspension is mixed with lentiviral supernatant and polybrene (Final Concentration: 8ug/ml) in a total volume of 400ul and transferred to a well of a 12 well plate. The plate is then centrifuged at 1800 rpm for 2 hours at 25°C. Following infection, the media is gently aspirated from the wells and the cells adhering to the plate are resuspended in an appropriate volume of PrEGM media.

18. Prepare cell suspension containing 10,000 cells per 50ul PrEGM media
19. Transfer 50ul of the cell suspension in a sterile tube
20. Mix the cell suspension with 50ul Matrigel and quickly plate it along the rim of a well of a 12 well plate. Swirl the plate to allow for even distribution of the cells.
21. Incubate for 30 min at 37°C to allow the Matrigel solidify
22. Gently add 1ml of pre-warmed PrEGM to the center of each well.
23. Incubate the plate in a 37°C/ 5% CO_2 incubator

Caution: Do not add cold media as Matrigel will melt

24. Change media every 3 days
25. Cells will grow as spheres and will be ready to be harvested by day 7-10

c) Harvesting prostate spheres:

1. Aspirate media and add 1ml of media containing Dispase.
2. Incubate the plate for 1hr at 37°C.
3. Collect the spheres and transfer them to a 15ml conical tube.
4. Spin down the spheres at 1000rpm for 5 min
5. Resuspend the spheres in harvest media and pass them through a 40um cell strainer to get rid of single cells as well as endogenous stromal cells
6. Flush the cell strainer from the side opposite to where the spheres were collected with harvest media to dislodge them into a well of a 6 well plate.
7. Transfer the spheres in a 15ml conical tube and spin them at 1000rpm for 5 min
8. Discard the supernatant and wash them with200ul of 1X PBS containing 0.5% BSA and 2mM EDTA.
9. Spin down the spheres at 1000rpm for 5min
10. Add 500ul of pre-warmed 0.05% Trypsin/EDTA solution and incubate for 10min at RT
11. Neutralize trypsin by adding equal volume of harvest media
12. Pass the cells through 21G needle 5-6 times followed by a 27 ½ G needle about 5-6 times to break the spheres into single cells
13. Pass the cells through a 40um cell strainer to obtain a single cell suspension.
14. Transfer the cells in a 15ml conical tube and spin at 1800rpm for 5min

15. Resuspend the cells in PrEGM media
16. Count the cells using Hemocytometer

d) Co-Culture assay (Fig. 3.1):

1. Prepare a cell suspension containing 5,000 PrEC and 5,000 UGSM cells in 50ul PrEGM media
2. Mix the cell suspension with 50ul of Matrigel and plate the mixture around the rim of a well in a 12-well plate
3. Incubate at 37°C incubator for 30 min to let the matigel-cell mixture solidify
4. Add 1ml of pre-warmed PrEGM media containing 5,000 UGSM cells/ml
5. Incubate the cells in 37°C incubator 5% CO2 for 6-7 days without media change
6. Count the number and measure the diameter/ area of the spheres

TIP: It is also possible to perform this co-culture assay with prostate epithelial stem cells sorted directly from dissociated prostate tissue based on cell surface markers.

e) Isolation of Urogenital Stromal Mesenchyme (UGSM) cells:

1. Harvest the Urogenital System (UGS) from a 16 day old mouse embryo. Refer to Fig. 3.3 for visual aid.
2. Transfer the UGS to a concave well glass slide.
3. Wash the UGS with three time with PBS
4. Incubate UGS with about 250ul of 1% Trypsin at 4°C for 90 min

5. After incubation, gently aspirate the trypsin and wash the UGS 2-3 times with media containing DNase I

Caution: Trypsinization results in cell death with concomitant release of DNA making the UGS clumpy. It is necessary to pay attention during washes so as to prevent inadvertent loss of UGS.

6. Using two 28G needles gently peel off the mesenchyme surrounding the epithelia. Discard the epithelial cells.
7. Wash the UGSM with PBS and transfer it to 15ml falcon tube containing 10ml digestion media.
8. Incubate at 37°C for 90 min on a rotator
9. Spin down the cells and resuspend the pellet in 5ml of UGSM media.
10. Transfer the cell suspension to a 6cm dish

Note: We generally seed cells obtained from about twenty UGS in a 6cm dish

11. Gently wash the cell with PBS next day to remove dead floating cells and add 5ml of media.
12. Change media every 2 days and split at a ratio of 1:2 when confluent

Caution: Do not passage the cells for more than 3-4 passages as these cells start losing their proliferative as well as differentiation capacity. Freeze down cells and store them in liq. Nitrogen for long term storage.

Tip: UGSM cells can be infected using lentiviruses at an MOI of 5-20 using standard infection procedure.

ANTICIPATED RESULT

The protocol we describe here will produce significantly larger spheres compared to the control (Fig. 3.2). In some instances, they form a multi-lobular structure however their relevance is yet to be understood. The investigator can alter gene expression in either epithelial cells or stromal cells or both and screen wide array of settings, developmental or pathophysiological, identifying the contribution of the epithelial compartment and stromal compartment.

TROUBLESHOOTING

Step	Problem	Cause	Suggestion
a17	Very few cells obtained	a) Excessive pressure applied when passing the prostate cells through syringe b) Trypsin/EDTA solution is not stored properly	a) Apply gentle pressure and avoid forming bubbles b) Store as 2-5ml one time use aliquots of Trypsin/EDTA at -20°C
b25	Few spheres observed	Cell apoptosis	Supplement the media with 10uM of ROCK inhibitor (Y-27632) for the first 3 days of culture
c5	Loss of spheres after passing through cell strainer	Attachment of spheres to the strainer membrane	Incubate the cell strainer in 10% FBS containing media for 20-30 min at RT to neutralize the membrane charge.
c10	Incomplete dissociation of spheres into single cells	a) Trypsin/EDTA solution is old/inactivated b) Reduced incubation in trypsin/EDTA solution c) Incorrect needle	a) Prepare single use aliquots of Trypsin/EDTA at -20°C b) Make sure the spheres are treated with trypsin/EDTA for 10 min at RT

		thickness (gauge)	c) Use a 27 ½ G or 28G needle
e5	Accidental loss of UGS	UGS being transferred with the viscous solution	Transfer the solution after washes to a sterile petri dish and check for presence of UGS before discarding it.
e12	UGSM cells not growing	Low seeding density	Increase the seeding density of the cells.

References:

1. Wang, Y., et al., *Cell differentiation lineage in the prostate.* Differentiation, 2001. **68**(4-5): p. 270-9.
2. Aumuller, G., et al., *Semiquantitative morphology of human prostatic development and regional distribution of prostatic neuroendocrine cells.* Prostate, 2001. **46**(2): p. 108-15.
3. English, H.F., R.J. Santen, and J.T. Isaacs, *Response of glandular versus basal rat ventral prostatic epithelial cells to androgen withdrawal and replacement.* Prostate, 1987. **11**(3): p. 229-42.
4. Kyprianou, N. and J.T. Isaacs, *Activation of programmed cell death in the rat ventral prostate after castration.* Endocrinology, 1988. **122**(2): p. 552-62.
5. Xin, L., et al., *Self-renewal and multilineage differentiation in vitro from murine prostate stem cells.* Stem Cells, 2007. **25**(11): p. 2760-9.
6. Ferraro, F., C.L. Celso, and D. Scadden, *Adult stem cels and their niches.* Adv Exp Med Biol, 2010. **695**: p. 155-68.
7. Cunha, G.R. and L.W. Chung, *Stromal-epithelial interactions--I. Induction of prostatic phenotype in urothelium of testicular feminized (Tfm/y) mice.* J Steroid Biochem, 1981. **14**(12): p. 1317-24.
8. Cunha, G.R. and B. Lung, *The possible influence of temporal factors in androgenic responsiveness of urogenital tissue recombinants from wild-type and androgen-insensitive (Tfm) mice.* J Exp Zool, 1978. **205**(2): p. 181-93.

9. Wan, X., et al., *Prostate cancer cell-stromal cell crosstalk via FGFR1 mediates antitumor activity of dovitinib in bone metastases.* Sci Transl Med, 2014. **6**(252): p. 252ra122.

Figures:

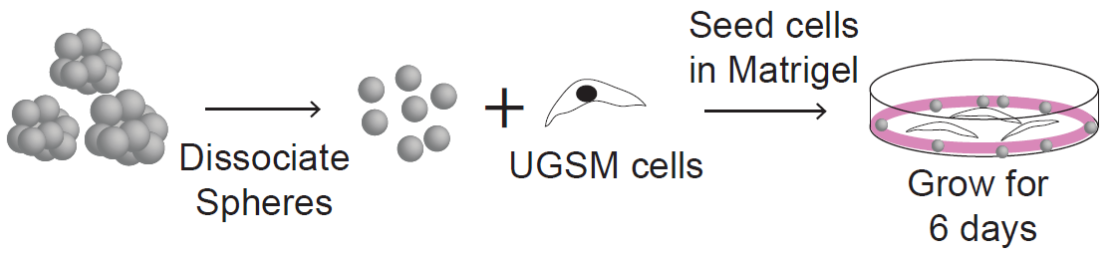

Figure 3.1 Schematic representation of prostasphere formation in the presence of stromal cells. Primary spheres are dissociated and the cells are seeded with UGSM cells in the matrix of Matrigel for six days without any media change.

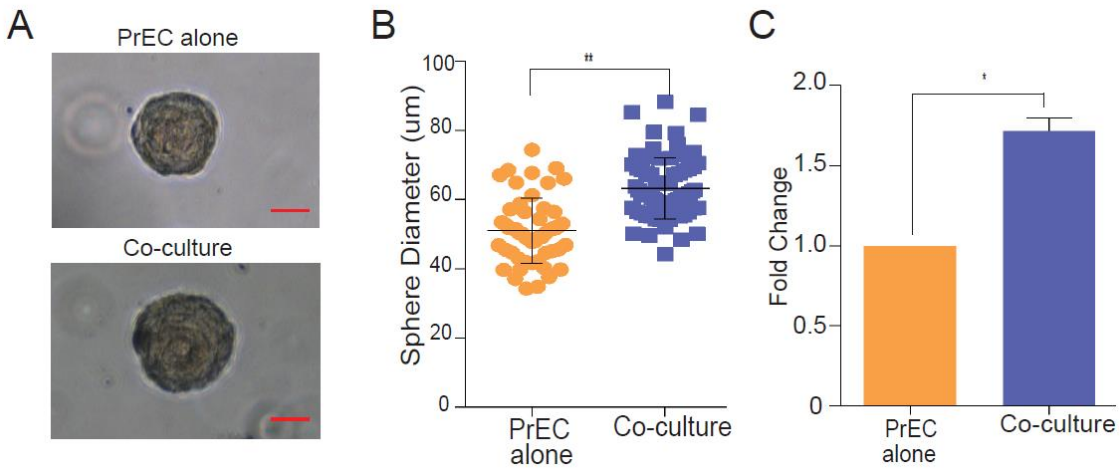

Figure 3.2 UGSM enhances sphere formation capacity. (A) Representative image of spheres grown in the presence and absence of UGSM. (B) Images of prostate spheres and bar graph comparing sphere size. Results show means ± SD from three independent experiments. (Scale = 25 µm). (C) Bar graph comparing sphere numbers. Results show

means ± SD from three independent experiments. Statistical significance was assessed by Student's t-test (*p < .05, **p < .01)

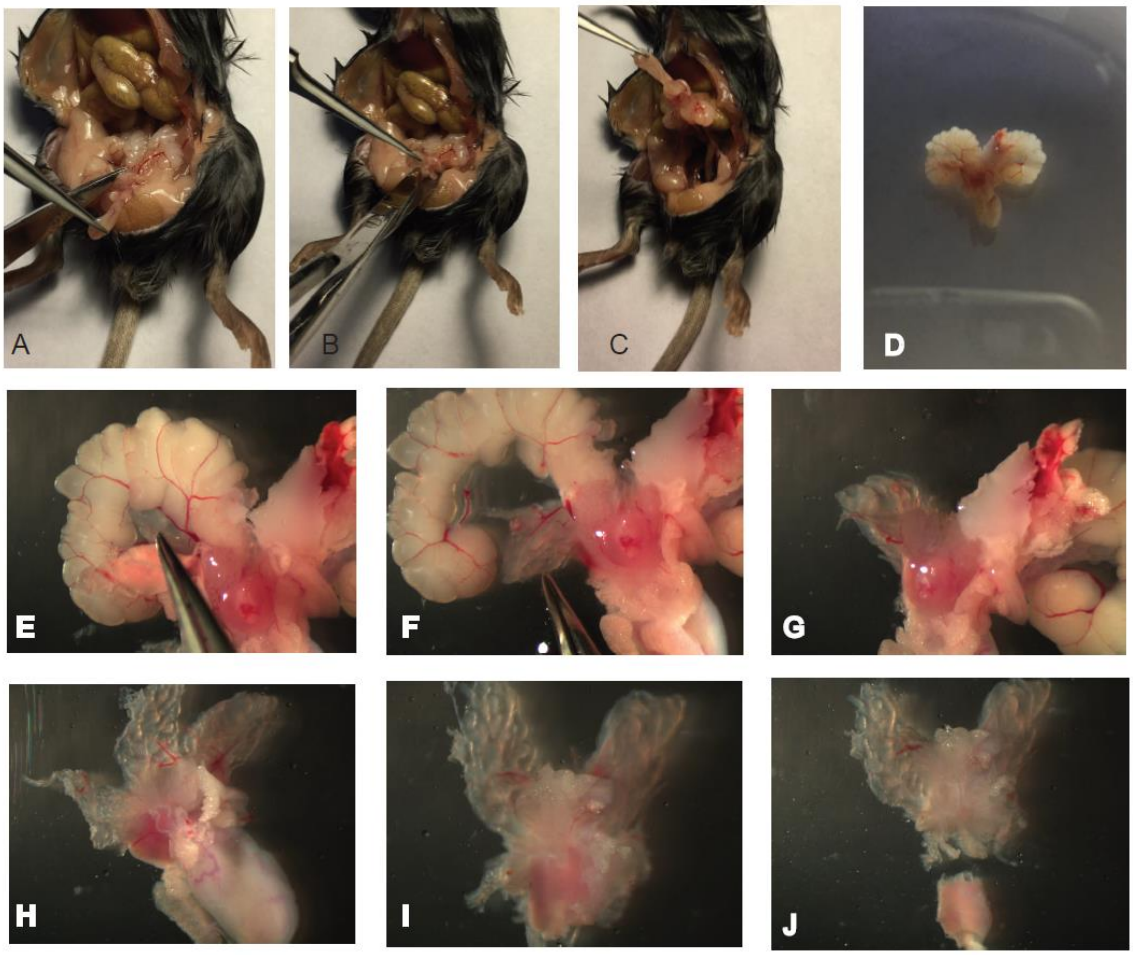

Figure 3.3 Procedure of isolating epithelial cells from prostate gland. (A) Exposed abdomen of a 6 week old male mice. (B, C) Bladder held with a forcep and incision made underneath to cut the connective tissue. (D) Harvested prostate in sterile PBS. (E, F, G) Anterior prostate lobe being released from the seminal vesicles. The seminal vesicle is cut. (H) Prostate gland after removal of both the seminal vesicles. (I) Bladder removed from the prostate. (J) Removal of urethra from the prostate.

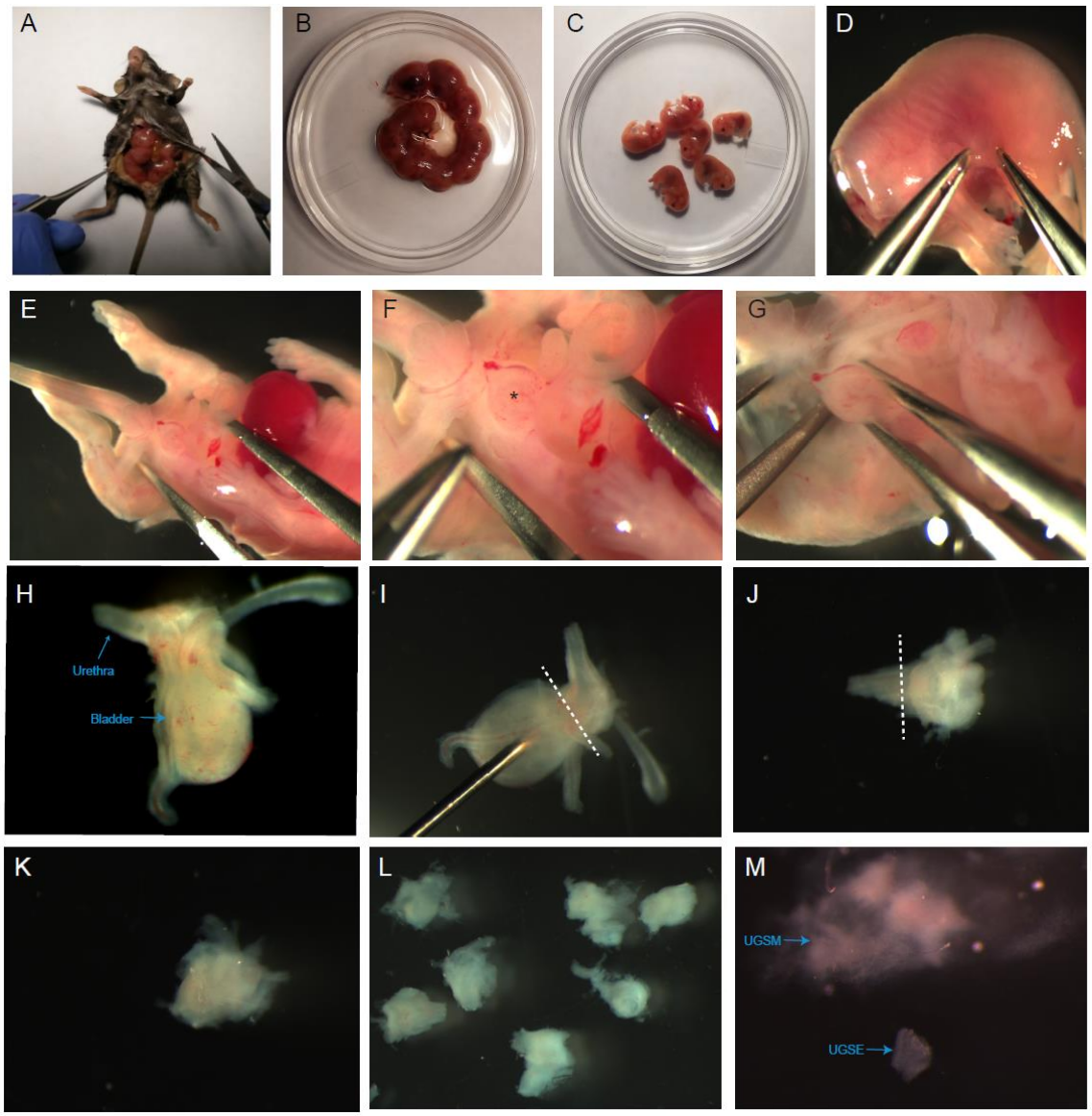

Figure 3.4 Procedure of isolating Urogenital Sinus Mesenchyme (UGSM) and its processing. (A) Exposed abdomen of a pregnant mouse at 16 day post coitum (d.p.c). (B) Uterine horns placed in sterile PBS in a petri dish (C) Embryos separated from their placenta and embryo sac. (D) Embryos cut in half and placed in a new petri dish with sterile PBS. (E) Exposed abdominal region of the embryo. (F) Magnified view of the Urogenital Sinus (UGS) (* indicates the bladder). (G) UGS is removed by pulling the

bladder gently. (H) Image of an intact UGS. (I, J and K) Removal of the bladder, urethra and the attached tubular structures. (L) Isolated UGS in a concave slide. (M) Representative image of cloudy urogenital sinus mesenchyme (UGSM) and the urogenital sinus epithelium (UGSE) having a shiny translucent appearance after mechanical separation.

CHAPTER 4

HEPARAN SULFATE IS INDISPENSIBLE FOR SPROUTING ANGIOGENESIS

Sumit Rai and Lianchun Wang. To be submitted to Arteriosclerosis, Thrombosis, and Vascular Biology.

Abstract:

Objective: Heparan sulfate (HS) is a ubiquitously expressed anionic polymer expressing diverse sulfated epitopes for interaction with signaling proteins like VEGF, HGF, PDGF, etc. involved in regulating angiogenesis. Previous report from our lab has demonstrated essential requirement of HS in mesoderm differentiation of mouse embryonic stem cells (mESCs). However, recent report suggest chondroitin sulfates (CS) can take over the functional role of HS during embryonic angiogenic sprouting. Thus, it is imperative to account for the discrepancy between the two findings.

Approach and Result: Embryoid bodies (EBs) formed from $Ext1^{f/f}$ and $Ext1^{-/-}$ mESCs were differentiated to endothelial cells on gelatin coated plates or embedded in collagen I matrix, in the presence of Vascular Endothelial Growth Factor (VEGF). Rescue experiments involved exogenous supplementation of heparin and chondroitin sulfate-A (CS-A) wherein it was found that $Ext1^{-/-}$ EBs sprout only in the presence of Heparin. Prolonged differentiation however promoted sprouting of $Ext1^{-/-}$ EBs but was highly diminished.

Conclusion: Our findings suggest that, in this particular model system, there exists no overlap between the functional role of HS and CS in mediating angiogenesis and that there exists a strict requirement of HS in this biological process.

Key Words: Heparan Sulfate, Chondroitin Sulfate, Sprouting Angiogenesis, Mouse Embryonic Stem Cells, Embryoid Body, Vascular Endothelial Growth Factor

Introduction

Embryogenesis is coupled with high metabolic investments fulfilled by the developing vascular system. In mammals, the vascular system originates from aggregates of mesodermal cells, the hemangioblasts, in the yolk sac forming a network of capillaries through a process termed as vasculogenesis[1]. As the embryo grows, the metabolic needs of the embryo intensify. To keep up with this heightened demand, the primitive vascular plexus expands through angiogenesis, formation of new blood vessels from pre-existing ones. Angiogenic processes are not restricted to the developing embryo, but continue postnatally for maintenance of normal physiology. They are also implicated in various patho-physiological conditions like cancer and metastasis. Sprouting angiogenesis is a highly coordinated multistep process with spatial and temporal restrictions [2]. A number of factors like vascular endothelial growth factor (VEGF), fibroblast growth factor (FGF) and hepatocyte growth factor (HGF) are known to interact with the heparan sulfate (HS) chains of various heparan sulfate proteoglycans (HSPG) and regulate this biological process.

Heparan sulfate is a linear polysaccharide, existing predominantly on the cell surface and in the extracellular matrix, composed of a backbone of N-acetyl glucosamine (GlcNAc) and glucuronic acid (GlcA) residues that further undergoes a number of modifications likes N-sulfation, epimerization and O-sulfation. Utilizing *in vitro* cell based assays and conditional knockout animal models has shed some light on the vascular development role of HS. Embryonic stem cell (ESC) when differentiated in suspension form aggregates termed as Embryoid Bodies (EBs) resembling a gastrulating embryo. When

cultured within a matrix of collagen I, in the presence of VEGF, these EBs recapitulate the process of sprouting angiogenesis [3]. Utilizing this assay, Le Jan et al recently demonstrated that *Ext1*$^{-/-}$ EBs are capable of undergoing sprouting angiogenesis with chondroitin sulfate (CS) taking over the functions of HS [4]. However, this is in contrast to our finding wherein *Ext1*$^{-/-}$ mESCs exhibit mesodermal differentiation defect [5]. To account for disparity between these two findings we performed the angiogenesis assay with the Ext1$^{f/f}$ mESC derived Ext1$^{-/-}$ESCs and found impaired sprouting in Ext1$^{-/-}$ EBs, validating our earlier finding.

Results

We have previously reported lineage commitment defect in Ext1-/- mESCs [6]. However, when forced to differentiate they exhibit mesodermal differentiation defect [5]. Forced differentiation of Ext1$^{-/-}$ EBs for 12 days, on gelatin coated plates, in the presence of VEGF, as expected, did not result in the emergence of endothelial cell (Fig. 4.1A). High doses of fibroblast growth factor (FGF) 2 as well as heparin, known to overcome this mesodermal differentiation block [5], gave rise to endothelial cells, the differentiation being further augmented by VEGF. However, supplementation of CS-A was unable to aid the differentiation process, even in presence of VEGF (Fig. 4.1A).

To determine if contrasting results obtained were a consequence of the monolayer differentiation of EB adopted, differentiation was performed in a matrix of collagen I. We found that in the presence of VEGF, at day 12 of differentiation, most Ext1$^{-/-}$ EBs failed to sprout while Ext1$^{f/f}$ EBs exhibited substantial sprouting phenotype. To determine the

identity of these sprouts, staining with endothelial cells marker, CD31 and VEGFR2 was performed. Sprouts from $Ext1^{f/f}$ EBs stained strongly for the two antigens (Fig. 4.1B, D). Heparin, a highly sulfated analogue of HS, is known to potentiate VEGF signaling [7]. Culturing $Ext1^{-/-}$ EBs, in presence of VEGF, with heparin resulted in vigorous sprouting and tube formation (Fig. 4.1C,D). To confirm the finding of functional overlap between HS and CS in mediating VEGF induced angiogenesis, we performed the assay in the presence of chondroitin sulfate-A. Interestingly, CS was unable to rescue the abolished sprouting phenotype of $Ext1^{-/-}$ EBs.

In the absence of HS, VEGF signaling is diminished but not completely lost. Prolonged culturing of $Ext1^{-/-}$ EBs thus might promote angiogenic sprouting, as observed in $Ndst1^{-/-}$ EBs [4]. Western blotting and qRT-PCR demonstrated the presence of endothelial cells at 17 days of $Ext1^{-/-}$ EB differentiation in monolayer culture suggesting a delayed differentiation of the HS-deficient cells (Fig. 4.1E, F).

Discussion:

Heparan sulfate (HS) chains bind to a plethora of growth factors regulating various biological processes. Numerous *in vitro* studies as well as research on conditional knockout animal models have established important roles of HS in vascular development both during embryogenesis and in adult. Previous report from our lab has demonstrated defective mesodermal differentiation of $Ext1^{-/-}$ mESCs [6]. This differentiation block can only be overcome in the presence of heparin or high doses of FGF-2 [5]. However, Le Jan et al recently reported evidence of sprouting angiogenesis and tube formation in $Ext1^{-/-}$ EBs, employing an *in-vitro* 3D angiogenesis model [4]. To investigate this discrepancy,

we first differentiated Ext1$^{-/-}$ EBs, on gelatin coated plates, in the presence of heparin and high doses of FGF2, both shown to facilitate mesodermal differentiation in HS deficient mESC [5]. Supplementing media with heparin and FGF2 promoted emergence of VE-Cadherin expressing endothelial cells with the differentiation being augmented in the presence of VEGF. VEGFR2 expression was not detected when differentiation proceeded in presence of FGF-2 possibly due to multiple mechanisms regulating high turnover of the receptor. In contrast, VE-Cadherin which is a structural protein mediating cell-cell adhesion and is not subjected to similar turnover rates under normal conditions. A higher level of differentiation was seen in heparin treated cultures due to its involvement in various signaling pathways e.g. BMP, Wnt, TGFβ [8] [9-11]. CS-A, even in the presence of VEGF, was unable to assist in the differentiation indicating the necessity of HS epitopes for appropriate regulation of vascular development.

These findings, in line with our previously published report, were in contrast with the studies of Le Jan et al requiring us to carry out the differentiation under similar conditions. Using this 3-D angiogenesis model we further establish that EBs derived from Ext1$^{-/-}$ mESCs were unable to sprout. Unlike CS-A, Heparin was able to rescue this sprouting defect, due to its well-known function in potentiating VEGF signaling. It is possible that the CS-A used in this study did not bear the structural determinants necessary to mediate VEGF induced angiogenesis in the absence of HS. However, a direct interaction of VEGF with CS-A is yet unknown. Prolonged differentiation of EBs, surprisingly, led to the emergence of endothelial cells as evidenced by western blot and qPCR analysis. The extended length of this differentiation regime might have pushed the

$Ext1^{-/-}$ EBs towards differentiation since VEGF signaling is not lost but diminished in the absence of HS.

Sprouting of $Ext1^{-/-}$ EBs, in Le Jan et al report, can possibly be attributed to HSPG's secreted by the feeder layer [13] which can compensate for the loss of HS in $Ext1^{-/-}$ mESCs pushing the cells from "naïve" state to differentiation primed state [14]. Another possibility resulting in sprouting of $Ext1^{-/-}$ EBs can be due contaminating mouse embryonic fibroblast (MEF) feeder cells. Even though the feeders are mitotically inactivated, either through gamma-radiation or mitomycin-C treatment, they are known to be carried over during routine culture of mESCs. By passaging the mESCs, in the absence of feeders, for four to five passages the contamination of feeders is reduced to less than 0.1% and completely lost by passage six or seven [15]. These HS expressing feeders can potentiate VEGF mediated signaling in an *in-trans* fashion and thus result in sprouting [16]. It is also possible that the discrepancy can be attributed to differences in mESC lines used for the assays. The two mESC lines used by Le Jan et al had different background and possibly different propensity to differentiate [17, 18]. However, the $Ext1^{-/-}$ mESCs, in our case, were derived from $Ext1^{flox/flox}$ mESC line isolated in-house thus providing us with a gold standard to compare our results with.

In conclusion, our current study reveals that HS is a crucial regulator of self-renewal and cell fate commitment in ESCs. We demonstrate that CS is unable to overcome mesodermal differentiation defect in $Ext1^{-/-}$ ESC and that there exist an essential requirement of heparan sulfate in regulating sprouting angiogenesis during early embryonic development.

Materials and Methods:

Culture of embryonic stem cells (ESCs): Establishment of $Ext1^{flox/flox}$ and $Ext1^{-/-}$ mESC was reported previously. Frozen stocks of Embryonic stem cells (ESCs) were thawed onto plates coated with irradiated mouse embryonic fibroblasts in DMEM-High Glucose with Gutamax (Thermo Fischer Scientific), 25mM HEPES (Thermo Fischer Scientific), 1.2mM sodium pyruvate (Thermo Fischer Scientific), 150uM monothioglycerol (Sigma), 15% fetal bovine serum (Atlanta Biologicals, Atlanta, GA), and 1000 units/ml of leukemia inhibitory factor (LIF). The colonies were trypsinized and mESCs thereafter were routinely cultured on 0.1% gelatin coated plates. Feeder cells were removed by transferring the trypsinized cell suspension to uncoated plate for 30min at 37°C, 5%CO_2. Feeder cells rapidly attach to the dish while the mESCs remain in suspension. The media is gently aspirated and unattached cells are transferred to gelatin coated plates and cultured. This selective depletion of feeders was performed for the first 3 passages and experiments were carried out only after cells have undergone 5 passages on gelatin coated plates to minimize contribution from contaminating feeder cells (capable of secreting cytokines and HSPGs in the surrounding media), if any.

Formation and culture of Embryoid Bodies: Briefly, at day 0, 1200 ESCs were aggregated in hanging drops (20 μl) without LIF. At day 4, single embryoid bodies was transferred to a gelatin coated 6 well plate or collagen I suspension (pH 7.2-7.4) composed of Ham's F12 medium (Corning), 6.26 mM NaOH (Sigma), 12.5 mM HEPES, 0.117% NaHCO3 (Sigma), 1% glutamax I (GIBCO), and 1.5 mg/ml collagen I (Trevigen, Gaithersburg,MD). Medium containing FGF2 (200ng/ml, R&D systems), VEGF165

(30ng/ml, R&D biotechnology), with or without heparin from pig intestine (M_r = 12,000–15,000) or CS-A from bovine trachea (Sigma), was changed every third day.

Immunostaining of Embryoid Bodies: Embryoid bodies in collagen gels were fixed in 4% p-formaldehyde in phosphate-buffered saline (PBS), blocked with 3% bovine serum albumin (BSA) followed by sequential overnight incubations with primary and secondary antibodies. DAPI was used to visualize the nuclei. The samples were analyzed using Nikon A1 confocal microscope (Nikon). The following primary antibodies were used: rat anti-mouse CD31 antibody (BD Biosciences, #550274) and rabbit anti-mouse VEGFR2 (CST, #5320). Secondary antibodies were: Alexa Fluor 488 goat anti-rat IgG and Alexa Fluor 594 goat anti-rabbit IgG.

RNA isolation and qRT–PCR: Total RNA was isolated from cells using the RNeasy Plus Mini kit (Qiagen, Valencia, CA). Reverse transcription was performed using iScript cDNA synthesis kit (Bio Rad, CA). qRT–PCR was performed using the iQ SYBR Green Supermix (Bio Rad, CA) on an ABI Step one plus real-time PCR system (Applied Biosystems, Foster City, CA). After synthesis, cDNA was used in PCR reaction with gene-specific primers for VE-Cadherin, forward primer: 5'-TTTGGAATCAAATGCACATCG-3' and reverse primer: 5'-AGCACATACTTAGCATTCTGG-3'; and VEGFR2, forward primer: 5'-ACATAGCCTCCACTGTTTATG-3' and reverse primer: 5'-GTTCTTGTTCTCGGTGATGTA-3'.

Western Blotting: Cells were lysed in RIPA buffer (20 mM Tris-HCl, pH 7.5, 150 mM NaCl, 1 mM Na_2EDTA, 1 mM EGTA, 1% NP-40, 1% sodium deoxycholate, 2.5 mM sodium pyrophosphate, 1 mM β-glycerophosphate and 1 mM Na3VO4) with protease inhibitors (Roche Applied Science) and phosphatase inhibitors 2 and 3 (Sigma). Protein concentrations were determined by a Bradford Assay kit (Bio-Rad). Protein was separated by 10% SDS/PAGE and transferred onto a Nitrocellulose membrane (Amersham Biosciences, Arlington Heights, IL). The membrane was blocked with 5% skim milk, and subsequently incubated with primary antibodies, rat anti-mouse VE-Cadherin antibody (Biolegend, # 138101) and rabbit anti-VEGFR2 (Cell signaling technology, #2479), at 4 °C overnight followed by incubation with peroxidase-conjugated goat anti-rat IgG or goat anti-rabbit IgG (CST, Danvers, MA), and developed with Amersham ECL reagent (GE Healthcare Ltd., Buckinghamshire, UK).

References

1. Haar, J.L. and G.A. Ackerman, *A phase and electron microscopic study of vasculogenesis and erythropoiesis in the yolk sac of the mouse.* Anat Rec, 1971. **170**(2): p. 199-223.
2. Ribatti, D. and E. Crivellato, *"Sprouting angiogenesis", a reappraisal.* Dev Biol, 2012. **372**(2): p. 157-65.
3. Feraud, O., Y. Cao, and D. Vittet, *Embryonic stem cell-derived embryoid bodies development in collagen gels recapitulates sprouting angiogenesis.* Lab Invest, 2001. **81**(12): p. 1669-81.
4. Le Jan, S., et al., *Functional overlap between chondroitin and heparan sulfate proteoglycans during VEGF-induced sprouting angiogenesis.* Arterioscler Thromb Vasc Biol, 2012. **32**(5): p. 1255-63.
5. Kraushaar, D.C., et al., *Heparan sulfate facilitates FGF and BMP signaling to drive mesoderm differentiation of mouse embryonic stem cells.* J Biol Chem, 2012. **287**(27): p. 22691-700.
6. Kraushaar, D.C., Y. Yamaguchi, and L. Wang, *Heparan sulfate is required for embryonic stem cells to exit from self-renewal.* J Biol Chem, 2010. **285**(8): p. 5907-16.
7. Ito, N. and L. Claesson-Welsh, *Dual effects of heparin on VEGF binding to VEGF receptor-1 and transduction of biological responses.* Angiogenesis, 1999. **3**(2): p. 159-66.

8. Lee, J., et al., *Structural determinants of heparin-transforming growth factor-beta1 interactions and their effects on signaling.* Glycobiology, 2015. **25**(12): p. 1491-504.

9. Jastrebova, N., et al., *Heparan sulfate-related oligosaccharides in ternary complex formation with fibroblast growth factors 1 and 2 and their receptors.* J Biol Chem, 2006. **281**(37): p. 26884-92.

10. Fuerer, C., S.J. Habib, and R. Nusse, *A study on the interactions between heparan sulfate proteoglycans and Wnt proteins.* Dev Dyn, 2010. **239**(1): p. 184-90.

11. Kuo, W.J., M.A. Digman, and A.D. Lander, *Heparan sulfate acts as a bone morphogenetic protein coreceptor by facilitating ligand-induced receptor hetero-oligomerization.* Mol Biol Cell, 2010. **21**(22): p. 4028-41.

12. Lu, H., et al., *Glycosaminoglycans in Human and Bovine Serum: Detection of Twenty-Four Heparan Sulfate and Chondroitin Sulfate Motifs Including a Novel Sialic Acid-modified Chondroitin Sulfate Linkage Hexasaccharide.* Glycobiol Insights, 2010. **2010**(2): p. 13-28.

13. Levenstein, M.E., et al., *Secreted proteoglycans directly mediate human embryonic stem cell-basic fibroblast growth factor 2 interactions critical for proliferation.* Stem Cells, 2008. **26**(12): p. 3099-107.

14. Nichols, J. and A. Smith, *Naive and primed pluripotent states.* Cell Stem Cell, 2009. **4**(6): p. 487-92.

15. Boheler, K.R. and K.V. Tarasov, *SAGE analysis to identify embryonic stem cell-predominant transcripts.* Methods Mol Biol, 2006. **329**: p. 195-221.

16. Jakobsson, L., et al., *Heparan sulfate in trans potentiates VEGFR-mediated angiogenesis.* Dev Cell, 2006. **10**(5): p. 625-34.

17. Lin, X., et al., *Disruption of gastrulation and heparan sulfate biosynthesis in EXT1-deficient mice.* Dev Biol, 2000. **224**(2): p. 299-311.

18. Nagy, A., et al., *Derivation of completely cell culture-derived mice from early-passage embryonic stem cells.* Proc Natl Acad Sci U S A, 1993. **90**(18): p. 8424-8.

Figure:

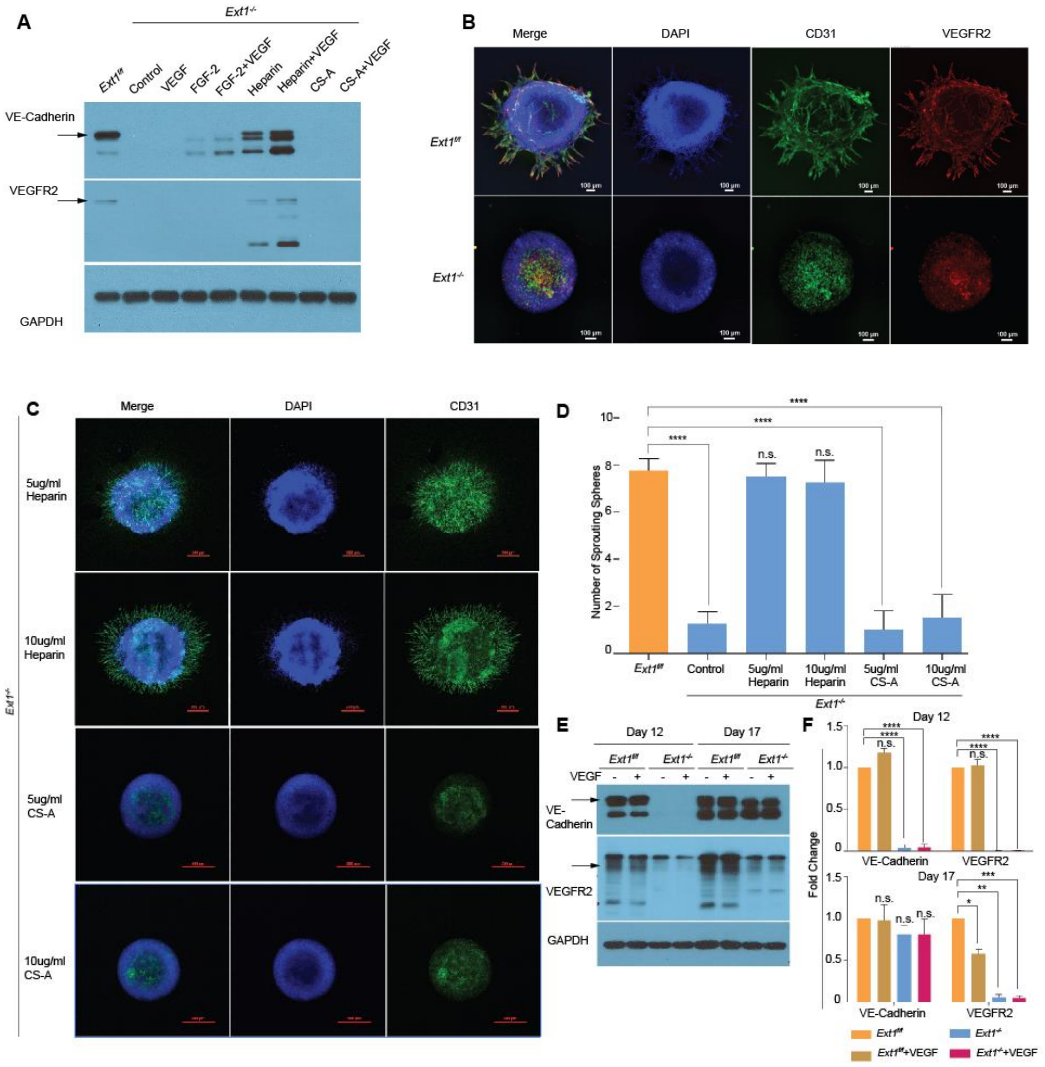

Fig. 4.1 HS is indispensable for sprouting angiogenesis. (A) Western Blot for endothelial specific marker after differentiation of $Ext1^{f/f}$ and $Ext1^{-/-}$ EBs on gelatin coated plates for 12 days. Arrows represent the correct band size. (B) $Ext1^{f/f}$ and $Ext1^{-/-}$ EBs grown in collagen I for 12 days in the presence of VEGFA (30 ng/ml). ECs were visualized by staining for CD31 and VEGFR2 (Scale=100µm). (C) $Ext1^{-/-}$ EBs grown in collagen I for 12 days in the presence of VEGFA (30 ng/ml) with exogenous

supplementation of heparin and CS-A. ECs were visualized by staining for CD31 (Scale = 500μm). (D) Bar graph comparing sprouted observed under different differentiation conditions. Results show means ± SD from four independent experiments. Statistical significance was assessed by Student's t-test (*p < .05, **p < .01, ***p<.001) (E) Western Blot for endothelial specific marker from EBs differentiated on gelatin coated plates for 12 and 17 days. (F) qRT-PCR analysis of endothelial specific markers after differentiation of $Ext1^{f/f}$ and $Ext1^{-/-}$ EBs on gelatin coated plates for 12 and 17 days. Results show means ± SD from three independent experiments. Statistical significance was assessed by Student's t-test (*p < .05, **p < .01, ***p<.001, ****p<0.0001)

CHAPTER 5.

APPLICATIONS AND FUTURE PERSPECTIVES

HS is a ubiquitously expressed polysaccharide bearing various sulfation modifications on a backbone of N-acetyl-glucosamine (GlcNAc) and glucuronic acid (GlcA) or iduronic acid (IdoA) residues [1]. The HS chains are found as glycocongugates covalently linked to a core protein forming the heparan sulfate proteoglycans (HSPGs) [2-4]. HSPGs are present on the cell surface (including syndecans and glypicans) and within the ECM (including perlecan, agrin and others) where they interact with numerous proteins including growth factors, morphogens, chemokines, extracellular proteases, and adhesive proteins [2-5]. The HS chain composition, charge density, degree and pattern of sulfation allows for highly specific interactions with various proteins. Spatiotemporal regulation of the enzymes involved in the biosynthesis as well as post-synthetic remodeling of the HS chains result in highly heterogeneous HS structures on the same cell [6-8]. These specific but promiscuous interactions of HS with various proteins have been well documented and implicated in a number of developmental as well as pathophysiological processes [9, 10] .

The contribution of heparan sulfate in self-renewal and cell fate commitment of prostate stem cells (PrSCs):

The role of HS has been extensively investigated in the context of early embryonic development [11, 12]. The generation of mice exhibiting conditional loss of HS biosynthetic enzymes have greatly improved our understanding of HS function in

mammalian organisms and further affirmed the importance of HS during vertebrate development (Table 5.1). Studies from our lab and others have reported essential role of HS in embryonic stem cell fate commitment and lineage establishment [10, 13-15]. However, the importance of HS in adult stem cell biology has largely been unexplored.

In this dissertation work, we have identified HS as a novel factor in the maintenance of the prostate stem cell (PrSC) function. Using an *in vitro* spheroid assay, we show that ablation of HS biosynthesis by genetic deletion of *Ext1*, the enzyme essential for HS biosynthesis, results in the loss of PrSC self-renewal potential. It is interesting to note that in the spheroid assay, PrSCs are embedded in Matrigel, a solubilized extracellular matrix (ECM) rich in HSPGs, to form spheroids. This allows for the likelihood of HSPGs or HS chains present in the matrix to sustain self-renewal of the PrSCs. This possibility is further supported by the observation that p63+ PrSCs in these spheroids are mostly present towards the periphery of the spheres found to be in direct contact with the ECM [16]. This is similar to *in vivo* situation wherein the $p63^{+}$ cells line the basement membrane, a rich source of HSPGs [17, 18]. Thus, enzymatic treatment of matrigel with heparitinase would result in efficient digestion of HS chains of the matrix and would provide insight into the role of matrix HS/ HSPGs in supporting self-renewal of PrSCs. Ablation of HS chains in the matrix through enzymatic treatment may improve efforts to maintain the PrSC state in culture. It is also possible that heparitinase treatment might remove growth factors supporting proliferation and self-renewal of PrSCs. However, this will still substantiate the role of HS interacting protein(s) that are required in maintaining stem cell identity.

The loss of PrSC HS lead to a decrease in the expression of PrSC marker, p63, with increased differentiation to $CK8^{+}$ luminal cells. This suggests a potential role of HS in cell fate commitment decisions mediating differentiation to luminal cell type. Identifying the spatiotemporal regulatory functions of HS in PrSCs would shed light on HS mediated molecular events that create a balance between self-renewal and cell fate commitment. The finding that luminal cell fate is default differentiation route for PrSCs in the absence of HS has profound implication especially in the field of cancer biology as the majority of prostate cancers exhibit luminal phenotype. *Ext1* is a tumor suppressor gene and was found to have a lower expression in benign prostatic hyperplasia (BPH) and prostate cancer in comparison with normal prostate tissue [19]. *Ext1* was also found to have a higher degree of hypermethylation in high Gleason score vs low Gleason score prostate cancer [20] suggesting a possibility that loss of HS expression can be one of the possible pathways allowing for greater differentiation to luminal cell phenotype.

Heparan sulfate has been extensively studied in model organisms such as *Drosophila* (Table 5.2) and has pioneered our understanding of the role of HS in developmental signaling and embryogenesis. Studies employing transgenic mice have elucidated and confirmed the importance of HS for development in higher organisms (Table 5.1). Thus, these transgenics may serve as important tools to study the role of various biosynthetic enzyme or the specific modifications they impart to the HS chains in regulating PrSC.

Loss of HS enhanced TGFβ inhibitory signals in prostate epithelial cells. However, inhibition of these signals only partially rescued sphere formation. Since HS is a promiscuous partner in many signal transduction cascades it is possible that other HS-

dependent pathways are also differentially modulated resulting in the phenotype [13, 21, 22]. On examination of other signaling pathways we found that Notch as well as Hedgehog signaling were altered (Fig. 5.1). Notch has been reported to prevent PrSC proliferation and to upregulate TGFβ ligands and receptors in the process [23] while the role of Hedgehog (HH) signaling was found to be stage specific during prostate morphogenesis. HH regulates epithelial proliferation and budding before birth while inhibiting epithelial proliferation and ductal branching postnatally. A recent report has showed that EXT1 negatively regulates Notch signaling by interacting with the notch intracellular domain (NICD) [24] supporting our finding of increased Notch signaling in the absence of EXT1 activity. In the absence of HS chains, we found a decrease in the expression of Gli3 transcription factor. Gli3 is a known repressor of the Hedgehog signaling pathway but can also function as an activator. Gli1 expression was not altered while Gli2 was not detected using the qPCR assay. It would be interesting to determine how loss of HS selectively inhibits Gli3 transcription and if this is a common mechanism between the various model systems.

A major finding of this study was the supportive role of urogenital sinus mesenchyme (stroma) HS during prostate development. An intimate relationship exists between the epithelial and the stromal compartment [25, 26]. The two compartment tightly regulate each other's activity in a juxtacrine and paracrine fashion. The stromal compartment maintained HS-depleted PrSCs and allowed for efficient integration of proliferative as well as differentiation signals resulting in efficient regeneration of the prostate tissue in the *in vivo* regeneration assay. It will be important to investigate if this supportive

function is mediated by cell surface or shed HS chains of the UGSM, helping in co-reception, as stromal cells are known to play an essential role in the development and progression of various cancers [27, 28].

Altogether this study has made valuable contributions to the understanding of HS in prostate development as well as PrSC differentiation and will likely lead to finding therapeutic targets in urogenital development, disorders and diseases.

Novel co-culture system to investigate stromal-epithelial stromal interaction during prostate development and carcinogenesis:

Epithelial-Mesenchymal interactions play an integral role during various developmental processes. These interactions have been well documented to allow paracrine as well as juxtacrine factors ensure proper development of the organ system. In rodents, urogenital sinus mesenchyme (UGSM) plays an inductive role in the formation of the prostate gland [26]. *In vivo* tissue recombination assay as well as prostate regeneration assays have been extensively used to study these interactive processes [29-31]. However, these assays are technically challenging and time intensive requiring about 6-8 weeks to reach the end-point. We have developed a novel *in vitro* co-culture system to quantify the interactions between stromal and epithelial compartments in a swift fashion. The assay is amenable to genetic manipulation of the two cellular compartments and is completed within a week. We have successfully employed this assay to determine how paracrine factors affect signaling pathways regulating self-renewal of PrSCs as spheres. It would, however, be interesting to determine if this assay can be used with tumor initiating cells (TICs) and/or myofibroblasts derived from the patient. Major reciprocal interactions, using this system,

can possibly be recognized in promoting carcinogenesis and thus can be utilized as a therapeutic target.

However, the extracellular matrix (ECM) is known to affect the biology of a cell. Since Matrigel is a highly complex and heterogeneous ECM [32], it might not mimic the *in vivo* environment. Therefore, it will be interesting to further develop this assay to employ defined matrix components or chemically synthesized 3D hydrogels to appreciate the importance of matrix components in developmental processes or cancer [33].

The development of the screening platform, reported in this work, allows rapid identification of the epithelial-stromal interactions aiding our understanding of the developmental processes as well as disorders. This assay system can also be employed in the other fields of developmental biology.

Heparan sulfate is required for embryonic sprouting angiogenesis:

The availability of ESCs with defective heparan sulfate (HS) synthesis has been useful in defining the role of HS in ESCs. ESCs provide a novel tool to investigate the molecular mechanisms during early embryonic development. Our lab has previously reported essential requirement of HS for mesodermal differentiation [10, 13]. Recent report suggest functional overlap between chondroitin sulfate (CS) and HS in mediating VEGF induced sprouting angiogenesis [34]. However, thorough investigation, as reported here, confirms our original finding of defective mesodermal differentiation in the absence of HS.

In this study, we show that most EBs formed from HS deficient mESCs were incapable of giving rise to endothelial cells that are known to be of mesodermal origin. However,

we did see formation of endothelial sprouts in some knockout EBs, though dramatically reduced. It would be useful to carry out differentiation in the absence of serum. Serum is known to contain HSPGs as well as various growth factors that can compensate for the loss of HS. This is of importance as it might uncover a novel mechanism wherein CS or other glycans can take over the functions of HS in pathophysiological conditions like cancer. Conditional ablation of HS biosynthesis in endothelial progenitors using transgenic animals would be useful in positively identifying the function in an *in vivo* setting.

Thus, this study demonstrates HS deficient mESC can differentiate to endothelial cells, under prolonged differentiation conditions, suggesting a possible role for other compensatory mechanisms to overcome HS deficiency. This will likely help in the understanding of the signals mediating angiogenesis signals during embryogenesis as well as in diseased state.

References:

1. Sugahara, K. and H. Kitagawa, *Heparin and heparan sulfate biosynthesis.* IUBMB Life, 2002. **54**(4): p. 163-75.
2. Bernfield, M., et al., *Functions of cell surface heparan sulfate proteoglycans.* Annu Rev Biochem, 1999. **68**: p. 729-77.
3. Esko, J.D. and S.B. Selleck, *Order out of chaos: assembly of ligand binding sites in heparan sulfate.* Annu Rev Biochem, 2002. **71**: p. 435-71.
4. Bishop, J.R., M. Schuksz, and J.D. Esko, *Heparan sulphate proteoglycans fine-tune mammalian physiology.* Nature, 2007. **446**(7139): p. 1030-7.
5. Forsberg, E. and L. Kjellen, *Heparan sulfate: lessons from knockout mice.* J Clin Invest, 2001. **108**(2): p. 175-80.
6. Hacker, U., K. Nybakken, and N. Perrimon, *Heparan sulphate proteoglycans: the sweet side of development.* Nat Rev Mol Cell Biol, 2005. **6**(7): p. 530-41.
7. Ornitz, D.M., *FGFs, heparan sulfate and FGFRs: complex interactions essential for development.* Bioessays, 2000. **22**(2): p. 108-12.
8. Pellegrini, L., *Role of heparan sulfate in fibroblast growth factor signalling: a structural view.* Curr Opin Struct Biol, 2001. **11**(5): p. 629-34.
9. Zhang, B., et al., *Heparan sulfate deficiency disrupts developmental angiogenesis and causes congenital diaphragmatic hernia.* J Clin Invest, 2014. **124**(1): p. 209-21.

10. Kraushaar, D.C., Y. Yamaguchi, and L. Wang, *Heparan sulfate is required for embryonic stem cells to exit from self-renewal.* J Biol Chem, 2010. **285**(8): p. 5907-16.

11. Lin, X., et al., *Disruption of gastrulation and heparan sulfate biosynthesis in EXT1-deficient mice.* Dev Biol, 2000. **224**(2): p. 299-311.

12. Stickens, D., et al., *Mice deficient in Ext2 lack heparan sulfate and develop exostoses.* Development, 2005. **132**(22): p. 5055-68.

13. Kraushaar, D.C., et al., *Heparan sulfate facilitates FGF and BMP signaling to drive mesoderm differentiation of mouse embryonic stem cells.* J Biol Chem, 2012. **287**(27): p. 22691-700.

14. Stelling, M.P., et al., *Matrix-bound heparan sulfate is essential for the growth and pluripotency of human embryonic stem cells.* Glycobiology, 2013. **23**(3): p. 337-45.

15. Forsberg, M., et al., *Undersulfation of heparan sulfate restricts differentiation potential of mouse embryonic stem cells.* J Biol Chem, 2012. **287**(14): p. 10853-62.

16. Xin, L., et al., *Self-renewal and multilineage differentiation in vitro from murine prostate stem cells.* Stem Cells, 2007. **25**(11): p. 2760-9.

17. Wang, Y., et al., *Cell differentiation lineage in the prostate.* Differentiation, 2001. **68**(4-5): p. 270-9.

18. Iozzo, R.V., *Basement membrane proteoglycans: from cellar to ceiling.* Nat Rev Mol Cell Biol, 2005. **6**(8): p. 646-56.

19. Suhovskih, A.V., et al., *Transcriptional Activity of Heparan Sulfate Biosynthetic Machinery is Specifically Impaired in Benign Prostate Hyperplasia and Prostate Cancer*. Front Oncol, 2014. **4**: p. 79.

20. Wu, Y., et al., *Methylation profiling identified novel differentially methylated markers including OPCML and FLRT2 in prostate cancer*. Epigenetics, 2016. **11**(4): p. 247-58.

21. Faham, S., et al., *Heparin structure and interactions with basic fibroblast growth factor*. Science, 1996. **271**(5252): p. 1116-20.

22. Chen, J., et al., *Exogenous Heparan Sulfate Enhances the TGF-beta3-Induced Chondrogenesis in Human Mesenchymal Stem Cells by Activating TGF-beta/Smad Signaling.* Stem Cells Int, 2016. **2016**: p. 1520136.

23. Valdez, J.M., et al., *Notch and TGFbeta form a reciprocal positive regulatory loop that suppresses murine prostate basal stem/progenitor cell activity*. Cell Stem Cell, 2012. **11**(5): p. 676-88.

24. Daakour, S., et al., *Systematic interactome mapping of acute lymphoblastic leukemia cancer gene products reveals EXT-1 tumor suppressor as a Notch1 and FBWX7 common interactor*. BMC Cancer, 2016. **16**: p. 335.

25. Sugimura, Y., G.R. Cunha, and A.A. Donjacour, *Morphogenesis of ductal networks in the mouse prostate.* Biol Reprod, 1986. **34**(5): p. 961-71.

26. Cunha, G.R., *The role of androgens in the epithelio-mesenchymal interactions involved in prostatic morphogenesis in embryonic mice.* Anat Rec, 1973. **175**(1): p. 87-96.

27. Mao, Y., et al., *Stromal cells in tumor microenvironment and breast cancer.* Cancer Metastasis Rev, 2013. **32**(1-2): p. 303-15.

28. Kruslin, B., M. Ulamec, and D. Tomas, *Prostate cancer stroma: an important factor in cancer growth and progression.* Bosn J Basic Med Sci, 2015. **15**(2): p. 1-8.

29. Cunha, G.R. and L.W. Chung, *Stromal-epithelial interactions--I. Induction of prostatic phenotype in urothelium of testicular feminized (Tfm/y) mice.* J Steroid Biochem, 1981. **14**(12): p. 1317-24.

30. Kinbara, H., et al., *Evidence of stem cells in the adult prostatic epithelium based upon responsiveness to mesenchymal inductors.* Prostate, 1996. **29**(2): p. 107-16.

31. Xin, L., et al., *In vivo regeneration of murine prostate from dissociated cell populations of postnatal epithelia and urogenital sinus mesenchyme.* Proc Natl Acad Sci U S A, 2003. **100 Suppl 1**: p. 11896-903.

32. Hughes, C.S., L.M. Postovit, and G.A. Lajoie, *Matrigel: a complex protein mixture required for optimal growth of cell culture.* Proteomics, 2010. **10**(9): p. 1886-90.

33. Tibbitt, M.W. and K.S. Anseth, *Hydrogels as extracellular matrix mimics for 3D cell culture.* Biotechnol Bioeng, 2009. **103**(4): p. 655-63.

34. Le Jan, S., et al., *Functional overlap between chondroitin and heparan sulfate proteoglycans during VEGF-induced sprouting angiogenesis.* Arterioscler Thromb Vasc Biol, 2012. **32**(5): p. 1255-63.

35. Lin, X., *Functions of heparan sulfate proteoglycans in cell signaling during development.* Development, 2004. **131**(24): p. 6009-21.

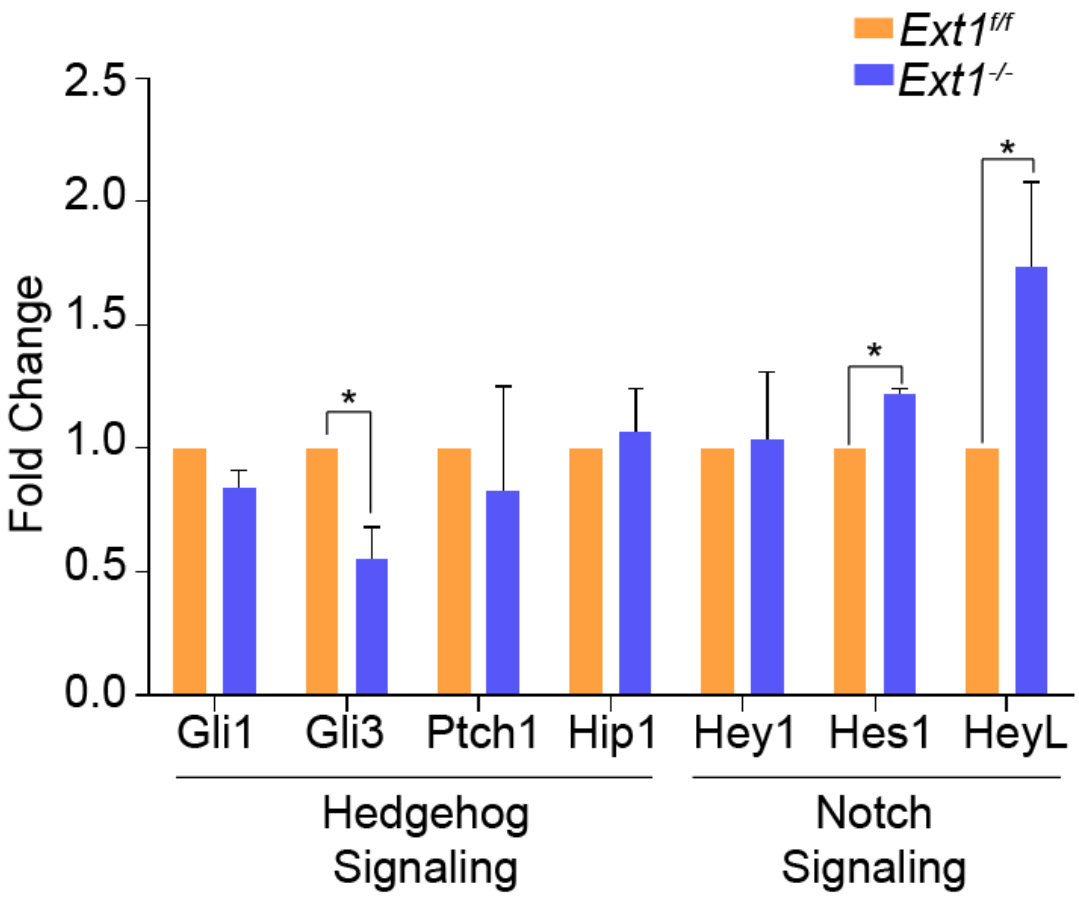

Figure 5.1 Differentially modulated signaling pathways in *Ext1*$^{-/-}$ PrECs. qPCR analysis of genes involved in Hedgehog and Notch signaling pathways. Fold Change normalized to Gapdh. Results represent the mean ± SD of three independent experiments. Statistical significance was assessed by Student's t-test (*$p < .05$).

Table 5.1 Mouse heparan sulfate biosynthesis enzyme mutants

Mutant (Null)	Phenotype	References
Ext1 Ext2	Embryonic lethal. Failure of gastrulation. Lack of primitive streak and malformation of extraembryonic structures	Lin *et al.,* 2000, Stickens *et al.,* 2005
NDST1	Cerebral hypoplasia, craniofacial defects, lens defects	Pan *et al.,* 2006, Grobe *et al.,* 2005, Pallerla *et al.,* 2007
NDST2	Defects in mast cell physiology	Forsberg *et al.,* 1999, Humphries *et al.* 1999
NDST3	Weak hematological phenotype	Pallerla *et al.* 2008
C-5 epimerase	Neonatal lethality. Kidney, lung and skeletal defects	Lin *et al.* 2003
Hs2st	Reduced proliferation of cerebral cortical precursor cells, renal agenesis	McLaughlin *et al.,* 2003, Bullock *et al.,* 1998
Hs3St1	Perinatal lethality, intrauterine growth retardation	Shworak *et al.,* 2002
Hs6st1	Late embryonic lethality. Abnormal placentation.	Habuchi *et al.* 2007

Table 5.2 Drosophila heparan sulfate biosynthetic enzyme mutants.

Modified from [35]

Gene	Mammalian Homolog	Effects on developmental signaling	References
Sugarless (sgl)	UDP-glucose dehydrogenase	Wnt signaling	Binari *et al*., 1997; Hacker *et al*.
Tout-velu (ttv)	Ext1	Hh signaling and movement, Wg signaling and distribution, Dpp signaling and distribution	Bellaiche *et al*., 1998; Bornemann *et al*., 2004; Gallet *et al*., 2003
Sister of ttv (sotv)	Ext2	Hh signaling and movement, Wg signaling and distribution, Dpp signaling and distribution	Bornemann *et al*., 2004; Han *et al*., 2004; Takei *et al*., 2004
Sulfateless (sfl)	N-deacetylase/N-sulfotransferase	FGF and ntsignaling	Han *et al*., 2004; Takei *et al*., 2004
Brother of ttv (botv)	Extl3	Hh signaling and movement, Wg signaling and distribution, Dpp signaling and distribution	Han *et al*., 2004; Takei *et al*., 2004
dHs3ST	Hs3st	Notch Signaling	Kamimura *et al*., 2004
dHs6ST	Hs6st	FGF signaling	Kamimura *et al*., 2001